CHARLES UNIVERSITY IN PRAGUE

Faculty of Science

Developmental and Cell Biology

Role of Genetic Factors Responsible for Development of Pancreatic Cancer

Ph.D. Thesis

Marianna Borecká

Supervisor: RNDr. Markéta Janatová, Ph.D.

Laboratory of Oncogenetics

Institute of Biochemistry and Experimental Oncology, First Faculty of Medicine

Prague, 2020

Statement

I hereby declare that I have completed this final thesis independently and that I have included all cited literature and used sources of information. Neither the work as a whole nor any of its substantial parts have been previously submitted to achieve a different or similar academic degree.

In Prague, 3 September 2020 Marianna Borecká

Acknowledgements

I would like to thank my supervisor RNDr. Markéta Janatová, Ph.D., M.Sc. Jan Ševčík, Ph.D., my colleagues, my family, and all those who never stopped asking when I am going to finish it.

Content

Abstract

Cancer is a major health problem, worldwide, and is the second-most frequent cause of death (www.uzis.cz). Research is urgently necessary to reduce cancer incidence and the costs associated with cancer management, to develop more efficient and effective risk prediction strategies and personalised patient treatment. Germinal mutations in genes that predispose individuals to hereditary cancer syndromes are clinically important and can be used to classify carriers being at high risk of cancer development. Identification of these mutations can influence the prognosis and treatment of probands and can be used to include their family members into high-risk groups with corresponding preventive strategies.

This study is focused on the currently underestimated description of newly identified genetic factors among the Czech population that predispose individuals to develop pancreatic ductal adenocarcinoma (PDAC). In 2017, the incidence of PDAC in the Czech Republic was 21 cases per 100,000 persons, and PDAC was the fourth-most frequent cause of death among all cancer diseases (www.svod.cz).

Using a variety of screening techniques, which included high-resolution melting (HRM) analysis, Sanger sequencing of whole genes, and next-generation sequencing (NGS), with a CZECANCA panel that was generated in our laboratory, we analysed several different cohorts of unselected PDAC patients and non-cancer controls. A role of PALB2 as a PDAC-predisposing gene in the Czech population was confirmed with the frequency of truncation mutations 1.97% (3/152) among unselected PDAC patients and 0.08% (1/1,226) in controls [odds ratio (OR)=24.66; 95% confidence interval (CI) 2.55-238.64; p=0.005]. Further, the recurrent Slavic mutation c.657_661del in *NBN* was found to have a higher frequency among unselected PDAC patients (5/241; 2.08%) than in controls (2/915; OR=9.65; 95% CI 1.9-50.2; p=0.006) and may represent another allele associated with an increased risk of PDAC occurrence. Moreover, NGS sequencing performed on 113 unselected PDAC patients revealed the presence of mutations in PDAC/HBOC (hereditary breast and/or ovarian cancer) predisposition genes in 15 patients [*BRCA1* (3x); *BRCA2* (5x); *PALB2* (1x); *ATM* (1x); *NBN* (1x); *CHEK2* (3x); and *BRIP1* (1x)]. The most promising new identified candidate gene was *LIG4,* which displayed a similar frequency of pathogenic variants as *BRCA1* and *CHEK2* (3x). In a unique group of 20 patients who survived more than 5 years after PDAC diagnosis, we identified five mutations in four genes, among four patients (4/20; 20%): *ATM* (1x), *MLH1* (1x), *RAD51D* (1x), and *CHEK2* (2x).

A set of missense *PALB2* sequence alterations, which were classified as variants of uncertain significance, were functionally characterised, *in vitro,* using a human U2 OS cell line as a model. The analysed sequence variants were first introduced into the genome using clustered regularly

interspaced short palindromic repeat (CRISPR)-based homology-directed repair. The primary PALB2 function within the DNA-damage response pathway during homologous recombination was determined in selected clones that harboured the analysed sequence alterations. The results showed no significant changes in homologous recombination activity among heterozygous clones with c.82_83delinsGC and c.3494C>T mutations, compared with the wild-type control.

Abstrakt

Nádorová onemocnění jsou jakožto druhá nejčastější příčina úmrtí globálním zdravotním problémem (www.uzis.cz). Vzniká tak urgentní potřeba výzkumu, aby díky efektivnější a výkonnější predikci rizika a více personalizovaným přístupem k pacientům, byla redukována incidence a asociované léčebné finanční náklady. Nosiči klinicky významných germinálních mutací v genech predisponujících k hereditárním nádorovým syndromům mají vysoké riziko nádorového onemocnění. Identifikace takovéto mutace může ovlivnit prognózu i léčbu probanda, ale také pomoci s prevencí rodinných příslušníků a jejich zařazení do vysoce rizikové skupiny.

Tato studie je zaměřena na dosud málo popsané genetické faktory predisponující k duktálnímu adenokarcinomu pankreatu (PDAC) v české populaci. V roce 2017 byla incidence PDAC v ČR 21 případů na 100 tisíc obyvatel a PDAC byl čtvrtý nejčastější důvod smrti mezi onkologickými pacienty (www.svod.cz).

Za použití široké škály metod včetně HRM analýzy (High Resolution Melting), Sanger sekvenování celého genu a sekvenování nové generace (NGS, Next Generation Sequencing) s pomocí CZECANCA panelu vyrobeného v naší laboratoři jsme analyzovali několik skupin neselektovaných PDAC pacientů a nenádorových kontrol. Byla potvrzena role *PALB2* jako PDAC predispozičního genu v české populaci s frekvencí trunkačních mutací u neselektovaných PDAC pacientů 1,97% (3/152) a 0,08% (1/1.226) v kontrolní skupině [OR=24,66 (odds ratio); 95% CI 2,55-238,64; p=0,005]. Dále byla nalezena vyšší frekvence rekurentní slovanské mutace c.657_661del v genu *NBN* u neselektovaných PDAC pacientů (5/241; 2,08%) oproti 0,22% (2/915) u kotrol, která tedy představuje další alelu zvyšující riziko vzniku PDAC (OR=9,65; 95% CI 1,9-50,2; p=0,006). V další části práce bylo vyšetřeno 113 neselektovaných PDAC pacientů pomocí NGS sekvenování. Byla potvrzena přítomnost mutací známých PDAC/HBOC (hereditary breast and/or ovarian cancer) predispozičních genů u 15 pacientů: *BRCA1* (3x), *BRCA2* (5x), *PALB2* (1x), *ATM* (1x), *NBN* (1x), *CHEK2* (3x) a *BRIP1* (1x). Jako nejslibnější nový kandidátní gen se jeví *LIG4* se stejnou frekvencí patogenních variant jako *BRCA1* a *CHEK2* (3x). V unikátní skupině dvaceti pacientů přeživších více než pět let po PDAC diagnóze jsme našli pět mutací u čtyř pacientů (4/20; 20%) – *ATM* (1x); *MLH1* (1x); *RAD51D* (1x) a *CHEK2* (2x).

Soubor *PALB2* missense variant nejasného významu byl funkčně charakterizován *in vitro* na modelu lidské U2 OS buněčné linie. Analyzované varianty byly nejprve zavedeny do buněčného genomu pomocí CRISPR technologie. Vzhledem k tomu, že PALB2 protein má důležitou funkci během oprav DNA zlomů, byla aktivita homologní rekombinace testována u selektovaných klonů. Výsledky neukázaly žádný signifikantní rozdíl aktivity homologní rekombinace mezi kontrolou s původní sekvencí a heterozygotními klony c.82_83delinsGC a c.3494C>T.

List of Abbreviations

AA	Amino Acids
AIM	ATM-Interacting Motif
ATM	Ataxia-Telangiectasia Mutated
ATP	Adenosine TriPhosphate
ATR	Ataxia-Telangiectasia and Rad3-related
BAM	Binary Alignment Map
BC	Breast Cancer
BMI	Body Mass Index
BRCA1	Breast Cancer 1
BRCA2	Breast Cancer 2
BRCT	BRCA1 Carboxy-Terminal domain
CADD	Combined Annotation Dependent Depletion
Cas9	CRISPR-Associated Protein 9
CC	Coiled Coil domain
CDK	Cyclin Dependent Kinase
ChAM	Chromatin-Association Motif
CHEK2	CHEckpoint Kinase 2
CI	Confidence Interval
CNV	Copy Number Variation
CRISPR	Clustered Regularly Interspaced Short Palindromic Repeats
CtBP	C-terminal Binding Protein
CtIP	CtBP-Interacting Protein
CUL3	Cullin-3
CZECANCA	CZech CAncer paNel for Clinical Application
DBD	DNA Binding Domain
DDSB	DNA Double-Strand Break
DMEM	Dulbecco´s Modified Eagle´s Medium
DNA	DeoxyriboNucleic Acid
dNTP	deoxyNucleoside TriPhosphate
DR-GFP	Direct Repeat-GFP assay
dsDNA	double strand DNA
EDTA	EthyleneDiamineTetraAcetic acid
ER	Estrogene Receptor
ExAC	Exome Aggregation Consortium
FA	Fanconi Anemia
FACS	Fluorescence-Activated Cell Sorter
FA-N	Fanconi Anemia type N
FANCN	Fanconi Anemia Complementation group N
FAN1	FANCD2/FANCI-Associated Nuclease 1
FBA	Fetal Bovine Albumine
FFPE	Formalin-Fixed Paraffin-Embedded
FHA	Fork-Head Associated domain
fPDAC	familial PDAC
GATK	Genome Analysis ToolKit
GERP	Genomic Evolutionary Rate Profiling
GFP	Green Fluorescent Protein
GPS	Glutamine-Penicillin-Streptomycin Solution
gRNA	guide RNA
HBOC	Hereditary Breast and/or Ovarian Cancer
HDR	Homology Direct Repeat

HER	Human Epidermal growth factor Receptor
HiDi	Highly Deionized
HP	Hereditary Pancreatitis
HR	Homologous Recombination
HRM	High Resolution Melting
ICL	Interstrand CrossLinking
IGV	Integrative Genomics Viewer
IR	Ionizing Radiation
KEAP1	Kelch-like ECH-Associated Protein 1
KO	Knock-Out
LIG4	DNA Ligase 4
LM-PCR	Ligation Mediated PCR
LOH	Loss Of Heterozygosity
MA	Mutation Assessor
MBD	MRG15 Binding Domain
MCF	Multiple Cancer Families
MDC1	Mediator of DNA Damage Checkpoint 1
MDM2	Mouse Double Minute 2 homolog
MIR	MRE11 Interaction Region
MLH1	MutL Homolog 1
MLPA	Multiplex Ligation-dependent Probe Amplification
MMC	MitoMycin C
MORF	Male-specific ORF protein
MRE11	Meiotic REcombination gene 11
MRG15	MORF-Related Gene on chromosome 15
MRN complex	MRE11-RAD50-NBN complex
NA	Not Available
NBN	NiBriN
NBS	Nijmegen Breakage Syndrome
NCCN	National Comprehensive Cancer Network
NES	Nuclear Export Signal
NGS	Next-Generation Sequencing
NHEJ	Non-Homologous End Joining
NLS	Nuclear Localisation Signal
NRF2	Nuclear Factor 2
OC	Ovarian Cancer
OR	Odds Ratio
PALB2	Partner And Localizer of BRCA2
PAM	Protospacer Adjacent Motif
PARP	Poly(ADP-ribose) Polymerase
PARPi	PARP inhibitors
PBS	Phosphate Buffered Saline
PC	Positive Control
PCR	Polymerase Chain Reaction
PDAC	Pancreatic Ductal AdenoCarcinoma
PEG	PolyEthylene Glycol
PID	PALB2-Interacting Domain
PMS2	PMS1 homolog 2
PP-2	PolyPhen-2
PR	Progesterone Receptor
qPCR	Real-time PCR
RAD50	RADiation gene 50

RAD51C	RAD51 paralog C
RNA	RiboNucleic Acid
RPA	Replication Protein A
RR	Relative Risk
SAM	Sequence Alignment Map
SDM	Site Directed Mutagenesis
sgRNA	structural gRNA
SIFT	Sorting Tolerant From Intolerant
SMN	Second Malignant Neoplasm
SNV	Single Nucleotide Variant
ssDNA	single stranded DNA
TE buffer	Tris EDTA buffer
Tm	meltign Temperature
TRF2	Telomeric Repeat-binding Factor 2
USP11	Ubiquitin Specific Peptidase 11
U2 OS	OsteoSarcoma cell line
VCF	Variant-Call Format
VUS	Variant of Uncertain Significance
WRN	WRN RecQ like helicase
WT	Wild Type
XRCC3	X-ray Repair Cross Complementing 3
XRS2	X-Ray Sensitivity 2

List of Tables

List of Figures

1. Introduction

1.1 Pancreatic Ductal Adenocarcinoma (PDAC)

Pancreatic cancer is a disease in which malignant cells arise in the tissue of pancreas. The pancreas has both an exocrine and endocrine function. The exocrine gland, acinar and ductal cells, produces pancreatic juice containing digestive enzymes and bicarbonate. The endocrine part, Langerhans cells, regulates blood glucose levels and carbohydrate metabolism. Depending on the origin of the cancer, we distinguish between exocrine and endocrine tumours. Pancreatic ductal adenocarcinoma (PDAC) is the most common and lethal among exocrine tumours (*1*). Other exocrine tumour types are, for example, acinar cell carcinoma, intraductal papillary mucinous neoplasm, mucinous cystic neoplasm and others. Endocrine tumours represent 7% of pancreatic cancers and they include, for example, insulinoma, glucagonoma and gastrinoma (*1*).

The incidence of PDAC in the Czech Republic reached 21 cases per 100,000 persons and a mortality of 19 cases per 100,000 persons in 2017 (Figure 1) (www.svod.cz). PDAC is the fourth most common cause of cancer death in the Czech population (*2*). It has one of the worst prognoses of any type of cancer, only 5%-9% of diagnosed patients survive 5 years (*3, 4*).

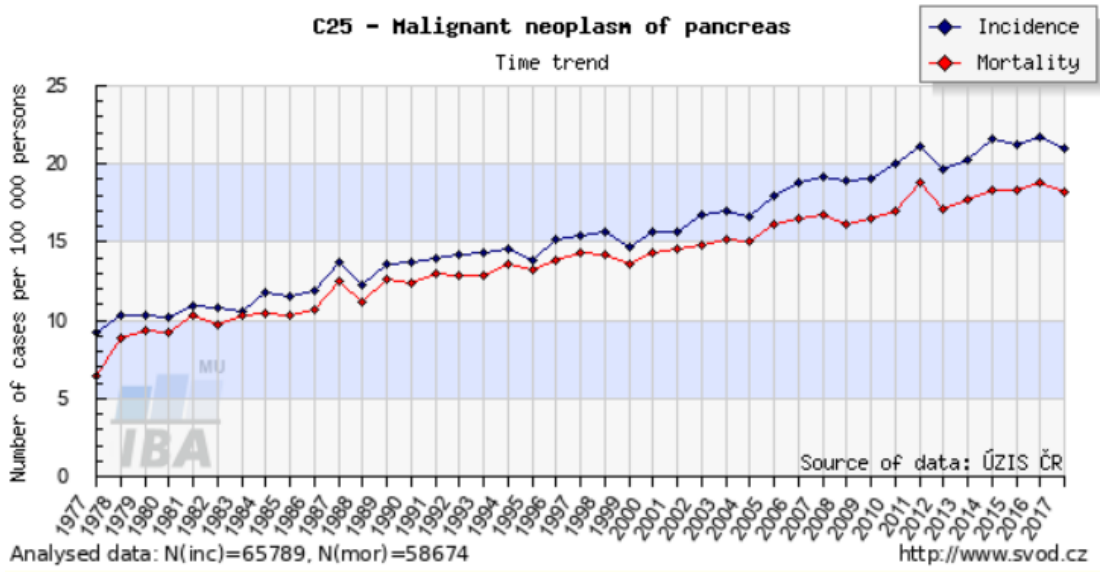

Figure 1. PDAC incidence and mortality per 100,000 persons in the Czech Republic in the years 1977-2017. (www.svod.cz)

PDAC has unspecific symptoms such as back pain, diabetes mellitus, jaundice, weight loss and nausea that usually occur in advanced stage of cancer. Over 80% of PDACs are diagnosed when already metastasized to other tissues (Figure 2). Therefore, most of the patients are not suitable for surgery, although a surgical resection is still the only effective treatment (*5*).

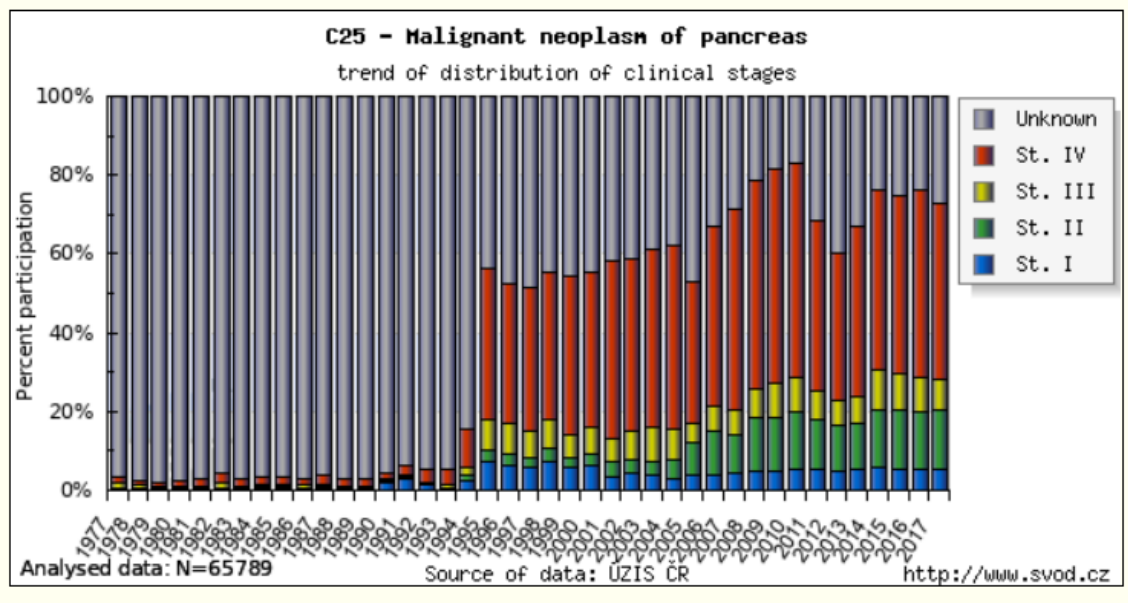

Figure 2. Clinical stage distribution of PDAC diagnosed in the Czech Republic in the years 1977-2017.
(www.svod.cz)

Various life-style factors contribute to the risk of PDAC. Cigarette smoking is the most established one and can increase the PDAC risk 2-3x (*6*). A higher risk of PDAC was also found for a high BMI (body mass index), alcohol consumption and diabetes mellitus (*7*). The main predisposition factor for developing PDAC is a positive family history (*8*).

1.1.1 Hereditary PDAC and Genes Associated with a PDAC Risk

Although the vast majority of PDAC are sporadic, about 5%-10% is associated with inherited predisposition. One of the highest PDAC risk factors is considered to be hereditary pancreatitis (HP) with a 40% risk of developing PDAC by 70 years of age. Activating germline mutations in *PRSS1* and inactivating in *SPINK1* genes are both associated with HP (*9*). Some hereditary cancer syndromes are also associated with a PDAC risk (Table 1).

Hereditary cancer syndrome	**Predisposition genes**	**Relative risk (RR) of PDAC**
Peutz-Jeghers syndrome	*STK11*	Up to 132-fold
Familial atypical multiple mole melanoma	*CDKN2A*	13- to 39-fold
Familial adenomatous polyposis	*APC* and *MUTYH*	5-fold
Lynch syndrome	*MLH1*, *MSH2*, *MSH6*, *PMS2*, and *EPCAM*	9- to 11-fold
Li-Fraumeni syndrome	*TP53*	7-fold
Hereditary breast and ovarian cancer syndrome (HBOC)	*BRCA1* *BRCA2* *PALB2*	2-fold 3- to 9-fold 6-fold

Table 1. List of hereditary cancer syndromes associated with PDAC risk.
(adapted from *1, 10*)

The predisposition genes often code for proteins involved in cell cycle control and DNA repair and Fanconi anemia pathways. Yet various other genes (*ATM*, *FANCC*, and *FANCG*) have also been associated with PDAC thus far (*11, 12*).

1.1.2 Benefits of Genetic Testing for PDAC Patients and Their Families

The symptoms of PDAC are very unspecific and therefore the tumours are often diagnosed in late stages. Thus, great effort is made to improve the prediction and early diagnosis of PDAC (*13*). The identification of causal mutations in families can help to define healthy carriers as high-risk individuals best eligible for screening methods (*14*). The 2020 PDAC NCCN (National comprehensive cancer network) guidelines recommend germline testing for all individuals diagnosed with exocrine pancreatic cancer (www.nccn.org).

The mutation status can also help with the choice of tailored treatment. Tumours with homologous recombination (HR) defects (e.g. *BRCA1*, *BRCA2*, or *PALB2* genes mutated) are sensitive to cytotoxic agents (e.g. Platinum derivatives, Mitomycin C). They directly bind to DNA, causing DNA strands crosslinking and inducing DNA double-strand breaks (DDSBs) (*15-17*). Moreover, inhibiting the base excision repair by PARP (Poly[ADP-Ribose] polymerase) inhibitors (PARPi) (e.g. Olaparib) leads to DDSBs after a DNA replication fork collapse and induces a synthetic lethality in these HR deficient tumours (Figure 3) (*18, 19*). The combination of PARPi and platinum-based therapy showed a good response with the overall survival of PDAC patients from 10 to 17 months (*20*).

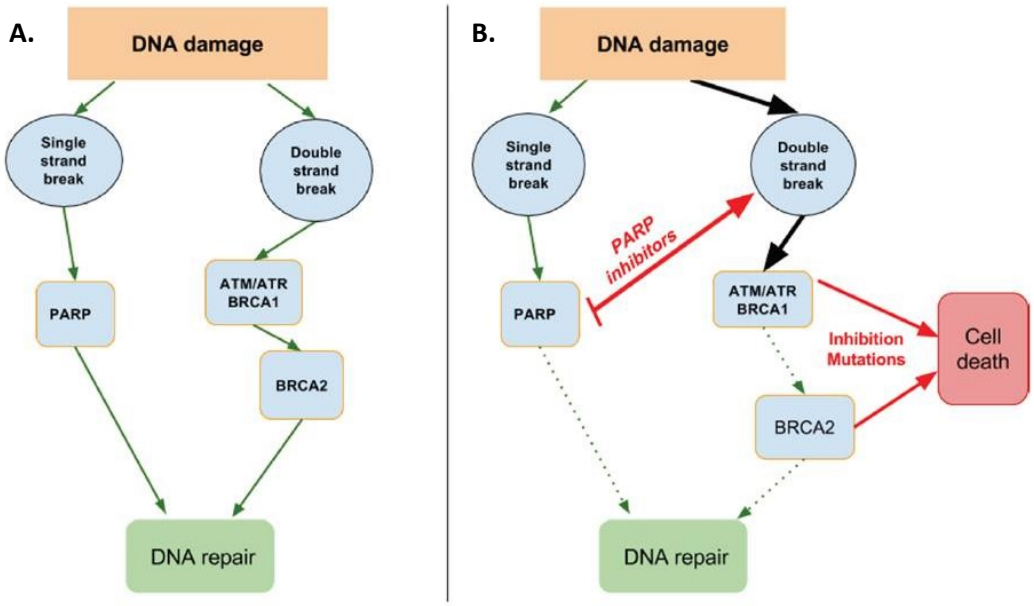

Figure 3. The mechanism of DNA damage repair and synthetic lethality.

- **A.** In healthy cells single strand DNA breaks are repaired with PARP and double strand breaks with ATM/ATR/BRCA1/BRCA2 pathways.
- **B.** Introducing PARP inhibitors in cells harbouring pathogenic mutations in double strand DNA repair pathways leads to gain of double strand breaks and hence results in synthetic lethality *(21).*

1.2 The Partner and Localiser of BRCA2 (*PALB2*) Gene

PALB2 was described as a nucleoprotein co-immunoprecipitating with BRCA2, helping its stabilisation and localisation to DDSBs sites (*22*). Xia et al. (*22*) also suggested a tumour suppression function of PALB2. The *PALB2* gene was later described as a Fanconi anemia gene *FANCN* (*23*) and as a BC susceptibility gene (*24*). PALB2 plays an important role in maintaining genome integrity through the error-free HR reparation of DDSBs (*25-27*). *PALB2* was also suggested as one of the PDAC susceptibility genes and therefore we focused on its mutation status among Czech PDAC patients (*28*).

1.2.1 Structure of *PALB2*

PALB2 is a 13-exons gene located on chromosome 16 (16p12.2) with one transcription variant. It codes for protein that is 1,186 amino acids (AAs) long and has 130kDa (Figure 4). PALB2 is a scaffold protein and thus contains various protein- and DNA-binding domains.

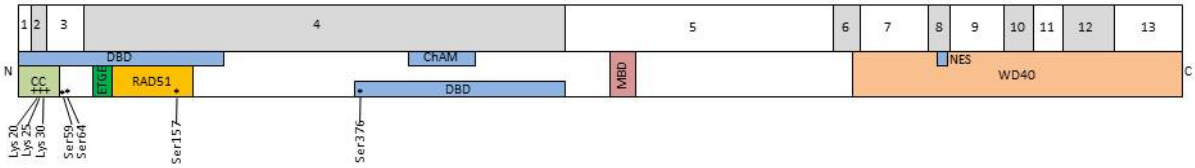

Figure 4. Diagram of the PALB2 protein structure.
Upper part: 13 exons of PALB2.
Bottom part: Functional domains of PALB2. **CC** (coiled coil domain, AAs 9-44); **DBD** (DNA binding domain, AAs 1-200 and AAs 372-561); ETGE motif (AAs 88-94); RAD51 binding site (AAs 101-184); **ChAM** (chromatin-association motif, AAs 395-450); **MBD** (MRG15 binding domain, AAs 611-29); WD40 domain (AAs 853-1186); **NES** (nuclear export signal, AAs 928-945); * phosphorylation sites; + ubiquitylation sites.

1.2.1.1 The C-terminus of PALB2

The WD40 domain (AAs 867-1186) is a protein-protein interaction domain on the C-terminus (Figure 5). It is folded into a seven-bladed β-propeller (*29*) and associates with BRCA2 and several other proteins including Polymerase η, RAD51, RAD51C and XRCC3 (*30-32*). Truncating mutations in the WD40 domain leaves the protein incompletely folded and prevents BRCA2 from localising to DDSB sites (*29*). This explains the pathogenicity of mutation p.Tyr1183Ter (c.3459C>G) that removes the last four residues of PALB2 (*29*).

A hidden nuclear export signal (NES) (AAs 928-945) within the WD40 domain was described by Pauty et al. (*33*). An unfolded WD40 domain exposes the NES sequence resulting in PALB2 mis-localisation to the cytoplasm instead of the nucleus (Figure 5) (*33*).

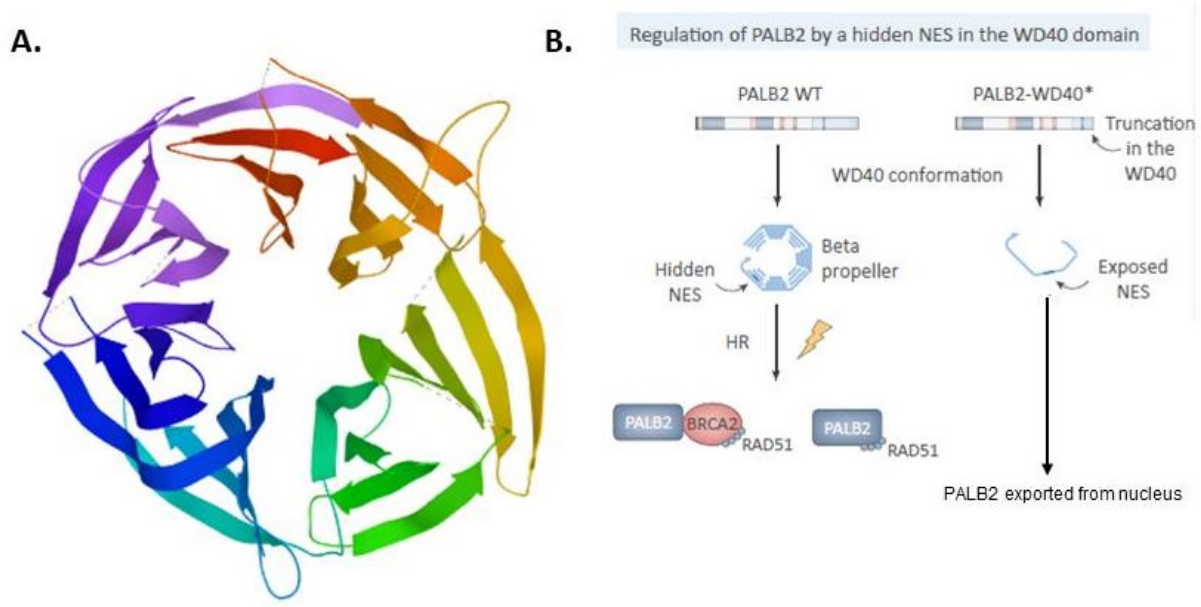

Figure 5. WD40 domain. – a seven-bladed β-propeller WD40 domain contains a hidden NES signal.

A. Structure of WD40 domain – a seven-bladed β-propeller (*29*).

B. Mis-folded PALB2 exposes the NES signal and PALB2 is then exported from nucleus (*34*). WT – wild type.

1.2.1.2 The N-terminus of PALB2

The N-terminus contains several binding domains – a coiled-coil domain (CC, AAs 9-44), RAD51 binding domain (AAs 101-184), DNA-binding domain (DBD, AAs 1-200) and KEAP1 binding ETGE motif (AAs 88-94).

The CC domain, known to mediate the protein-protein interaction, participates in both PALB2-BRCA1 binding and PALB2 homo-oligomerisation. The competition between PALB2 oligomerisation and PALB2-BRCA1 binding is a switch allowing the HR and is believed to be triggered by Cyclin dependent kinase (CDK) phosphorylation of PALB2 after DNA damage (*25, 35, 36*). The PALB2-PALB2 interaction thus prevents unscheduled DNA recombination in the absence of a sister chromatid (*34*).

Next to the CC domain is a conserved ETGE motif (AAs 88-94) important for interaction with the KELCH domain on KEAP1 E3 ubiquitin ligase (Kelch-like ECH-associated protein 1). This interaction is important for the maintenance of cellular redox homeostasis.

1.2.1.3 The Central Region of PALB2

In the middle region, there lies a second DBD (AAs 372-561) (*37*) and an evolutionary conserved chromatin-association motif (ChAM, AAs 395-450), which mediates PALB2 association with nucleosome core histones H3 and H2B. The primary AA sequence of the ChAM does not present any similarities with other known nucleosome-binding domains (*38*).

The MBD (MRG15 binding domain) (AAs 611-629) interacts with a chromodomain protein MORF-related gene on chromosome 15 (MRG15; a part of the histone acetyltransferase/deacetylase

complex) and its close homologue MRGX (*39*). The MRG15 recognises histone H3 trimethylated at lysine 36 (H3K36me3), which is enriched at highly active genes, thus targets PALB2 to actively transcribed genes and protects them from DNA damage. The permanent chromatin association of PALB2 contributes to protect active genes from stress arising during DNA replication (*40*). In agreement with these reports, PALB2 genome-wide chromatin occupancy contained 373 genes with high transcription activity and co-localised extensively with BRCA1 and RNA polymerase II. These genes included ribosomal proteins, histones, growth regulators and modulators of inflammation and stress (*41*).

1.2.1.4 Post-translational Modification of PALB2

During the initial phase of HR, CDKs phosphorylate PALB2 at Ser64, preventing BRCA1 interaction with PALB2. The later formation of single stranded DNA (ssDNA) leads to ATR activation. The ATR regulates PALB2 by driving a phosphorylation switch on Ser64 to Ser59 and thus favours PALB2-BRCA1 interaction (*42*). There are at least three ATM/ATR recognised phosphorylation sites on the PALB2 sequence (Ser59, Ser157, and Ser376) (*43*). Phospho-deficient PALB2 mutants in all three AAs are unable to support proper RAD51 foci formation during HR (*44*).

The E3 ubiquitin ligase CUL3 (Cullin-3) targets the PALB2 residues Lys20, Lys25, and Lys30 in the CC domain for ubiquitylation and inhibits BRCA1-PALB2 binding during the G1 phase. The cell cycle controlled deubiquitylase USP11 (Ubiquitin specific peptidase 11) converts this interaction and thus induces HR repair (*45, 46*).

1.2.2 Function of PALB2

1.2.2.1 Homologous Recombination (HR)

DDSBs are the most dangerous DNA lesions. If left unrepaired, they can cause chromosomal mutation or large genomic rearrangement with a devastating effect on genomic stability and cellular homeostasis. With regard to the severity of DDSBs, the cell has two separate mechanisms for their repair – non-homologous end joining (NHEJ) and HR. Many proteins directly participating in either of these DNA repair processes are coded by tumour suppressor genes. Their inactivation is linked with a number of cancer syndromes. The PALB2 protein is an important factor for HR (Figure 6). It acts as a protein interaction modulator bringing BRCA1, BRCA2, and RAD51 together in a pre-complex (*38, 40, 47*).

After DDSB recognition by the MRN sensor complex (MRE11-RAD50-NBN), ATM kinase is activated (*48*) and orchestrates HR through the phosphorylation of its downstream mediators of a DNA damage response pathway. The DNA repair complex assembly starts by the H2A histone

phosphorylation by activated ATM. This modification marks the site of the DNA damage and brings other factors to the place where they are required. After a regulated DNA resection, the formed 3´-end ssDNA tails are capped and protected by phosphorylated Replication protein A (RPA) (*34*). In a further step, PALB2 protein binds BRCA1 anchored in the DDSB and tethers BRCA2 by a protein-protein interaction mediated by its WD40 domain (*36*). Together, the BRCA1-PALB2-BRCA2 complex assists the RPA removing and RAD51 forming its nucleoprotein filaments. They promote a homology search and strand invasion into the sister chromatid (*49*). The 3´-end ssDNA tails pair with homologous regions on the sister chromatid and serve as the primers for DNA synthesis. HR is restricted to the S and G2 phases of the cell cycle due to the necessity of the sister chromatid (*26, 27, 37, 39, 50*).

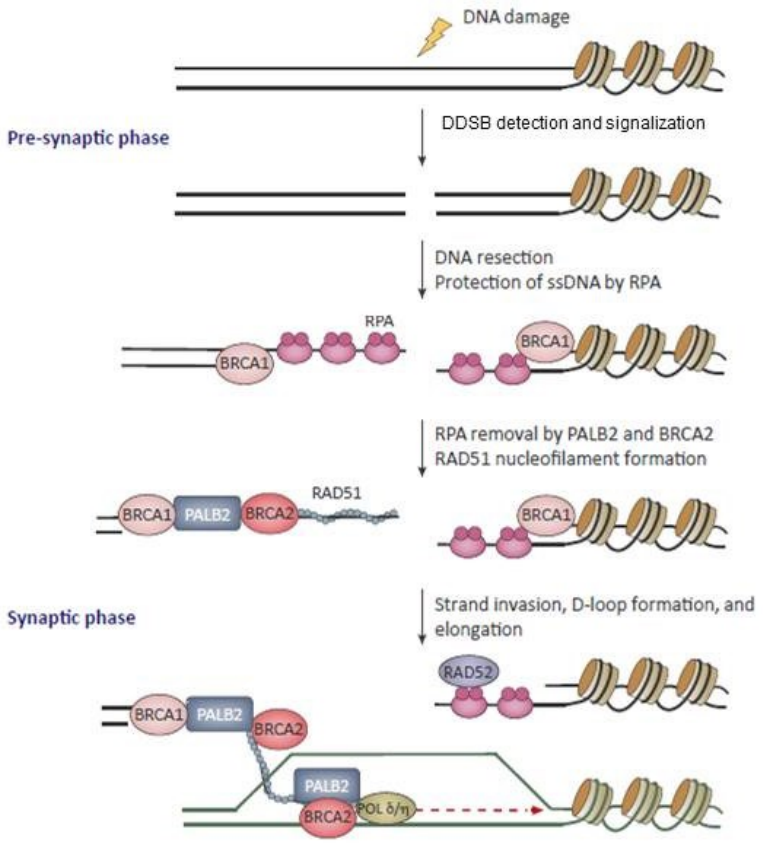

Figure 6. PALB2 function during HR.
After DDSB occurs in the cell nucleus, the 5´-ends are resected and the resulting single stranded DNA is capped by RPA protein. PALB2 forms a complex together with BRCA1 and BRCA2 and together they help with the formation of RAD51 nucleofilaments, which later help pairing with homologous regions on the sister chromatid (*34*).

1.2.2.2 Replication Stress Recovery

PALB2 has a crucial role in the recovery of replication stress caused by stalled forks during the S phase (Figure 7). Following replication fork stalling, RPA is phosphorylated by CDK2 and ATR. The phosphorylated RPA binds to ssDNA sites and marks the DNA damage, localises PALB2 and BRCA2 to

nuclear foci and stabilises the replisome. Deregulating these processes leads to significant DNA damage after replication stress (*51-53*). BRCA2 and PALB2 are needed for the proper localisation of Polη on blocked replication forks and stimulate Polη to initiate DNA synthesis on strand invasion (*30*).

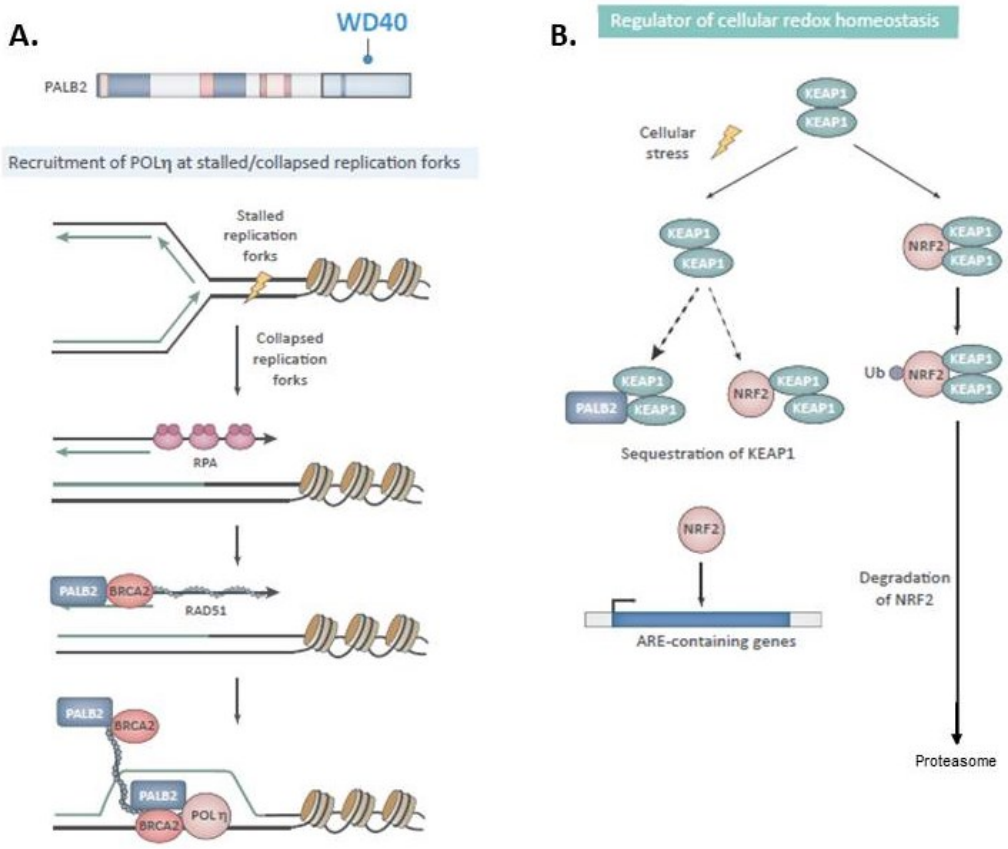

Figure 7. PALB2 functions during replication stress recovery and cellular redox homeostasis.

A. Collapsed replication forks results in DDSB. PALB2 helps with localising of BRCA2 and Polη to the site and thus enables its recovery.
B. PALB2 binding to KEAP1 releases NRF2 antioxidant transcription factor from KEAP1 inhibition and later degradation (*34*).

1.2.2.3 Regulation of Cellular Redox Homeostasis

KEAP1 is an oxidative stress sensor that targets the antioxidant transcription factor NRF2 (Nuclear factor 2) for degradation. PALB2 binds to KEAP1 and prevents NRF2 from KEAP1-mediated inhibition. Thus, PALB2 increases levels of NRF2 in the nucleus and lowers the cellular reactive oxygen species level (Figure 7). This could explain the fact that Fanconi anemia cells are hypersensitive to oxidative stress (*45*).

1.2.3 *PALB2* Mutations and Associated Diseases

1.2.3.1 Fanconi Anemia Complementation Group N (FA-N)

Fanconi anemia (FA) is a bone marrow failure syndrome characterised by increased cancer risk (mainly haematological malignancies), growth retardation, genomic instability on the cellular level

and the formation of DNA ICLs (interstrand crosslinks). FA is caused by biallelic mutations in one of 22 FA genes (*54, 55*). Inactivation in both *PALB2* alleles causes the FA type N (FA-N). FA-N shares a similar phenotypic spectrum (hyper-sensitive to ICL agents, a high risk of childhood solid tumours, mainly Wilms tumour and medulloblastoma), with FA type D1 arising from *BRCA2* biallelic mutations (*23, 56, 57*).

From the FA-N patients described so far in the literature, nine have clear pathogenic *PALB2* mutations leading to a severe form of FA (Table 2). However, two patients (siblings, #10/11) were diagnosed with a mild form of FA-N (no severe developmental defect, B cell non-Hodgkin lymphoma) having one truncating mutation resulting in protein of 561 AAs and one splicing mutation resulting in the in-frame skipping of exon 6 (24 AAs). PALB2-Δ6 is proposed to be a hypomorphic mutation that does not impair BRCA1/2 interactions. It is able to interact with BRCA2 and, although patient cells do not form RAD51 foci, cells with biallelic PALB2-Δ6 are able to recruit RAD51 (*58*).

Patient	First mutation		Second mutation		Reference
	Nucleotide change	Protein change	Nucleotide change	Protein change	
1	c.1653T>A	p.Tyr551Ter	Δ2-6	p.Leu17_Lys862del	(*23*)
2	c.395delT	p.Val132fs	c.3113+5G>C	p.Ala946fs	(*56*)
3	c.757_758delCT	p.Leu253fs	c.3294_3298delGACGA	p.Lys1098fs	(*56*)
4	c.2257C>T	p.Arg753Ter	c.3549C>A	p.Tyr1183Ter	(*56*)
5	c.2393_2394insCT	p.Thr799fs	c.3350+4A>G	p.Phe1118fs	(*56*)
6	c.2521delA	p.Thr841fs	c.3323delA	p.Tyr1108fs	(*56*)
7	c.2962C>T	p.Gln988Ter	c.3549C>G	p.Tyr1183Ter	(*56*)
8	c.3116delA	p.Asn1039fs	c.3549C>G	p.Tyr1183Ter	(*56*)
9	c.1676_1677delAAinsG	p.Gln559fs	c.1676_1677delAAinsG	p.Gln559fs	(*59*)
10 (11)	c.1676_1677delAAinsG	p.Gln559fs	c.2586+1G>A	p.Thr839_Lys862del	(*58*)

Table 2. List of eleven described FA-N patients and their *PALB2* mutations.
Δ – deletion of whole exon(s).

1.2.3.2 PALB2 Mutations and Cancer Risk

1.2.3.2.1 Breast Cancer

PALB2 germline variants were associated with a breast cancer (BC) risk shortly after PALB2 discovery (*24*). Rahman et al. (*24*) proposed that *PALB2* mutation carriers have a 2.3-fold higher risk of BC. Since then, many studies were published screening *PALB2* mutations with various frequencies in BC patients from 0.6% (*60*) to 3.9% (*61*). The risk of BC to an age of 80 years for female *PALB2* mutation carriers was recently calculated to be 53% (*62*). A meta-analysis of *PALB2* mutations in high-risk BC patients showed a carrier frequency of 1.55% (91/5,862) and odds ratio (OR)=21.40 (95% CI 10.10-45.32) (*63*). Recently, a meta-analysis of *BRCA1* and *BRCA2* non-mutated patients showed the frequency of *PALB2* germline mutations in familial BC patients at 1.29% with OR=8.45 (95% CI 6.42-11.14) and the frequency among unselected BC patients at 4.76 with OR=4.76 (95% CI 3.37-6.72) (*64*).

1.2.3.2.2 PDAC

Jones et al. (*28*) was the first to show the association of *PALB2* germline mutations with PDAC incidence. Nowadays, *PALB2* is considered to be one of the four most frequently mutated PDAC genes together with *BRCA1*, *BRCA2,* and *CDKN2A*. Next generation sequencing (NGS) studies show the *PALB2* mutations frequency among sporadic PDAC patients at 0.71% (range 0%-1.64%) and 1.05% among familial PDAC (fPDAC, range 0.54%-3.70%) (Table 3). The mutations in *PALB2* were described as increasing the risk of pancreatic cancer in an international study of 524 families (RR=2.37) (*62*). A large case-control sequencing study described the OR for *PALB2* mutations in pancreatic cancer to be 7.69 (*65*).

Mutations	No of cases	Frequency	Country	Study
Unselected or sporadic PDAC patients; 0.71% (62/8,778)				
0	180	–	Canada	(*66*)
0	96	–	USA	(*67*)
3	190	1.58%	USA	(*68*)
1	385	0.26%	Aus/USA/Italy	(*69*)
1	176	0.57%	USA	(*70*)
2	854	0.23%	USA	(*71*)
1	298	0.34%	USA	(*72*)
1	437	0.23%	USA/Canada/Aus	(*73*)
12	3,030	0.40%	USA	(*74*)
20	1,217	1.64%	USA	(*75*)
2	274	0.73%	USA	(*76*)
1	289	0.35%	USA	(*77*)
18	1,352	1.33%	USA	(*65*)
fPDAC patients; 1.05% (10/956)				
1	1	100%	USA	(*28*)
0	2	–	USA	(*11*)
1	5	20%	Canada	(*78*)
0	71	–	Canada	(*66*)
5	638	0.78%	USA	(*79*)
2	54	3.70%	Japan	(*80*)
1	185	0.54%	USA	(*81*)

Table 3. Overview of *PALB2* germline mutations found in NGS studies of PDAC patients.
Aus – Australia; fPDAC – familial PDAC.

1.2.3.2.3 Association with Other Cancers

The importance of *PALB2* germline mutations in a predisposition to ovarian cancer (OC) is not convincing. Most of the studies did not find evidence for this association (in summary 0.27%; 15/5,502) (*68, 82, 83*). Norquist et al. (*84*) suggested *PALB2* as an OC risk gene with OR=4.4 (95% CI 2.1-9.1) in an NGS study of 1,915 OC patients (*84*) whereas our recent paper shows a lower risk of OC for *PALB2* mutation carriers OR=1.5 (95% CI 0.5-4.5) (*85*). The cumulative risk of OC for *PALB2* mutation carriers to an age of 80 years was calculated to be 5% (*62*).

Pakkanen et al. (*86*) and Erkko et al. (*87*) together found a 0.27% frequency of *PALB2* germline mutation among familial prostate cancer cases and 0.19% among unselected prostate cancer cases in the Finnish population. No germline pathogenic mutation was found in 95 prostate cancer high-risk families from North America (*88*), nor has an increased risk of prostate cancer been found in recent meta-analysis (*62*).

The sequencing data of 201 melanoma patients (*89*) and 53 families with familial melanoma did not support a case for *PALB2* association with melanoma (*90*).

1.2.3.2.4 Characteristics of Tumour Tissues from Patients with Germline *PALB2* Mutations

BCs with *PALB2* truncating mutations are associated with an aggressive tumour phenotype with a higher tumour grade and higher levels of the proliferation marker protein Ki-67 (*91*). A 10-year survival rate for *PALB2* mutated BCs was 48.0% compared to 74.7% for BCs with *PALB2* wild type (WT) sequences (*92*).

First observations suggested that *PALB2* mutated tumours could share a phenotypic characteristic with *BRCA2* mutated tumours rather than *BRCA1* mutated tumours (Estrogene receptor positive – ER+; Progesterone receptor positive – PR+; Human epidermal growth factor receptor 2 negative expression – HER2-) (*87, 93, 94*).

Lee et al. showed bi-allelic inactivation of *PALB2* in 10 (six times loss of heterozygosity – LOH and four times somatic mutations) out of 15 invasive BCs from patients carrying a germline pathogenic mutation (*95*). Li et al. found eleven LOH and five somatic mutations among 24 BC patients (*96*). It is inconclusive whether promotor hypermethylation could be an epigenetic inactivation mechanism for *PALB2* deficient tumours (*97-100*). An alternative mechanism of *PALB2* functional inactivation, such as haploinsufficiency or a dominant-negative effect of the truncated proteins in the remaining tumours without identified somatic inactivation of a second allele, is probable (*93*).

1.2.3.2.5 Treatment of *PALB2* Mutated Tumours

Identification of pathogenic germline *PALB2* variants may be also beneficial for the clinical management, prognosis, and treatment of patients. *PALB2* deficient cancers showed sensitivity to platinum derivatives and PARPi treatment the same way as *BRCA1/2* deficient cancers. Germline variants in DNA repair genes, including *PALB2*, were identified in the group of triple negative BC patients who responded to neoadjuvant treatment with a mitotic inhibitor and intercalating agent (*101*). Among OC patients, *PALB2* mutations were associated with higher platinum sensitivity (*102*). Villarroel et al. (*103*) presented a pancreatic cancer patient deficient for *PALB2* with a long-lasting response to the ICL agent Mitomycin C (MMC) (*103*). A more recent report also shows a positive response of the PDAC tumour to platinum ICL-agent-based chemotherapy at a *PALB2* heterozygous background (*104*). PARPi was tested with PALB2-deficient Willms tumour xenografts and showed a complete response maintained for four weeks (*105*).

1.3 The *NBN* Gene

Nibrin protein is encoded by the *NBN* gene (*NBS1, NBS, ATV, AT-V1*, or *p95*). It is a member of the MRE11-RAD50-NBN (MRN) complex, which has a crucial role in several stages of DDSBs repair through HR and NHEJ. It is also important in the repairing of DDSBs arisen during replication, meiosis, V(D)J recombination, class switch recombination and telomere maintenance (*106, 107*). Biallelic mutations in *NBN* cause a severe disease, Nijmegen breakage syndrome (NBS), characterised by chromosomal instability and an increased risk of lymphoid malignancies and other cancers (*108*).

1.3.1 Structure of *NBN*

The *NBN* gene is located on chromosome 8 (8q21.3) and consists of 16 exons. It encodes a 754-AA-long protein with a molecular mass of 85kDa (Figure 8). The Nibrin has two different transcripts – one full version with 754 AAs and a second transcript encoding shorter protein beginning from AA 83.

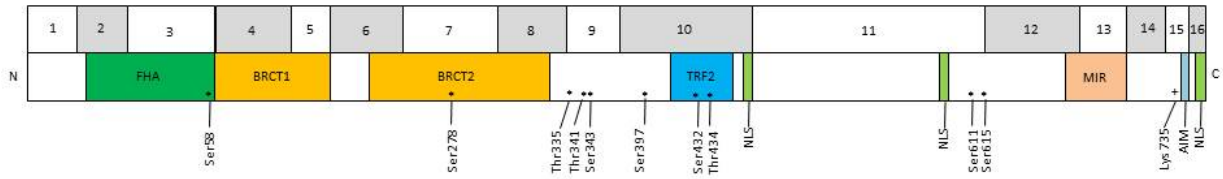

Figure 8. Diagram of the Nibrin protein structure.
Upper part: 16 exons of *NBN*.
Bottom part: Functional domains of Nibrin. **FHA** (fork-head associated domain, AAs 24-108); **BRCT1** and **BRCT2** (BRCA1 carboxy-terminal domains, AAs 108-196, AAs 221-330); **TRF2** binding site (Telomeric repeat-binding factor 2, AAs 419-449); **NLS**s (nuclear localisation signal, AAs 461-467, AAs 590-594, and AAs 751-754); **MIR** (MRE11 interaction region, AAs 665-693); **AIM** (ATM-interacting motif, AAs 734-754); * phosphorylation sites; + ubiquitylation sites.

1.3.1.1 The C-terminus of Nibrin

The C-terminus contains two binding domains and a nuclear localisation signal (NLS, AAs 751-754) (*109*). The MRE11 interaction region (MIR, AAs 665-693) and ATM-interacting motif (AIM, AAs 734-754) are protein binding domains (*110, 111*).

1.3.1.2 The N-terminus of Nibrin

The N-terminus of Nibrin consists of a fork-head associated domain (FHA, AAs 24-108) and two BRCA1 carboxy-terminal domains (BRCT1 and BRCT2, AAs 108-196 and AAs 221-330) that are responsible for binding to phosphorylated H2AX and other serine-phosphorylated factors (MDC1, MDM2, CtIP, ATR, WRN helicase).

1.3.1.3 The Central Region of Nibrin

A TRF2 (Telomeric repeat binding factor 2) binding site (AAs 419-449) (*112*) and another two NLSs (AAs 461-467 and AAs 590-594) are present in the central region of Nibrin. They seem to be redundant (*109*).

1.3.1.4 Post-translational Modification of Nibrin

ATM dependent phosphorylation induced by DNA damage was found on three sites – Ser343, Ser397, and Ser615 (*113*). The phosphorylation of residues Ser278, Ser343, and Ser397 of Nibrin was required for the stabilisation and accumulation of Nibrin-ATM binding at the sites of DDSBs (*114*). CDK2 phosphorylation of Ser432 during the S/G2 phase is required for the maintenance of telomeres (*112*). Nibrin is ubiquitylated by E3 ubiquitin ligase Skp2 (S phase kinase-associated protein 2) on Lys735 within the AIM motif. This allows ATM to bind to Nibrin (*115*).

1.3.2 Nibrin is a Member of MRN Complex

Nibrin is a component of the MRN protein complex together with the MRE11 and RAD50 (MRE11-RAD50-NBN) proteins. The MRN complex is most likely a part of larger macromolecular complex that defines its multiple functions. It is a key player in the sensing, signalling and regulation of responses to DDSBs. It controls the optimal response to DDSBs and activation of cell cycle checkpoints (*116*).

1.3.2.1 MRN Complex Structure

The MRN complex is a hetero-hexamer of nuclease activity containing dimers of each subunit ($M_2R_2N_2$) forming a bipolar structure (Figure 9). Its globular head binds to DNA and consists of MRE11 and RAD50, a long coiled-coil tail is formed by RAD50, and Nibrin forms a flexible adapter domain (*117*).

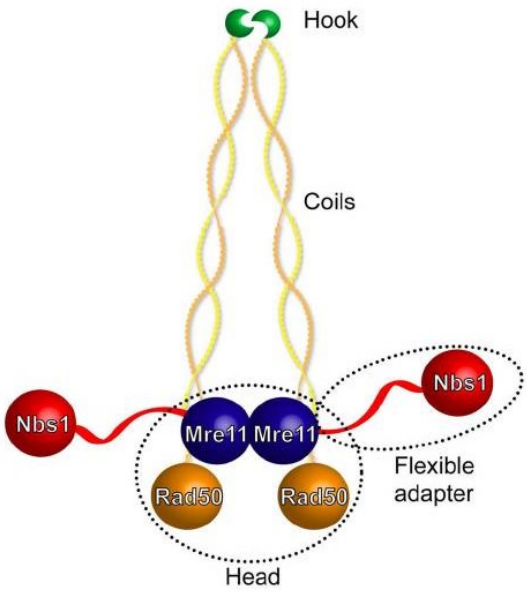

Figure 9. MRN complex structure.
The MRN complex consists of two MRE11, two RAD50 and two Nibrin (NBS1) proteins. The MRE11 and RAD50 proteins make a head of the complex. RAD50 is reaching out of the head as a coiled-coil tail and terminates with a zinc hook. Nibrin protein forms a flexible adapter (*116*).

The RAD50 protein contains two globular ATPase/DNA binding domains interacting with MRE11 and a coiled-coil structure binding Zn-hook important for the tail-to-tail dimerisation of RAD50. The dimerisation of RAD50 is required for the tethering of DNA ends or sister chromatids (*118, 119*). The ATPase activity of RAD50 drives conformational changes of the MRN complex from a closed state (ATP binding), which recognise DDSBs and tethers DNA ends, to an open state (ATP hydrolysis) with exposed MRE11 nuclease active sites and the processing of DDSBs (*117, 120*).

MRE11 has dual ssDNA endonuclease and 3´-5´ double strand DNA (dsDNA) exonuclease activities, a RAD50 interaction site and two DNA binding domains (*121*).

Nibrin is a scaffold protein responsible for the nuclear localisation of the MRN complex and its indirect recruiting to DDSB sites. In the absence of Nibrin, the remaining MRE11/RAD50 complex stays in cytoplasm (*122, 123*).

1.3.2.2 MRN Complex Function during DDSBs Repair

The MRN complex plays an important role in the initial processing of DDSBs before repairing by HR or NHEJ. The MRN complex also participates in activating the checkpoint kinase ATM in response to DNA damage.

Upon DDSBs, ATM phosphorylates all three members of the MRN complex along with hundreds of other ATM substrates important as effectors of the DDSB response, like BRCA1 and histone H2AX at the surrounding chromatin. A phosphorylated MRN complex acts in a positive feedback loop and maintains ATM activity (*114, 124-126*).

1.3.2.3 Other MRN Complex Functions

DDSBs are also formed during the meiotic recombination of homologous chromosomes and are processed by the MRN complex. This could be essential for embryonic development and cell viability and thus explain embryo lethality after the depletion of the MRN complex proteins (*127*).

The MRE11 conformations distinguish between binding to 2-ended breaks – DDSBs (activating ATM signalling) and binding to 1-ended breaks – stalled replication forks (activating ATR signalling). The MRN complex is thus capable to repair ssDNA breaks from collapsed replication forks (*116, 128*).

Another MRN complex function is the maintenance of telomeres. During the S phase, Nibrin interacts with TRF2 at telomeres. After Ser432 CDK2 phosphorylation during the S/G2 phase, Nibrin dissociates, hence TRF2 can protect telomeric ends (*112*).

1.3.3 *NBN* Mutations and Associated Diseases

1.3.3.1 Nijmegen Breakage Syndrome (NBS)

Biallelic mutations of *NBN* lead to a chromosome instability syndrome called Nijmegen breakage syndrome (NBS). NBS is an autosomal recessive disorder characterised by high sensitivity to IR (ionising radiation), a high number of DDSBs and a high frequency of malignancies. NBS patients often feature microcephaly, stunted growth, mental deficiency, immunodeficiency and chromosomal instability. The primary cause of death among NBS patients is cancer of lymphoid origin – especially non-Hodgkin lymphoma. Over 40% of patients develop a malignant disease by the age of 20 (*129, 130*).

The majority of NBS patients have a biallelic recurrent Slavic founder mutation, c.657_661del (p.Lys219AsnfsTer16). This mutation is localised between the BRCT domains and results in the expression of two shortened proteins of 26 kDa and 70 kDa. The 70 kDa protein is associated with the MRN complex (*131*). Another mutation was described in NBS twins heterozygous for c.657_661del and c.643C>T (p.Arg215Trp) mutations. Variant c.643C>T reduces stability of the protein and the level of ATM phosphorylation (*132*). The frequency of diagnosed NBS patients in the Czech Republic is 1/271,000. The frequency of NBS in non-Slavic populations is unknown (*133*).

The frequency of *NBN* mutations among randomly-selected Czech new-borns was calculated at 0.65% (8/1,234) (*133*), which is lower but not significantly different from the frequency among healthy Czech bone marrow donors 1.04% (4/383, p=0.5) (13-64 years old) (*134*).

1.3.3.2 NBN Mutations and Cancer Risk

1.3.3.2.1 Non-Hodgkin Lymphoma

The most frequent diagnosis associated with *NBN* mutations is non-Hodgkin lymphoma (NHL) and the combined frequency of c.657_661del germline mutation among Czech, Polish and Russian patients with NHL is 2.12% (12/566) (*135-138*).

1.3.3.2.2 PDAC

In 2016, two studies suggested *NBN* as a PDAC predisposition gene. Together, the genotyping of Slavic founder mutation c.657_661del in Czech and Polish patients showed a frequency of 2.08% (OR=4.33; 95% CI 2.2-8.56; p=0.0001) (*139, 140*). Recent NGS studies have found a lower frequency of 0.18% in unselected PDAC patients and 0.11% in fPDAC patients, but all of them were performed in non-Slavic populations (Table 4).

Mutations	No of cases	Frequency	Country	Study
Unselected or sporadic PDAC patients; 0.18% (10/5,727)				
1	96	1.04%	USA	(*67*)
0	190	–	USA	(*68*)
0	385	–	Aus/USA/Italy	(*69*)
0	176	–	USA	(*70*)
0	298	–	USA	(*72*)
2	437	0.46%	USA, Canada, Aus	(*73*)
4	3,030	0.13%	USA	(*74*)
2	552	0.36%	USA	(*75*)
0	274	–	USA	(*76*)
1	289	0.35%	USA	(*77*)
fPDAC patients; 0.11% (1/885)				
0	1	–	USA	(*28*)
0	2	–	USA	(*11*)
0	5	–	Canada	(*78*)
0	638	–	USA	(*79*)
0	54	–	Japan	(*80*)
1	185	0.54%	USA	(*81*)

Table 4. Overview of *NBN* germline mutations found in NGS studies of PDAC patients.
Aus – Australia; fPDAC – familial PDAC.

1.3.3.2.3 Associations with Other Cancers

NBN is now considered an intermediate-risk BC susceptibility gene (*141*). A meta-analysis concerning the frequency of c.657_661del mutation carriers among BC patients showed OR=2.66 (95% CI 1.82-3.90) (*142*). Gao et al. (*143*) analysed c.657_661del mutation frequency in 60 articles in several cancer types and found OR=2.51 (95% CI 1.68-3.73) for BC and OR=5.87 (95% CI 2.51-13.75) for prostate cancer (*143*).

The frequency of *NBN* germline mutations in OCs ranges from 0.12% in Susswein et al. (*68*) up to 0.47% in the Norquist et al. (*84*) NGS study (9/1,915; OR=2.3; 95% CI 0.99-5.4).

Pearlman et al. (*144*) tested the association of *NBN* mutations with colorectal cancer by NGS sequencing and found no germline mutation in *NBN* among 450 early-onset colorectal cancer patients. In the Czech population, three variants were found in 771 colorectal cancer patients (0.40%), but the frequency did not differ from the control group (5/1,432, 0.35%) (*145*).

In German melanoma patients, a 0.72% frequency of *NBN* germline mutations was revealed (1/376) (*146*). A United States multi-cancer study did not find any germline mutation of the *NBN* gene in endometrial, colon, stomach or PDAC cancers (*68*).

1.3.3.2.4 Characteristics of Tumour Tissues from Patients with *NBN* Mutations

The loss of WT allele among *NBN* mutation carriers has not been broadly studied. Cybulski et al. (*147*) observed 7 LOH events out of 8 prostate cancer patients with the *NBN* c.657_661del mutation in Poland. Among five Russian BC patients with c.657_661del, a loss of WT allele was displayed in three tumour tissues (*148*).

2 Aims of the Study

The genetic background of PDAC is highly heterogeneous and the genetic basis of a majority of familial PDAC cases has not been explained yet. Identification of inherited forms of a disease in patients enables precise decision about treatment strategies and subsequent management and specialised prevention and early diagnostics in their families.

This work focused on unravelling of the genetic background in unselected PDAC patients in the Czech Republic, addressing few partial goals:

- Examine the importance of the *PALB2* gene germline mutations among unselected PDAC patients in the Czech Republic.
- Examine the importance of the *NBN* gene recurrent Slavic mutation among unselected PDAC patients in the Czech Republic.
- Characterise the prevalence and spectrum of mutations in known and candidate PDAC predisposition genes using NGS.
- Evaluate the genetic involvement in the development of secondary malignancies in long-term PDAC survivors.
- Determine the pathogenicity of selected *PALB2* missense variants with functional analysis.

3 Methods

3.1 Mutation Analysis of the *PALB2* Gene in Unselected Pancreatic Cancer Patients in the Czech Republic

3.1.1 PDAC Patients and Controls Included in the *PALB2* Study

A cohort of 152 unselected histopathologically-verified PDAC patients with origin from the Czech Republic (National Institute of Public Health in Prague) was analysed. Patients were diagnosed between the years of 2004 and 2012, median age at diagnoses was 63 years (40-82 years), and 59 patients (38.82%) were females. Germline DNA was isolated from peripheral blood samples collected into EDTA containing tubes by Wizard Genomic DNA Purification System (Promega) following the manufacturer´s instructions. Identified germline variants were confirmed from an independent blood sample.

Control cohort consisted of 756 non-cancer individuals and 470 blood donors of Czech origin. Genotyping of control group was performed previously by Janatova et al. (*61*).

3.1.2 Polymerase Chain Reaction

PALB2 exons 4, 5, and 6 (66.70% of the *PALB2* sequence) were amplified by polymerase chain reaction (PCR) and subsequently Sanger sequenced (Chapter 3.1.4). PCR was performed by FastStart LA Taq DNA Polymerase (Roche) according the protocol in Table 5 with primers listed in Table 6.

ddH_2O	7.52 µl	
PCR Reaction Buffer with 20mM $MgCl_2$ 10x	1 µl	
dNTP (10 mM)	0.2 µl	
Primer Forward (30 pmol/µl)	0.1 µl	
Primer Reverse (30 pmol/µl)	0.1 µl	
DNA (0.1 µg/µl)	1 µl	
FastStart LA Taq DNA Polymerase (5 U/µl)	0.08 µl	
95°C	5 minutes	
95°C	30 seconds	40x
60°C	30 seconds	
72°C	1 minute	
72°C	7 minutes	

Table 5. PCR amplification of DNA.

Name	Sequence 5´-3´	Tm (°C)
PB2_4AF	TCATCTGCCTGAATGAAATGTCAC	55.6
PB2_4HR	ACTTGGCCCTGTCACTTTTTAGA	56.1
PB2_5AF	TGTTGGGTTTTGTTACTATTTTGTGAC	54.9
PB2_5CR	GCAAGTCATGCTGTTTACATTCAC	55.4
PB2_6F	AGTGGGTAATGCAGGCAGA	55.1
PB2_6R	CATATGTAAGACACGAGACACTGG	55.0

Table 6. List of PCR primers for exons 4, 5, and 6 of the *PALB2* gene.

3.1.3 Agarose Gel Electrophoresis

The efficiency of PCR was controlled by electrophoresis on 1% agarose gel (UltraPure Agarose, Gibco). To visualise DNA fragments GelRed Nucleic Acid Gel Stain 10.000x (Biotium) was added to the gel and the lengths of fragments were compared to GeneRuler DNA Ladder Mix (Thermo Scientific).

3.1.4 Sanger Sequencing

Successfully amplified PCR reactions were then processed by ExoSAP-IT (USB Corp.) to degrade remaining PCR primers and nucleotides (Table 7). Purified PCR products underwent sequencing reaction with BigDye Terminator v3.1 cycle sequencing kit (Applied Biosystems, Table 8). The long exons 4 and 5 were sequenced in two overlapping fragments. The same PCR primers were used for sequencing as well. Products of sequencing reaction were precipitated and dissolved in HiDi Formamide (Applied Biosystems, Table 9). The ABI Prism 3130 genetic analyser (Applied Biosystems) was used for the analysis. Raw data were processed by Sequencing Analysis v.2.5.5 software (Applied Biosystems) and visualised in FinchTV (Geospiza, Figure 10).

ExoSAP-IT	0.6 µl
ddH_2O	1.2 µl
PCR reaction	1 µl
37°C	15 minutes
80°C	15 minutes

Table 7. Degradation of redundant primers and nucleotides by ExoSAP-IT.

ExoSAP-IT reaction	2.8 µl	
ddH_2O	0.8 µl	
BigDye Terminator Sequencing Buffer 5x (MCLAB)	1 µl	
Sequencing Primer (30 pmol/µl)	0.2 µl	
BigDye Ready Reaction Premix	0.4 µl	
96°C	1 minute	
96°C	10 seconds	25x
50°C	5 seconds	
60°C	4 minutes	

Table 8. Sequencing reaction with BigDye Terminator.

BigDye reaction	5.2 µl
EDTA (0.125M)	1.3 µl
NaAc (3M)	1.3 µl
Ethanol (100%)	30 µl
Centrifugation	20 minutes, 4°C, 3000 rpm
Discarding supernatant	
Ethanol (70%)	50 µl
Centrifugation	20 minutes, 4°C, 3000 rpm
Discarding supernatant	
95°C	5 minutes
Drying	20 minutes, RT
HiDi Formamide (Applied Biosystems)	12 µl
95°C	5 minutes

Table 9. Precipitation of sequencing reaction.

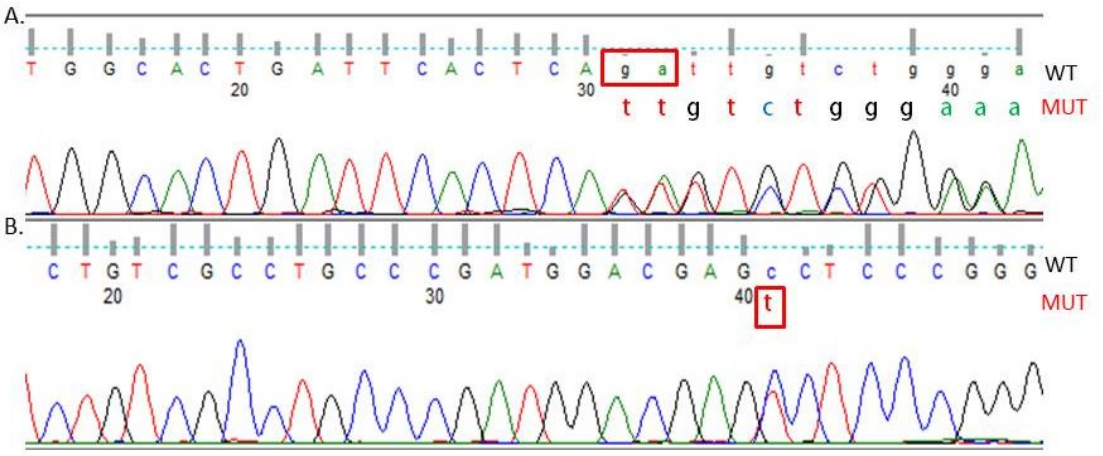

Figure 10. An example of electrophoretograms of *PALB2* sequencing visualised in FinchTV.

A. The frame-shift *PALB2* mutation c.509_510del.

B. The missense *PALB2* mutation c.10C>T.

3.1.5 High Resolution Melting Analysis

Remaining ten *PALB2* exons were screened using high resolution melting (HRM) analysis. After a PCR amplification of DNA in the presence of fluorescent intercalating dye the resulting reaction is gradually melted and a melting curve is acquired (primers listed in Table 12). While the DNA denatures with the increasing temperature the fluorescence signal decreases depending on the sequence of the PCR product. Thus a PCR product with a mutation displays a different melting profile. HRM analysis was performed with HOT FirePol EvaGreen HRM Mix (Solis BioDyne) on Light Cycler 480 (Roche, Table 10 and Table 11). Melting profiles were evaluated at LightCycler 480 Software ver. 1.5.0 SP4 (Roche, Figure 11). Identified variants were confirmed by Sanger sequencing from independent PCR reaction.

ddH_2O	4.44 µl	
HOT FirePol EvaGreen HRM Mix 5x	1.2 µl	
Primer Forward (30 pmol/µl)	0.03 µl	
Primer Reverse (30 pmol/µl)	0.03 µl	
DNA (0.1 µg/µl)	0.4 µl	
95°C	15 minutes	
95°C	15 seconds	55x
60°C	20 seconds	
72°C	25 seconds	

Table 10. Protocol of HRM analysis PCR reaction with HOT FirePol EvaGreen HRM Mix.

Temperature	Time	Ramp rate (°C/s)
95°C	1 minute	4.8
40°C	1 minute	2.5
68°C	1 second	1
Continuous up to 95°C	Acquiring 25x per 1°C	0.02
40°C	10 seconds	2.5

Table 11. Conditions for acquiring melting curves during HRM analysis.

Name	Sequence 5´-3´	Tm (°C)
PB2_1F	GGCTGCTCTTTTCGTTCTGTC	56.2
PB2_1R	GACACAAAGCCAGGCCTAAA	54.8
PB2_2F	GACTCCACCTTTCCACTTGC	55.2
PB2_2R	GAGACAAAAACAGCCCCAGAAA	55.4
PB2_3F	AGAAAACGTATTTCTGGGGCTG	55.1
PB2_3R	CAATAGCCAAAATATACCTGGGAAATG	54.6
PB2_7F	TGCTTTGCATAAAACAGCACTC	54.6
PB2_7R	TGGTAAGCTGCCCATCTACA	54.7
PB2_8F	ACCAAGCATAATTTTTGGCTGC	54.8
PB2_8R	TGCACTTAAAACCAGCTGACA	54.6
PB2_9F	ATTAAAAGGTTACTCCTCACATCACC	54.8
PB2_9R	TTACCCAACTTTCTCTGAAACCTG	54.8
PB2_10F	CCTAGAGACTGCTTTAGTGCAAAG	55.4
PB2_10R	CTACAGATGAGGGAACTGAGGAC	55.6
PB2_11F	GTTTGTTGGAAGAATGTGATCAGC	55.1
PB2_11R	CTGCTTATGACTTACTGCTCTCAC	55.2
PB2_12F	GTTTGGTTTTTGTCTCTGCCAG	54.8
PB2_12R	GTGTTTGCACAGTGCCTTTC	54.9
PB2_13F	TTTGGATATGTAATCTGAATTATATCTTCTTTG	53.0
PB2_13R	AGGCCCAATATATCCAGAAAATTG	53.0

Table 12. Primers used for HRM analysis of *PALB2* exons.

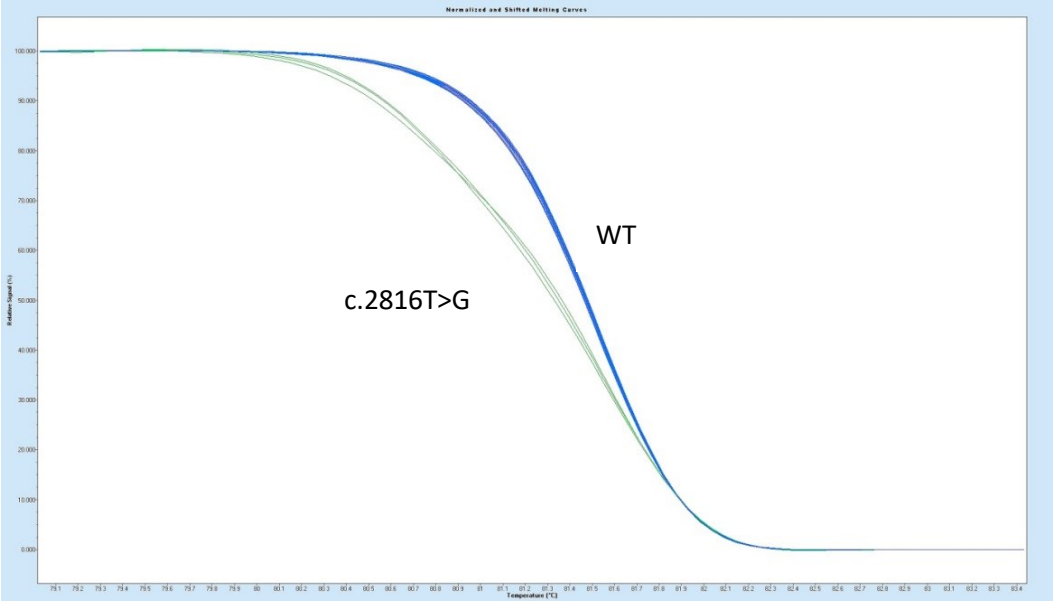

Figure 11. An example of melting curves from HRM Analysis showing three carriers of *PALB2* mutation c.2816T>G (green).

3.1.6 Multiplex Ligation-dependent Probe Amplification

Multiplex ligation-dependent probe amplification (MLPA) analysis is a tool for detecting copy number variations (CNVs) of one or more exons of an analysed gene. PCR reaction results in amplicons of unique length for each exon. These products are denaturated in HiDi Formamide (Applied Biosystems) and separated by capillary electrophoresis on ABI Prism 3130 genetic analyser (Applied Biosystems). The relative intensity for every exon is compared with reference samples and

duplication or deletion of exons can be determined in Coffalyzer software (MRC-Holland, Figure 12). The SALSA MLPA probe mix P260 (MRC-Holland) was used to analyse CNVs of *PALB2* gene (Table 13Table 14).

DNA (0.1 µg/µl)	1 µl	
ddH_2O	1.5 µl	
98°C	5 minutes	
25°C	Pause	
SALSA MLPA Buffer	0.75 µl	
Probemix P260	0.75 µl	
95°C	1 minute	
60°C	Overnight	
54°C	Pause	
ddH_2O	12.5 µl	
Ligase Buffer A	1.5 µl	
Ligase Buffer B	1.5 µl	
SALSA Ligase-65	0.5 µl	
54°C	15 minutes	
98°C	5 minutes	
20°C	Pause	
ddH_2O	3.75 µl	
SALSA PCR Primer Mix	1 µl	
SALSA Polymerase	0.25 µl	
95°C	30 seconds	35x
60°C	30 seconds	
72°C	1 minute	
72°C	20 minutes	

Table 13. MLPA analysis procedure with SALSA MLPA probe mix P260 for *PALB2* gene.

MLPA reaction	1 µl
GeneScan 600 Liz Size Standard (Applied Biosystems)	0.4 µl
HiDi Formamide (Applied Biosystems)	9 µl
95°C	2 minutes
Cooling on ice	

Table 14. Preparation of MLPA sample for capillary electrophoresis.

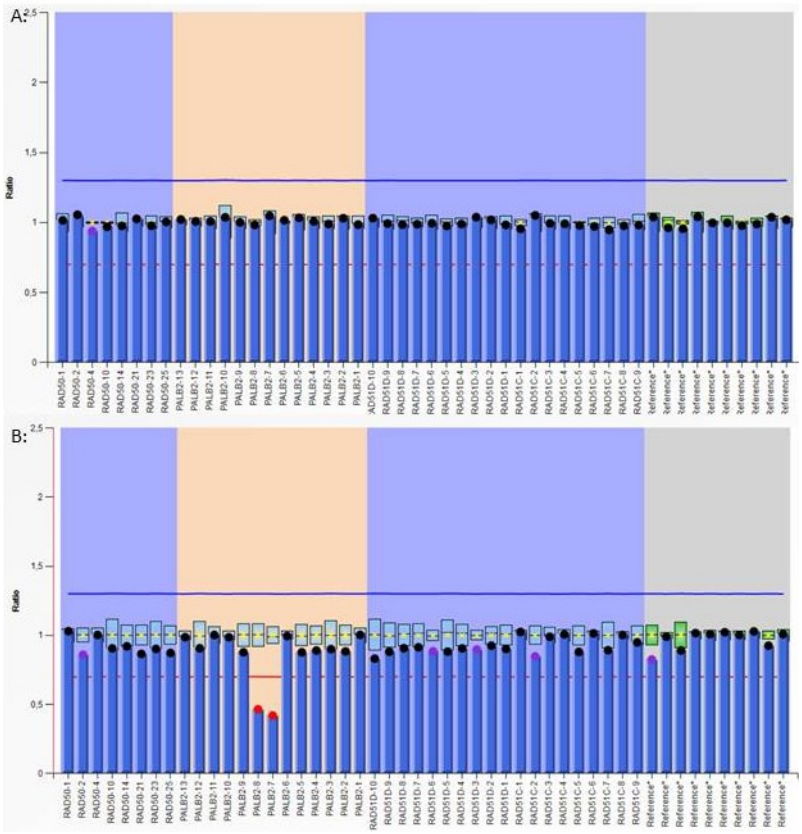

Figure 12. An example of MLPA results visualised in the Coffalyzer software.
The SALSA MLPA probe mix P260 includes probes for PALB2, RAD51D, and RAD51C.
A. The PALB2 WT sequence.
B. The PALB2 heterozygous deletion of exons 7 and 8 found previously by Janatova el al. (*61*).

3.1.7 Variant Prioritisation of *PALB2* Single Nucleotide Variants

Frame-shift, stop-gain and consensus splice-site (±1/2) variants were considered as pathogenic. Missense variants were filtered according to the frequency in Exome aggregation consortium database (ExAC) (http://exac.broadinstitute.org/). Their pathogenicity was evaluated by seven prediction programs: Sorting tolerant from intolerant (SIFT), PolyPhen-2 (PP-2), Mutation assessor (MA), Phylop, Genomic evolutionary rate profiling (GERP), Combined annotation dependent depletion (CADD) scaled score, and Spidex (Table 15). Variant with at least six predictions exceeding the thresholds limits were considered potentially pathogenic.

Prediction program	Thresholds	Website
SIFT	≤0.05	http://sift.jcvi.org/
PP-2	≥0.85	http://genetics.bwh.harvard.edu/pph2/
MA	≥1.9	http://mutationassessor.org/r3/
Phylop	≥0	http://compgen.cshl.edu/phast/background.php
GERP	≥2	http://mendel.stanford.edu/SidowLab/downloads/gerp/
CADD scaled score	≥15	http://cadd.gs.washington.edu/
Spidex	>|2|	http://tools.genes.toronto.edu/

Table 15. List of prediction tools, their thresholds, and websites used for prioritisation of variants.

3.1.8 Statistical Analysis

Fisher's exact test was used to compare frequencies of carriers between cases and controls. Mann-Whitney test was used to calculate levels of significance for age-related analysis. A p-value less than 0.05 was considered statistically significant.

3.2 The c.657_661del Variant in the *NBN* Gene Predisposes to Pancreatic Cancer

3.2.1 PDAC Patients and Controls Included in the *NBN* Study

Genotyping of a Slavic founder mutation c.657_661del in the *NBN* gene was executed on a cohort of 241 unselected PDAC patients of Czech origin – 152 patients (59 females, 38.82%) from the National Institute of Public Health and 89 patients (49 females, 55.06%) from the Department of Oncology, General University Hospital in Prague. Median age at diagnosis was 63 (ranged 40-82) and 64 (ranged 38-84) respectively. Germline DNA was isolated from peripheral blood samples and collected into EDTA containing tubes by Wizard Genomic DNA Purification System (Promega) following the manufacturer´s instructions. Identified variants were confirmed from an independent blood sample.

Control cohort consisted of 915 non-cancer individuals of Czech origin and genotyping of *NBN* exon 6 in controls was completed previously by Mateju et al. (*149*).

3.2.2 High Resolution Melting Analysis

Genotyping of *NBN* exon 6 (Figure 13) was performed by HRM analysis (Chapter 3.1.5) with primers listed in Table 16. Potential mutations were confirmed by Sanger sequencing from an independent PCR reaction (Chapters 3.1.2-3.1.4).

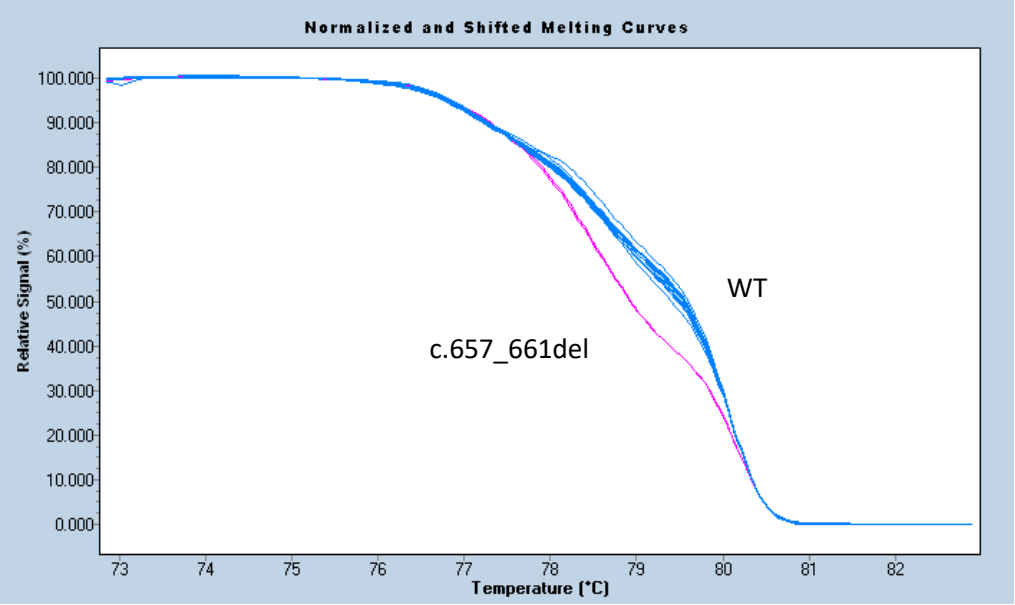

Figure 13. An example of *NBN* exon 6 HRM Analysis showing two carriers of c.657_661del mutations (pink).

Name	Sequence 5´-3´	Tm (°C)
NBN_6F	CAGATAGTCACTCCGTTTACAA	51.8
NBN_6R	CCCAAAATGAAATACGTTAACAAC	51.6

Table 16. Primers used for HRM analysis of *NBN* exon 6.

3.2.3 DNA Isolation from Paraffin Fixed Tumour Tissue

One sister of the *NBN* mutation carrier suffered from gastric cancer and her tumour tissue was available for further DNA analysis. Isolation of DNA from FFPE (formaldehyde fixed-paraffin embedded) tumour tissue was performed using the Cobas DNA Sample Preparation Kit (Roche) according to manufacturer´s instructions. PCR and Sanger sequencing were used to confirm the mutation (Chapters 3.1.2-3.1.4).

3.2.4 Statistical Analysis

Statistical analysis was calculated with the same method like in Chapter 3.1.8.

3.3 Germline Multi-gene Panel Testing in PDAC Patients

3.3.1 Patients and Controls Included in the PDAC Study

A distinct cohort of 113 unselected PDAC patients was analysed in the ongoing project of portraying the landscape of hereditary mutations contributing to PDAC risk. Patients of Czech origin were diagnosed with PDAC between the years 2005-2018 (one patient 1997) and collected in our laboratory. In case of positive cancer family history, patients were categorised into three groups (Table 17) – familial PDAC group, families with history of both PDAC and HBOC, and multiple cancer families.

(1) Familial PDAC (fPDAC) group was defined according to Stoffel et al. (*150*) as: (A) two first-degree relatives suffered from PDAC, (B) at least three relatives from one side of family were diagnosed with PDAC or (C) patient meet the criteria for other genetic syndromes associated with PDAC (*150*). Families which did not meet the criteria for fPDAC were further divided into (2) PDAC with hereditary breast and/or ovarian cancer (PDAC+HBOC) in the family history or (3) multiple cancer families (MCF) with family history without BC and OC.

Non-cancer control cohort consists of 766 Czech origin individuals ≥60 years old without personal or family cancer history in first-degree relatives. Control group consists of 78 males and 538 females and was analysed within other research project in our laboratory (*85*).

	PDAC patients (N=113)	
	N	**%**
Gender		
Females	61	53.98
Males	52	46.02
Median age at diagnosis	All 64.0 (39-92.6)	
Year (range)	Females 63.5 (39-79)	
	Males 64.2 (40-92.6)	
Age at diagnosis categories		
<50	13	11.51
50-54.9	11	9.73
55-59.9	21	18.58
60-64.9	17	15.04
65-69.9	29	25.66
70-74.9	16	14.16
75-79.9	3	2.66
80-84.9	2	1.77
85-89.9	–	–
90-94.9	1	0.89
Localisation		
Head of pancreas	68	60.18
Body of pancreas	16	14.16
Tail of pancreas	16	14.16
NA	13	11.50
Grade		
1	5	4.43
2	25	22.12
3	26	23.01
NA	57	50.44
Personal history		
Breast cancer	2	1.77
Ovarian cancer	2	1.77
Ovarian and breast cancer	1	0.89
Male breast cancer duplicity	1	0.89
Endometrial cancer	1	0.89
Kidney cancer	1	0.89
Urinary bladder cancer	1	0.89
Lymphoma	1	0.89
PDAC only	100	88.50
NA	3	2.66
Family history		
fPDAC	15	13.27
PDAC+HBOC	22	19.47
MCF	42	37.17
Negative	31	27.43
NA	3	2.66

Table 17. PDAC patient's clinical and histopathological characteristics.
NA – not available.

3.3.2 Next Generation Sequencing

Next generation sequencing (NGS) was performed with a CZECANCA v.1.0 (Czech cancer panel for clinical application) custom panel designed in our laboratory. This panel targets coding sequences and exon-intron junctions of 219 genes (NimbleGen Seq-Cap EZ Choice; Roche) (*151*). These genes include known cancer-susceptibility genes associated with various hereditary cancer syndromes and other candidate cancer predisposing genes participating in DNA repair and cell cycle control (Table 18). The final panel target size reached 328,069 bases.

AIP; ALK; APC; APEX1; ATM; *ATMIN (86%);*ATR; ATRIP; AURKA; AXIN1; BABAM1; BAP1; BARD1; BLM; BMPR1A; BRAP; BRCA1; BRCA2; BRCC3; BRE; BRIP1; BUB1B; C11orf30; C19orf40; CASP8; CCND1; CDC73; CDH1; CDK4; CDKN1B; *CDKN1C (68%);* CDKN2A; CEBPA; CEP57; CLSPN; CSNK1D; CSNK1E; CWF19L2; CYLD; DCLRE1C; DDB2; *DHFR (85%)*; DICER1; DMC1; DNAJC21; DPYD; EGFR; EPCAM; EPHX1; ERCC1; ERCC2; ERCC3; ERCC4; ERCC5; ERCC6; ESR1; ESR2; EXO1; EXT1; EXT2; EYA2; EZH2; FAM175A; FAM175B; FAN1; FANCA; FANCB; FANCC; FANCD2; *FANCE (95%);* FANCF; FANCG; FANCI; FANCL; FANCM; FBXW7; FH; FLCN; GADD45A; GATA2; GPC3; GRB7; HELQ; HNF1A; HOXB13; HRAS; HUS1; CHEK1; *CHEK2 (77%)*; KAT5; KCNJ5; KIT; LIG1; LIG3; LIG4; LMO1; LRIG1; MAX; MCPH1; *MDC1 (67%)*; MDM2; MDM4; MEN1; MET; MGMT; MLH1; MLH3; MMP8; MPL; MRE11A; MSH2; MSH3; MSH5; MSH6; MSR1; MUS81; MUTYH; NAT1; NBN; NCAM1; NELFB; *NF1 (84%*); NF2; *NFKBIZ (98%)*; NHEJ1; NSD1; OGG1; PALB2; PARP1; PCNA; PHB; PHOX2B; PIK3CG; PLA2G2A; PMS1; POLB; POLD1; *POLE (99%);* PPM1D; PREX2; PRF1; PRKAR1A; PRKDC; PTEN; PTCH1; PTTG2; RAD1; RAD17; RAD18; RAD23B; RAD50; RAD51; RAD51AP1; RAD51B; RAD51C; RAD51D; RAD52; RAD54B; RAD54L; RAD9A; RB1; RBBP8; RECQL; *RECQL4 (98%)*; RECQL5; *RET (98%);* RFC1; RFC2; RFC4; RHBDF2; RNF146; RNF168; RNF8; RPA1; RUNX1; SDHAF2; SDHB; SETBP1; SETX; SHPRH; SLX4; SMAD4; SMARCA4; SMARCB1; SMARCE1; STK11; SUFU; TCL1A; TELO2; TERF2; *TERT (94%);* TLR2; TLR4; TMEM127; TOPBP1; TP53; TP53BP1; TSC1; TSC2; TSHR; UBE2A; UBE2B; UBE2I; UBE2V2; UBE4B; UIMC1; VHL; WRN; WT1; XPA; XPC; XRCC1; XRCC2; XRCC3; XRCC4; XRCC5; XRCC6; ZNF350; ZNF365

Table 18. List of 219 CZECANCA panel genes.
Genes in italics are not fully covered; the percentage of targeted sequence is in brackets.

The workflow of NGS experiments is shown in Figure 14. During library preparation genomic DNA is ultrasonically fragmented and ligated with adapters called i5 and i7. Adapters include P5 and P7 sequences complementary to ligation mediated PCR (LM-PCR) primers used to amplify DNA sample library. These primers contain indexes which serve to tag individual samples and to allow pooling. The sample library is then hybridised with CZECANCA panel probes to capture target sequences. After their recovering, the captured DNA is amplified by second LM-PCR. If the resulting library meets all the quality control criteria experiment proceeds to a preparation of sequencing sample and sequencing on MiSeq System platform.

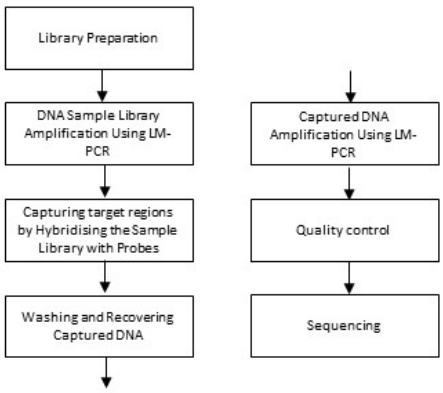

Figure 14. The NGS workflow from genomic DNA to sequencing sample.

3.3.2.1 Library Preparation

One run of NGS with CZECANCA panel was typically composed of 30 DNA samples. Fragmented samples were treated with KAPA HTP Library Preparation Kit (Roche) according to workflow in Figure 15. Sheared genomic DNA was blunt-ended (End Repair) and dAMP was added at 3´ends (A-tailing). A fork shaped DNA adapters were ligated to 3´-A-Tailed ends (Adaptor Ligation; Table 19-Table 26). AMPure XP magnetic beads (Beckmann Coulter) were used repeatedly for purifying fragments. Double-sided size selection on AMPure XP magnetic beads (Beckmann Coulter) served to obtain fragments of an ideal length about 250-450 bp (Table 27).

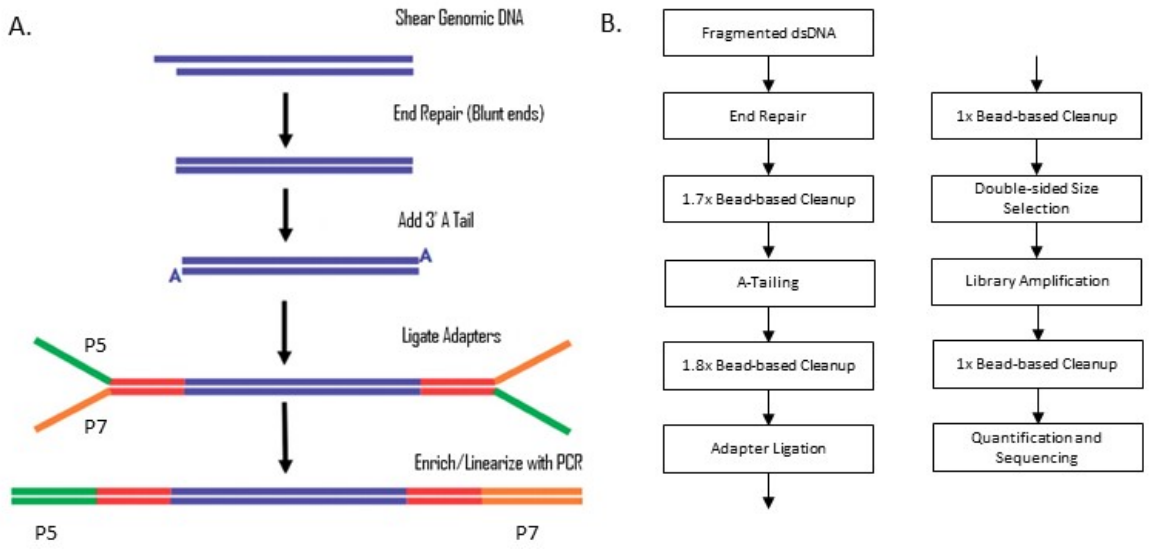

Figure 15. The library preparation and amplification workflow.

A. A graphic illustration of library preparation. Fork shaped adapters are in red/green/orange colour. Green and orange represent P5 and P7 primers´ recognition sites. Red represents sequencing primers´ recognition site. Adapted from http://tucf-genomics.tufts.edu/home/faq.
B. KAPA HTP Library Preparation Kit workflow. Adapted from KAPA HTP Library Preparation Kit manual.

DNA Shearing

A 500 ng of each genomic DNA sample was diluted separately in a total volume of 53 µl of low TE buffer (10 mM Tris-HCl, 1 mM EDTA, pH 8) and ultrasonically sheared by Covaris E220 model (Covaris Inc) to fragments of medium length 200 bp.

End Repair and Cleanup

Fragmented DNA	50 µl
End Repair Buffer 10x (KAPA)	7 µl
End Repair Enzyme Mix (KAPA)	5 µl
ddH_2O	8 µl
20°C	30 minutes

Table 19. End repair of sheared DNA samples by KAPA HTP Library Preparation Kit (Roche).

End repair reaction	70 µl	
AMPure XP Magnetic Beads	120 µl	
RT	5 minutes	
Placing tubes on magnet		
Discarding supernatant		
Ethanol (80%)	190 µl	2x
RT	30 seconds	
Discarding the ethanol		
Drying ethanol	3-4 minutes	
Removing from magnet		

Table 20. Cleanup of end repair reaction with AMPure XP Magnetic Beads.

A-Tailing and Cleanup

AMPure Beads with End repaired DNA	–
A-Tailing Buffer 10x (KAPA)	5 µl
A-Tailing Enzyme (KAPA)	3 µl
ddH_2O	42 µl
30°C	30 minutes

Table 21. A-Tailing of end repaired DNA by KAPA HTP Library Preparation Kit (Roche).

A-Tailing reaction	50 µl	
20% PEG/NaCl Solution (KAPA)	90 µl	
RT	5 minutes	
Placing tubes on magnet		
Discarding supernatant		
Ethanol 80%	190 µl	2x
RT	30 seconds	
Discarding the ethanol		
Drying ethanol	3-4 minutes	
Removing from magnet		

Table 22. Cleanup of A-Tailing reaction with AMPure XP Magnetic Beads.

Adapter Ligation and Cleanup

Name	Sequence 5´-3´
i5_Adapter	ACACTCTTTCCCTACACGACGCTCTTCCGATC*T
i7_Adapter	pGATCGGAAGAGCACACGTCTGAACTCCAGTCAC

Table 23. Sequences of i5 and i7 Adapters.
* – phosphothiolate bond; p – 5´phosphate.

i5_Adapter (100 pmol/µl)	20 µl	
i7_Adapter (100 pmol/µl)	20 µl	
Tris:NaCl Buffer Mix (50 mM Tris:HCl pH 7.5; 50 mM NaCl)	10 µl	
97°C	2 minutes	
97°C (-1°C per cycle)	1 minute	72x
25°C	5 minutes	
Tris:NaCl Buffer Mix	26.6 µl	
ddH_2O	57 µl	

Table 24. Preparation of forked iAdapter_Work Solution (15 µM).

AMPure Beads with A-Tailed DNA	-
Ligation Buffer 5x (KAPA)	10 µl
iAdapter_Work Solution (15 µM)	3.5 µl
DNA Ligase (KAPA)	5 µl
ddH_2O	31.5 µl
20°C	15 minutes

Table 25. Adapter ligation to A-Tailed DNA by KAPA HTP Library Preparation Kit (Roche).

Adapter ligation reaction	50 µl	
20% PEG/NaCl Solution (KAPA)	50 µl	
RT	5 minutes	
Placing tubes on magnet		
Discarding supernatant		
Ethanol 80%	190 µl	2x
RT	30 seconds	
Discarding the ethanol		
Drying ethanol	3-4 minutes	
Removing from magnet		

Table 26. Cleanup of adapter ligation reaction with AMPure XP Magnetic Beads.

Double-sided Size Selection

AMPure Beads with adapter-ligated DNA	–	
Elution Buffer (10mM Tris-HCl, pH 8.0, no EDTA)	100 µl	
RT	2 minutes	
20% PEG/NaCl Solution (KAPA)	60 µl	
RT	5 minutes	
Placing tubes on magnet		
Transferring 155 µl of supernatant into new tubes		
AMPure XP Magnetic Beads	20 µl	
RT	5 minutes	
Placing tubes on magnet		
Discarding supernatant		
Ethanol 80%	190 µl	2x
RT	30 seconds	
Discarding the ethanol		
Drying ethanol	3-4 minutes	
Removing from magnet		
Elution Buffer	26 µl	
RT	2 minutes	
Placing tubes on magnet		
Transferring 23 µl of supernatant into new tubes		

Table 27. Double-sided size selection of adapter-ligated DNA with AMPure XP Magnetic Beads and KAPA HTP Library Preparation Kit (Roche).

3.3.2.2 Sample Library Amplification

Sample library was amplified by ligation mediated PCR (LM-PCR) using P5 and P7 primers complementary to the adapters ligated to DNA fragments previously (Table 28). These indexing primers carry barcodes (indexes; 8 nucleotides sequences) which were used in unique combination for each DNA sample to distinguish them when pooled together (Table 29-Table 31).

LM-PCR

Sample library	23 µl	
HiFi HotStart ReadyMix 2x (KAPA)	25 µl	
P5 and P7 indexing primers mix (25 µM each)	2 µl	
98°C	45 seconds	
98°C	15 seconds	6x
65°C	30 seconds	
72°C	30 seconds	
72°C	5 minutes	

Table 28. LM-PCR amplification of sample library by KAPA HTP Library Preparation Kit (Roche).

Name	Sequence 5´-3´
P5_D501	AATGATACGGCGACCACCGAGATCTACACTATAGCCTACACTCTTTCCCTACACGACGCTCTTCCGATC*T
P5_D502	AATGATACGGCGACCACCGAGATCTACACATAGAGGCACACTCTTTCCCTACACGACGCTCTTCCGATC*T
P5_D503	AATGATACGGCGACCACCGAGATCTACACCCTATCCTACACTCTTTCCCTACACGACGCTCTTCCGATC*T
P5_D504	AATGATACGGCGACCACCGAGATCTACACGGCTCTGAACACTCTTTCCCTACACGACGCTCTTCCGATC*T
P5_D505	AATGATACGGCGACCACCGAGATCTACACAGGCGAAGACACTCTTTCCCTACACGACGCTCTTCCGATC*T
P7_D701_R	CAAGCAGAAGACGGCATACGAGATCGAGTAATGTGACTGGAGTTCAGACGTGTGCTCTTCCGAT*C
P7_D702_R	CAAGCAGAAGACGGCATACGAGATTCTCCGGAGTGACTGGAGTTCAGACGTGTGCTCTTCCGAT*C
P7_D703_R	CAAGCAGAAGACGGCATACGAGATAATGAGCGGTGACTGGAGTTCAGACGTGTGCTCTTCCGAT*C
P7_D704_R	CAAGCAGAAGACGGCATACGAGATGGAATCTCGTGACTGGAGTTCAGACGTGTGCTCTTCCGAT*C
P7_D705_R	CAAGCAGAAGACGGCATACGAGATTTCTGAATGTGACTGGAGTTCAGACGTGTGCTCTTCCGAT*C
P7_D706_R	CAAGCAGAAGACGGCATACGAGATACGAATTCGTGACTGGAGTTCAGACGTGTGCTCTTCCGAT*C

Table 29. List of P5 and P7 indexing primers for LM-PCR.
* – phosphothiolate bond. Unique 8-nucleotide barcodes are in red.

P5/P7	D701	D702	D703	D704	D705	D706
D501	D501+D701	D501+D702	D501+D703	D501+D704	D501+D705	D501+D706
D502	D502+D701	D502+D702	D502+D703	D502+D704	D502+D705	D502+D706
D503	D503+D701	D503+D702	D503+D703	D503+D704	D503+D705	D503+D706
D504	D504+D701	D504+D702	D504+D703	D504+D704	D504+D705	D504+D706
D505	D505+D701	D505+D702	D505+D703	D505+D704	D505+D705	D505+D706

Table 30. Combinations of P5 and P7 indexes for different DNA samples.

Library Amplification Cleanup

LM-PCR reaction	50 µl	
AMPure XP Magnetic Beads	90 µl	
RT	5 minutes	
Placing tubes on magnet		
Discarding supernatant		
Ethanol 80%	190 µl	2x
RT	30 seconds	
Discarding supernatant		
Drying ethanol	3-4 minutes	
Removing from magnet		
ddH_2O	52 µl	
RT	2 minutes	
Placing tubes on magnet		
Transferring 50 µl of supernatant into new tubes		

Table 31. Cleanup of LM-PCR reaction with AMPure XP Magnetic Beads.

3.3.2.3 Quantity and Quality Control during Preparation

A quantity and quality control of amplified sample library was performed before proceeding to hybridisation. The concentration of each sample after LM-PCR was measured with the Qubit Quantification Platform (Life Technologies) using dsDNA HS Assay Kit following the manufacturer's instructions (ideal concentration 10 ng/µl).

Fragments´ size distribution throughout the sample library preparation was checked in three steps: (1) after DNA shearing, (2) after double-sided size selection and (3) after LM-PCR. Samples were diluted 5x, 2x, and 5x respectively and analysed on Agilent 2100 Bioanalyzer System using the Agilent High Sensitivity DNA Kit (Agilent Technologies, Figure 16).

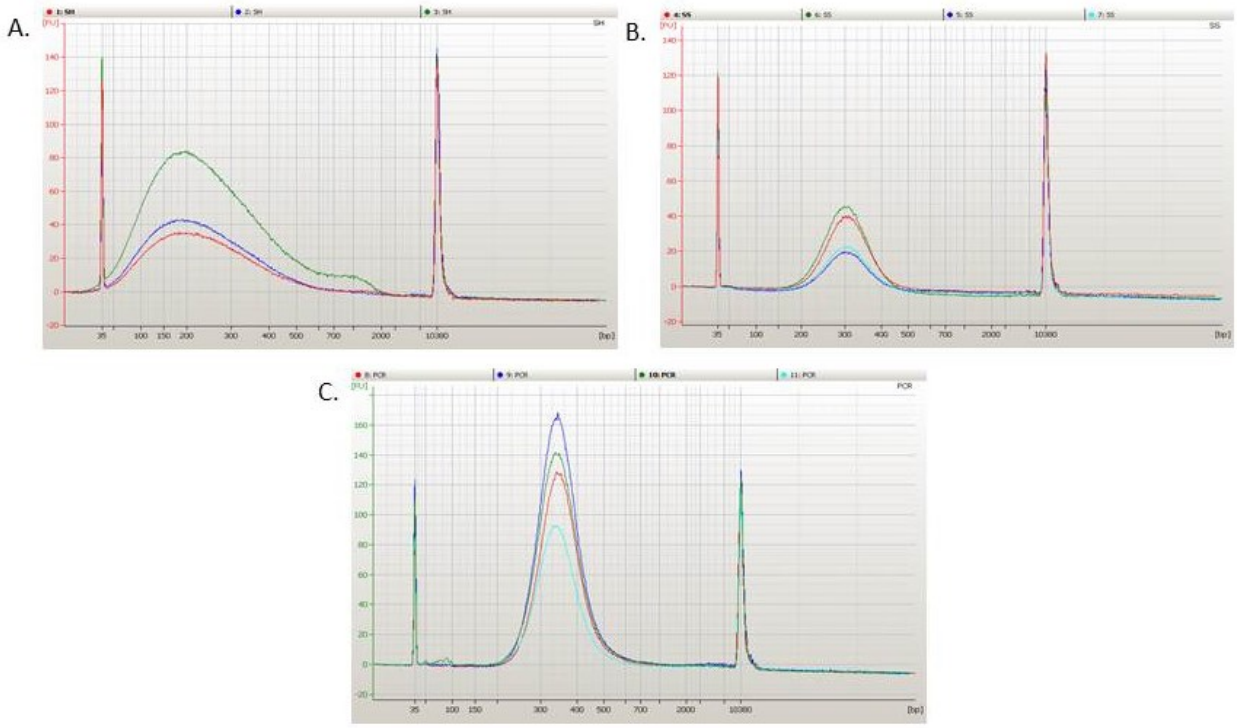

Figure 16. An example of DNA fragments length distribution analysed on Agilent 2100 Bioanalyzer.

A. After fragmentation with the peak at 200bp.
B. After double-sided size selection with the peak at 300 bp.
C. After LM-PCR with the peak at 350 bp.

3.3.2.4 Hybridisation of Amplified Sample Library

Equal amounts of 33 ng of every sample were pooled into one tube (1 µg of DNA in total) together with 5 µl of 1 mg/ml COT Human DNA (Roche) to prevent unspecific hybridisation to repetitive elements and with 2 µl of 1,000 pmol/µl BarBlock Mix – oligonucleotides that blocks indexes´ sequences. The hybridisation and enrichment of targeted regions of the amplified sample library with CZECANCA probes (biotinylated oligonucleotide probes) was performed with NimbleGen SeqCap EZ Hybridization and Wash Kit (Roche, Table 32-Table 33).

Amplified sample library (33 ng of each)	1 µg in total
COT Human DNA (1 mg/ml)	5 µl
BarBlock Mix (1,000 pmol/µl of each)	2 µl
Drying in a DNA vacuum concentrator	60°C
Hybridization Buffer 2X (NimbleGen)	7.5 µl
Hybridization Component A (NimbleGen)	3 µl
Vortexing	10 seconds
Centrifugation	10 seconds
95°C	10 minutes
Centrifugation	10 seconds
CZECANCA probes	4.5 µl
Vortexing	3 seconds
Centrifugation	10 seconds
47°C	64-72 hours

Table 32. Hybridisation of amplified sample library with CZECANCA probes by NimbleGen SeqCap EZ Hybridization and Wash Kit (Roche).

Name	Sequence 5´-3´
block_P5_D501	AATGATACGGCGACCACCGAGATCTACACTATAGCCTACACTCTTTCCCTACACGACGCTCTTCCGATCT
block_P5_D502	AATGATACGGCGACCACCGAGATCTACACATAGAGGCACACTCTTTCCCTACACGACGCTCTTCCGATCT
block_P5_D503	AATGATACGGCGACCACCGAGATCTACACCCTATCCTACACTCTTTCCCTACACGACGCTCTTCCGATCT
block_P5_D504	AATGATACGGCGACCACCGAGATCTACACGGCTCTGAACACTCTTTCCCTACACGACGCTCTTCCGATCT
block_P5_D505	AATGATACGGCGACCACCGAGATCTACACAGGCGAAGACACTCTTTCCCTACACGACGCTCTTCCGATCT
block_P7_D701_R	CAAGCAGAAGACGGCATACGAGATCGAGTAATGTGACTGGAGTTCAGACGTGTGCTCTTCCGATC
block_P7_D702_R	CAAGCAGAAGACGGCATACGAGATTCTCCGGAGTGACTGGAGTTCAGACGTGTGCTCTTCCGATC
block_P7_D703_R	CAAGCAGAAGACGGCATACGAGATAATGAGCGGTGACTGGAGTTCAGACGTGTGCTCTTCCGATC
block_P7_D704_R	CAAGCAGAAGACGGCATACGAGATGGAATCTCGTGACTGGAGTTCAGACGTGTGCTCTTCCGATC
block_P7_D705_R	CAAGCAGAAGACGGCATACGAGATTTCTGAATGTGACTGGAGTTCAGACGTGTGCTCTTCCGATC
block_P7_D706_R	CAAGCAGAAGACGGCATACGAGATACGAATTCGTGACTGGAGTTCAGACGTGTGCTCTTCCGATC

Table 33. Sequences of BarBlock oligonucleotides.

3.3.2.5 Washing Captured DNA

After hybridisation the captured DNA was obtained by binding CZECANCA biotinylated probes to Streptavidin M-270 Dynabeads (Invitrogen) using NimbleGen SeqCap EZ Hybridization and Wash Kit (Roche, Table 34-Table 35).

Preparing the Streptavidin Dynabeads and Binding of DNA

Streptavidin M-270 Dynabeads (10 mg/ml)	100 µl	
Placing on magnet		
Bead Wash Buffer 1x (NimbleGen)	195 µl	2x
Vortexing	10 seconds	
Placing back on magnet		
Discarding supernatant		
Bead Wash Buffer 1x (NimbleGen)	100 µl	
Placing on magnet		
Discarding supernatant		
Transferring the hybridised captured DNA to the Streptavidin M-270 Dynabeads	15 µl	
47°C	45 minutes	
Vortexing for 3 seconds every 15 minutes of incubation		

Table 34. Preparing Streptavidin M-270 Dynabeads and binding of hybridised captured DNA by NimbleGen SeqCap EZ Hybridization and Wash Kit (Roche).

Washing the Streptavidin Dynabeads Plus Bound DNA

Streptavidin M-270 Dynabeads and hybridised captured DNA	15 µl
Wash Buffer I 1x (pre-heated on 47°C) (NimbleGen)	100 µl
Placing on magnet	
Discarding supernatant	
Removing from magnet	
Stringent Wash Buffer 1x (pre-heated on 47°C) (NimbleGen)	200 µl
47°C	5 minutes
Placing on magnet	
Discarding supernatant	
Removing from magnet	
Stringent Wash Buffer 1x (pre-heated on 47°C) (NimbleGen)	200 µl
47°C	5 minutes
Placing on magnet	
Discarding supernatant	
Removing from magnet	
Wash Buffer I 1x (NimbleGen)	200 µl
Vortexing	2 minutes
Placing on magnet	
Discarding supernatant	
Removing from magnet	
Wash Buffer II 1x (NimbleGen)	200 µl
Vortexing	1 minute
Placing on magnet	
Discarding supernatant	
Removing from magnet	
Wash Buffer III 1x (NimbleGen)	200 µl
Vortexing	30 seconds
Placing on magnet	
Discarding supernatant	
Removing from magnet	
ddH_2O	50 µl

Table 35. Washing of Streptavidin M-270 Dynabeads and hybridised captured DNA.

3.3.2.6 Captured DNA Amplification Using LM-PCR

To minimise bias the captured DNA was amplified by two separate Post-capture LM-PCR reactions. These were pooled before washing (Table 36-Table 38).

Streptavidin M-270 Dynabeads and hybridised captured DNA	20 µl	
HiFi HotStart Ready Mix (KAPA)	25 µl	
Post-capture LM-PCR Primers P5F + P7R (5 µM each)	5 µl	
98°C	45 seconds	
98°C	15 seconds	11x
60°C	40 seconds	
72°C	30 seconds	
72°C	1 minute	

Table 36. LM-PCR amplification of captured DNA by KAPA HTP Library Preparation Kit (Roche).

Name	Sequence 5´-3´
Post-Capture LM-PCR Primer P5F	AATGATACGGCGACCACCGAGATCTACAC
Post-Capture LM-PCR Primer P7R	CAAGCAGAAGACGGCATACGAGAT

Table 37. Sequences of Post-capture LM-PCR primers.

Captured DNA Amplification Cleanup

Pooled post-capture LM-PCR reactions	100 µl	
AMPure XP Magnetic Beads	180 µl	
RT	5 minutes	
Placing on magnet		
Discarding supernatant		
Ethanol 80%	190 µl	2x
RT	30 seconds	
Discarding supernatant		
Drying ethanol	3-4 minutes	
Removing from magnet		
ddH_2O	52 µl	
RT	2 minutes	
Placing on magnet		
Transferring 50 µl of the amplified captured DNA into new tube		

Table 38. Cleanup of post-capture LM-PCR reaction with AMPure XP Magnetic Beads.

Amplified Captured DNA Quality Control

The concentration of amplified captured DNA sample was measured with the Qubit Quantification Platform (Life Technologies) using dsDNA HS Assay Kit following the manufacturer's instructions (ideal concentration 2 ng/µl).

3.3.2.7 Enrichment Quality Control

Real-time PCR (qPCR) was used to control proper enrichment of target fragments. PRE-capture sample was pooled from 4 different LM-PCR amplified samples (Chapter 3.3.2.2) and diluted to 1 ng/µl. POST-capture sample was prepared from post-capture LM-PCR (Chapter 3.3.2.6) and diluted to the same concentration. The PRE- and POST-capture samples from previous NGS experiment were used as an internal control. Four different PCR fragments were analysed (list of primers in Table 39) in qPCR reaction with HOT FIREPol EvaGreen qPCR Mix Plus (Solis Biodyne) on Light Cycler 480 (Roche, Table 39-Table 41, Figure 17). A successfully amplified POST-capture sample should have a lower average Cp (crossing point) value of at least 8 cycles than PRE-capture sample.

Name	Sequence 5´-3´
qPCR NGS-0237 F	CGCATTCCTCATCCCAGTATG
qPCR NGS-0237 R	AAAGGACTTGGTGCAGAGTTCAG
qPCR NGS-0247 F	CCCACCGCCTTCGACAT
qPCR NGS-0247 R	CCTGCTTACTGTGGGCTCTTG
qPCR NGS-0268 F	CTCGCTTAACCAGACTCATCTACTGT
qPCR NGS-0268 R	ACTTGGCTCAGCTGTATGAAGGT
qPCR NGS-0272 F	CAGCCCCAGCTCAGGTACAG
qPCR NGS-0272 R	ATGATGCGAGTGCTGATGATG

Table 39. List of qPCR primers (Roche) for enrichment quality control.

HOT FIREPol EvaGreen qPCR Mix Plus 5x	1.2 µl	
Primer Forward + Reverse (1 pmol/µl each)	1 µl	
DNA (1 ng/µl)	0.4 µl	
ddH_2O	3.4 µl	
95°C	5 minutes	
95°C	15 seconds	55x
60°C	25 seconds	
72°C	15 seconds	

Table 40. Enrichment quality control qPCR reaction.

Temperature	Time	Ramp rate (°C/s)
95°C	5 seconds	4.8
72°C	1 second	2.5
Continuous up to 95°C	Acquiring 8x per 1°C	0.07
40°C	10 seconds	2

Table 41. Conditions for acquiring melting curves during enrichment quality control.

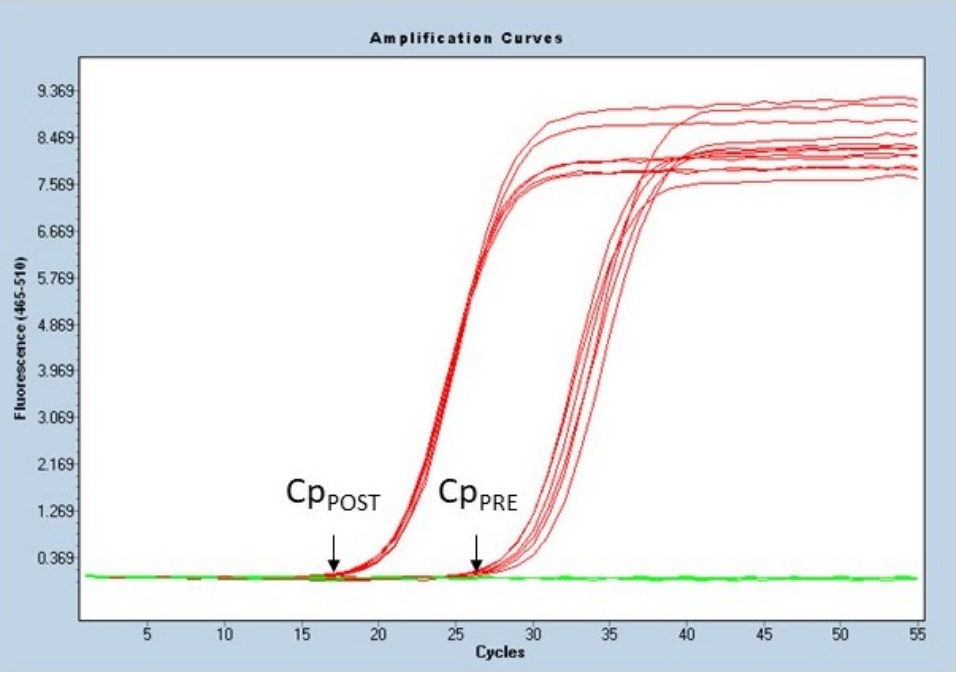

Figure 17. An example of amplification curves with PRE and POST-capture samples.
Average Cp (crossing point) value of POST-capture sample should be lower than average Cp value of PRE-capture sample.

3.3.2.8 Preparation of Library for Sequencing in MiSeq System Instrument

The NGS sequencing was performed on MiSeq System platform (Illumina) and MiSeq Reagent kit v3 was used for the preparation of sequencing sample (Table 42-Table 44). Final library concentration was adjusted to 14 pM. A library derived from bacteriophage PhiX (Illumina) was used as a control for cluster generation, sequencing, and alignment.

PhiX Control v3 (pre-diluted 4 nM) (Illumina)	0.5 µl
0.2 M NaOH	0.5 µl
RT	5 minutes
Pre-chilled HT1 (MiSeq Reagent)	141.9 µl

Table 42. Preparation of 14 pM PhiX Control.

Amplified captured DNA (4 nM)	10 µl
0.2 M NaOH	10 µl
RT	5 minutes
Only 7 µl of amplified captured DNA (2 nM) with NaOH for next dilution	
Pre-chilled HT1 (MiSeq Reagent)	993 µl

Table 43. Denaturation and dilution of amplified captured DNA to 14 pM with MiSeq Reagent kit v3.

Amplified captured DNA (14 pM)	980 µl
PhiX Control (14 pM)	20 µl

Table 44. Preparation of final 14 pM sequencing sample.

3.3.2.9 Sequencing on Illumina MiSeq System Instrument

The sequencing procedure can be separated into two steps: (1) generation of clusters and (2) sequencing by synthesis. (1) The adapter-modified amplified captured DNA is added to the flow cell and hybridised to the oligonucleotide anchors complementary to P5 and P7 adapters. The DNA templates are amplified by bridge PCR when DNA strands are arching over and hybridising to an adjacent anchor oligonucleotide. Each strand forms a cluster of DNA molecules with the same sequence. (2) Subsequently, reverse strands are washed away, and a sequencing primer is hybridised to adapter. In every cycle, a polymerase and fluorescently marked reversible terminators are added to the flow cell and one terminator is complementarily incorporated. Fluorescence of specific terminator is imaged, the dye is cleaved and the next cycle can follow (*152*) (Figure 18Figure 19).

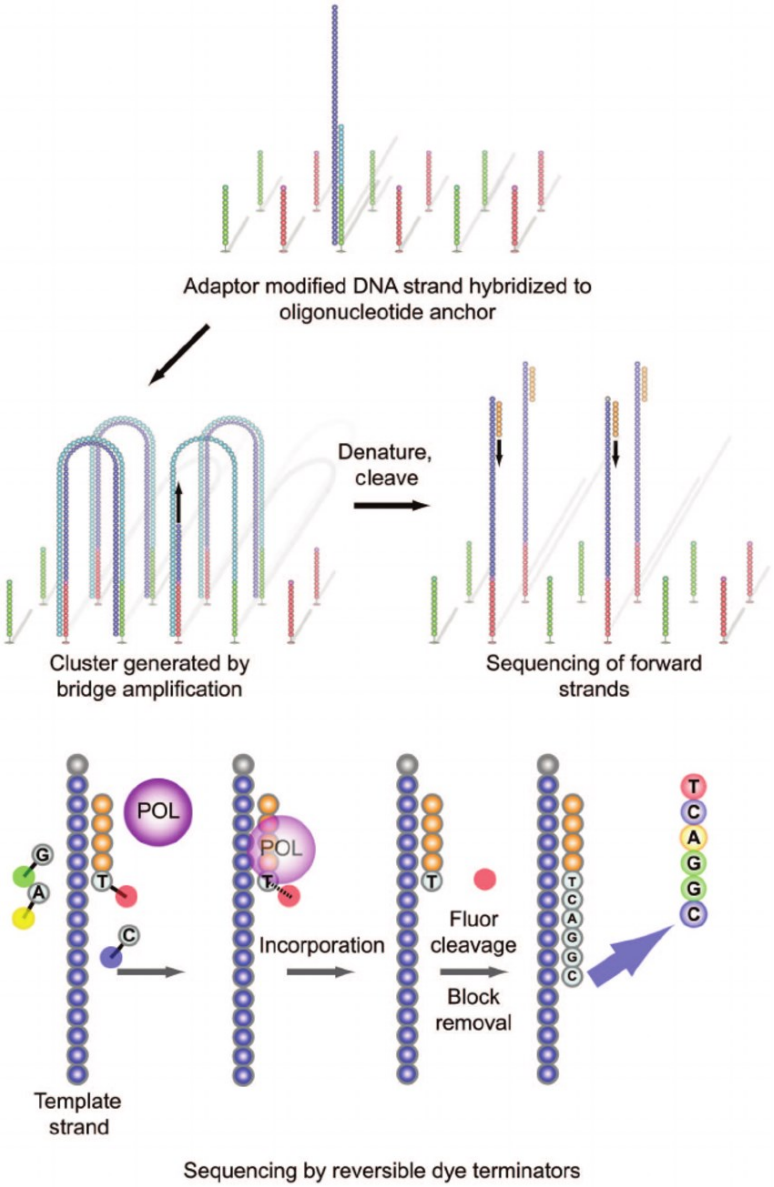

Figure 18. Principe of Illumina MiSeq platform sequencing.
Adaptor modified DNA strands bind to oligonucleotide anchors and generate clusters by bridge amplification. Reverse strands are cleaved and removed. Forward strands are sequenced by synthesis in cycles ***(152)***.

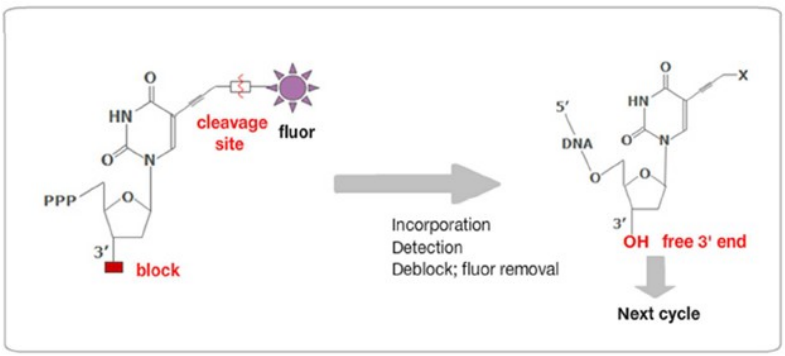

Figure 19. An example of reversible dye terminator.
Adapted from www.Illumina.com.

3.3.2.10 Bioinformatics

The processing of FASTQ files generated by MiSeq System was performed according to the in-house bioinformatics pipeline developed by Mgr. Petra Zemánková, PhD., a member of our laboratory, and described in Soukupova et al. (*151*). FASTQ files were mapped to GRCh37/hg19 by Novoalign v2.08.03 generating sequence alignment map (SAM) files which were transformed to binary alignment map (BAM) files using Picard tools v1.129. The quality of mapped bases was checked using Genome analysis toolkit (GATK) v3.3, converted to a variant-call format (VCF) containing alternative variants only and annotated by ANNOVAR. The Integrative genomics viewer (IGV) was used to visualise variants. The detection of medium sized indels was performed by Pindel software. CNVs were analysed by CNVkit.

3.3.3 Variant Prioritisation

Genes included in CZECANCA panel were divided into three groups (Table 45). First group was called "PDAC genes" and 11 PDAC susceptibility genes were included based on PDAC NCCN guidelines 2020. Three other genes (*APC*, *MUTYH*, and *EPCAM*) were included based on predisposition to hereditary genetic syndromes associated with PDAC. *PMS2* and genes associated with familial pancreatitis (*PRSS1, SPINK1, and CFTR*) are not included in the CZECANCA panel and thus are not included in the list. Second group, "HBOC genes" consisted of 19 genes associated with HBOC syndrome (except *PMS2*) according to HBOC NCCN guidelines 2020. Third group included all remaining 195 genes in the CZECANCA panel and is referred as "Other genes".

Name of group	Genes
PDAC genes	*APC*$^{+}$, ***ATM***, ***BRCA1***, ***BRCA2***, *CDKN2A*, ***EPCAM***$^{+}$, *FANCC, FANCG,* ***MLH1, MSH2, MSH6,*** *MUTYH*$^{+}$, ***PALB2***, and ***STK11***
HBOC genes	***ATM***, *BARD1,* ***BRCA1***, ***BRCA2***, *BRIP1, CDH1, CHEK2*,* ***EPCAM, MLH1, MSH2, MSH6,*** *NBN, NF1*,* ***PALB2***, *PTEN, RAD51C, RAD51D,* ***STK11,*** and *TP53*
Other genes	Remaining 195 genes

Table 45. 219 genes from the CZECANCA panel were divided according to their susceptibility to PDAC and HBOC cancers. **BOLD** – genes in both PDAC and HBOC genes groups; + – genes included based on genetic syndromes they cause; * – not fully covered genes in the panel.

Variants with sequence quality >100 and allelic frequencies in 1,000 Genomes Project <0.01 (http://www.internationalgenome.org/) were selected for further analysis. Splicing variants were considered if the mutation affected canonical splice site ±1/2 bases. Variants found more than twice in a control group were filtered out. Frameshift, nonsense, splicing variants, and CNVs together with variants of known pathogenicity according to ClinVar database (https://www.ncbi.nlm.nih.gov/clinvar/) were classified as pathogenic. Other variants of uncertain significance (VUSs) were prioritised based on predictive values from selected prediction algorithms (see Chapter 3.1.7).

3.3.4 Confirmation of Found Variants

All pathogenic variants in genes from either PDAC genes or HBOC genes groups were confirmed by Sanger sequencing (Chapters 3.1.2-3.1.4) with primers in Table 46. Other identified variants of uncertain significance were visually inspected in an IGV viewer.

Name	Sequence 5´-3´	Tm (°C)
BRCA2_5F	AACAATTTATATGAATGAGAATC	45.0
BRCA2_5R	AATTGTTAAGTTTTATTTTTATTA	41.9
BRCA1_11EF	AGAGCTGAAGTTAACAAATGCACC	56.0
BRCA1_11ER	GTGGGCAGAGAATGTTGCAC	56.2
NBN_6F	CAGATAGTCACTCCGTTTACAA	51.8
NBN_6R	CCCAAAATGAAATACGTTAACAAC	51.6
BRCA1_11IF	AGCTTCCCTGCTTCCAACAC	56.9
BRCA1_11IR	TGTGCTCCCCAAAAGCATAAAC	55.8
BRCA2_14F	TGCAACAAAGGCATATTCCT	52.0
BRCA2_14R	CAAAGGGGGAAAACCATCAG	53.0
MUTYH_12F	GCCCTCTTGGCTTGAGTAGG	56.5
MUTYH_13R	CAACATCCTTGGCTATTCCGC	56.0
BRCA2_11AS	GTGAAAAATATTTAGTGAATGTGATTGATGGTAC	56.1
BRCA2_11AA	CATGACTAGGTTTGACAGAACATCC	55.5
BRCA2_11ES	GAAGTGCCTGAAAACCAGATGAC	56.1
BRCA2_11EA	TTCTTCAACAAAAGTGCCAGTAGTC	55.8
CHEK2_13F	ATTGTCTTCTGTCCAAGTGCG	55.2
CHEK2_14R	CTCTTCTGAGTTTTAATCCACGGTC	55.6
CHEK2_11F	TAATTTAAGCAAAATTAAATGTCC	46.8
CHEK2_11R	GTGACTTCATCTAATCACCT	48.5
BRCA2_10CS	GAAGCCATTAAATGAGGAAACAGTG	54.8
BRCA2_10CA	AAAACACAGAAGGAATCGTCATCTA	54.4
PALB2_4BF	CCAGGAGGATTACCTATACAAAGAACA	55.8
PALB2_4BR	ACTGGTTCTGGAGAATCTGGAAG	55.7
ATM_52F	TCCTTAGAAGTTTGCTTTTTTC	49.4
ATM_52R	CTGGACCAAGTGCTAGGAAT	53.3
BRIP1_9F	GGTTGGCCATAGTGCTTCAG	55.3
BRIP1_9R	CTGGCAAGGAACAATTCATTTCCC	56.8
MUTYH_6F	AAGGGAAGGGTCATGGGTCAG	57.6
MUTYH_7R	GCCATCCCCTTACCTTCCG	56.4

Table 46. List of PCR and sequencing primers used to confirm mutations found during PDAC patients' germline DNA sequencing.

3.3.4.1 Confirmation of CHEK2 Deletion of Exons 9 and 10

Two sets of primers were used to confirm deletion of 5,395bp including exons 9 and 10 (Δ9-10) in *CHEK2* gene (Table 47-Table 48). They were designed to amplify short fragments at the deletion break points so PCR of the WT allele resulted in two products (379bp and 525bp). In case of gene rearrangement one of each set of the primers could not hybridise to mutated allele and only one PCR product would emerge from the reaction (450bp) (Figure 20).

ddH_2O	7.32 µl	
PCR Reaction Buffer with 20mM $MgCl_2$ 10x	1 µl	
dNTP (10 mM)	0.2 µl	
Primer CHEK2_9F/1 (30 pmol/µl)	0.1 µl	
Primer CHEK2_9R/1 (30 pmol/µl)	0.1 µl	
Primer CHEK2_10F/1 (30 pmol/µl)	0.1 µl	
Primer CHEK2_10R/1 (30 pmol/µl)	0.1 µl	
DNA (0.1 µg/µl)	1 µl	
FastStart LA Taq DNA Polymerase (5 U/µl)	0.08 µl	
95°C	5 minutes	
95°C	20 seconds	35x
56°C	20 seconds	
72°C	40 seconds	
72°C	10 minutes	

Table 47. Confirmation of Δ9-10 in *CHEK2* gene.

Name	Sequence 5´-3´	Tm (°C)
CHEK2_9F/1	TGTAATGAGCTGAGATTGTGC	52.7
CHEK2_9R/1	CAGAAATGAGACAGGAAGTT	49.3
CHEK2_10F/1	CTCTGTTGTGTACAAGTGAC	50.5
CHEK2_10R/1	AGTGTCTCAAACTTGGCTGCG	57.7

Table 48. List of primers used for confirmation of Δ9-10 in *CHEK2* gene.

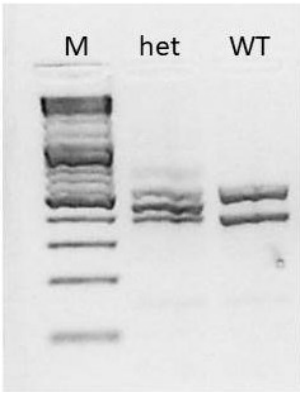

Figure 20. An example of electrophoresis of PCR products confirming the Δ9-10 CHEK2 large deletion.
WT sample consists of two bands (379bp and 525bp). Carrier of heterozygous *CHEK2* Δ9-10 variant shows three bands (379, 450, and 525bp). M – marker; het – patient heterozygous for *CHEK2* Δ9-10 variant.

3.3.5 Statistical Analysis

Statistical analysis was calculated with the same method like in Chapter 3.1.8.

3.4 Genetic Analysis of Second Neoplasms in PDAC Long-term Survivors

3.4.1 Patients and Controls Included in the PDAC Long-term Survivors Study

Among 118 PDAC patients treated in University Hospital Olomouc between the years 2006-2011 only 22 (18.64%) patients survived more than five years after surgery. Mean age at diagnoses of long-term

PDAC survivors was 61.7 (range 44-75 years). A second malignant neoplasm (SMN) was developed by six of them (27.27%) within the median time to diagnosis of SMN 52.5 months and mean age at PDAC diagnosis 66.7 (range 51-75 years). Twenty of these twenty-two long-term surviving patients were analysed by NGS sequencing on CZECANCA panel. Two patients suffering from rectal SMN cancers died before DNA samples could be collected. DNA was isolated from peripheral blood samples collected into EDTA containing tubes by Wizard Genomic DNA Purification System (Promega) following the manufacturer´s instructions. Identified variants were confirmed from an independent blood sample.

3.4.2 Next Generation Sequencing

Protocol for NGS analysis was identical to the previous one in Chapter 3.3.2.

3.4.3 Variant Prioritisation

Variants with low sequence quality <30, variants with allelic frequencies >0.01 in ESP6500 (https://evs.gs.washington.edu/EVS/) and 1,000 Genomes Project databases and variants present >2x among 507 non-cancer from our laboratory (unpublished data) controls were excluded. Truncating and splicing variants (±1/2) of known PDAC and HBOC predisposition genes were classified as pathogenic. Other variants were classified according to the ClinVar database and prioritised by CADD scaled score (≥15) and GERP (≥2). Prioritised variants were further characterised by SIFT (≤0.05), PP-2 (≥0.85), MA (≥1.9), Phylop (≥0), and Spidex (>|2|) prediction programs. Variants with at least three predictions (on top of CADD and GERP) above the thresholds were considered potentially deleterious.

3.4.4 Confirmation of Found Variants

All detected pathogenic variants were confirmed by Sanger sequencing from PCR reaction (Chapters 3.1.2-3.1.4) with primers in Table 49.

Name	Sequence 5´-3´	Tm (°C)
CHEK2_11F	TCAACAGCCCTCTGATGCATG	56.9
CHEK2_15R	TTCCAGTAACCATAAGATAATA	45.6
RAD51D_4F	TGGCCAGTGATGTTCAAAGA	53.7
RAD51D_5R	CAACACAAATGGGCTGAGTC	53.8
MLH1_5F	GGGATTAGTATCTATCTCTCTACTGG	52.8
MLH1_5R	GCTTCAACAATTTACTCTCCC	51.2
ATM_28F	TGCTGATGGTATTAAAACAGTTT	50.8
ATM_28R	GGTTGGCTATGCTAGATAATGAT	52.0
CHEK2_11F	TAATTTAAGCAAAATTAAATGTCC	46.8
CHEK2_11R	GTGACTTCATCTAATCACCT	48.5

Table 49. List of PCR and sequencing primers used to confirm mutation found during PDAC long-term surviving patients germline DNA sequencing.

3.4.5 Statistical Analysis

Statistical analysis was calculated with the same method like in Chapter 3.1.8.

3.5 Functional Characterisations of *PALB2* Missense Variants

3.5.1 Method Overview

Risk estimates for *PALB2* sequence variants have mainly been based on protein truncating variants (frame-shift, non-sense, splice-site mutation etc.) causing complete loss of function. Missense variants could cause subtle changes in the biological activity of protein product that disables precise determination of associated cancer risk. Regarding that, most of missense alterations are classified as VUSs. Unclassified variants are the major clinical challenge as they complicate reporting of genetic testing results and genetic counselling, limit patient eligibility for intensive surveillance and gene-targeted therapies, and prevent predictive gene testing of relatives. Thus a robust method for interpreting VUSs is urgently needed. One possible approach is functional characterisation of the impact of sequence alteration on activity of the protein product.

We have therefore decided to perform a functional analysis using stable human osteosarcoma-derived cell line U2 OS model system (Figure 21). First, we have picked out novel not classified missense variants detected during our genetic screening of BC and PDAC patients (*61, 153*). CRISPR-Cas9 (Clustered regularly interspaced short palindromic repeats-CRISPR-associated protein 9) system was used for genome modification of *PALB2* sequence following protocol from Ran et al. (*154*) and the functionality of modified proteins was determined by checking the ability to repair DDSBs by HR assay (*155*).

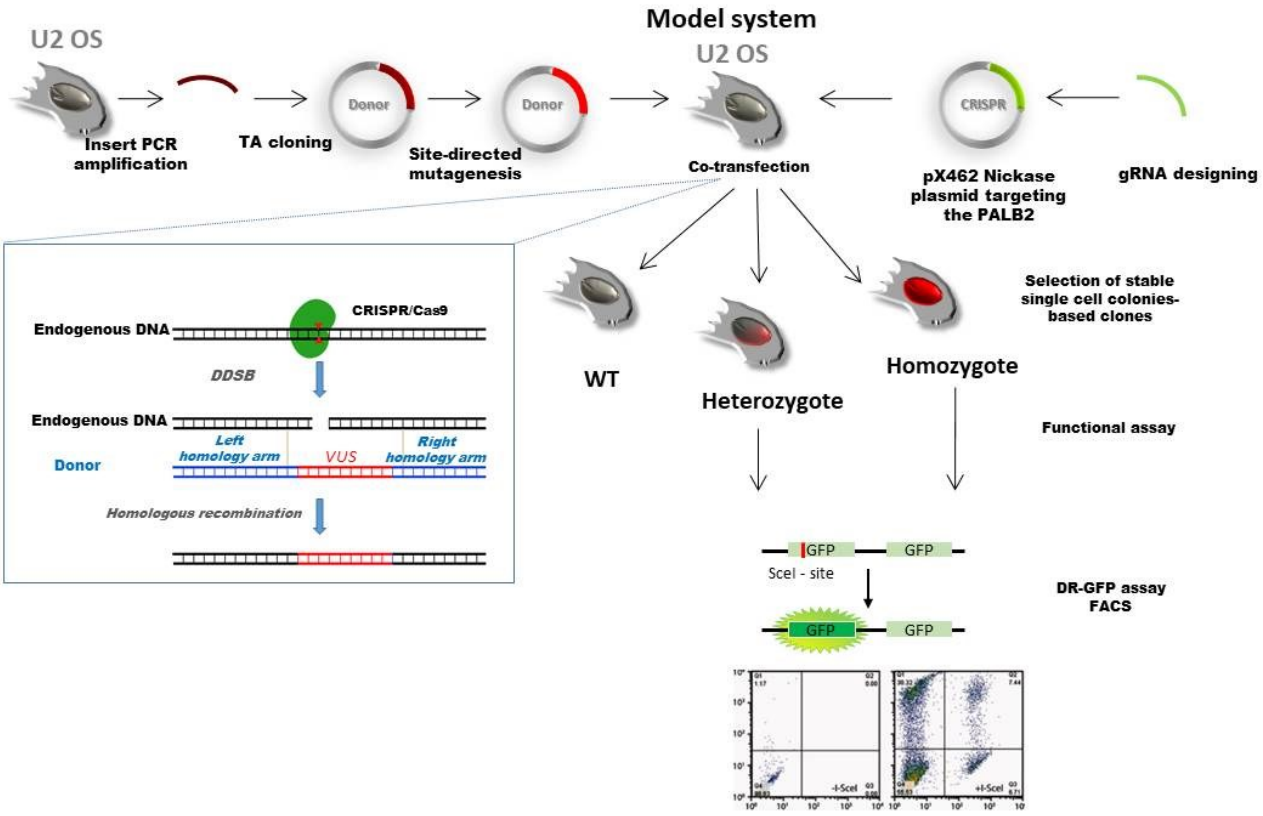

Figure 21. Overview of functional characterisations of *PALB2* VUSs methodology.
The U2 OS cell line enables a direct scoring of HR activity by a Direct repeat-green fluorescent protein (DR-GFP) assay. The targeted genome modification was achieved by simultaneous CRISPR-based (px462 Nickase expression vector) site specific introduction of DDSBs followed by homology-mediated repair. CRISPR plasmid was targeted to the desired *PALB2* region by homology-mediated interaction of guiding RNA (gRNA) in CRISPR with endogenous nuclear DNA. Plasmid donor for this modification was prepared by ligating a homologous region of *PALB2* into the vector backbone. Studied sequence alteration was subsequently introduced by site-directed mutagenesis. Donor was co-transfected together with CRISPR vector into the U2 OS model cells by chemical transfection. By a high dilution of cell population after transfection the single-cell colony clones with homo, or heterozygous alteration were selected. The activity of HR in the set of clones was scored directly by DR-GFP assay and flow cytometry (FACS).

3.5.2 Selection of Variants

For the analysis we selected novel not previously reported and clinically unclassified variants detected in cohort of BC and PDAC patients in our laboratory (*61, 153*). As a positive controls (PCs) we chose missense variant c.82_83delinsGC (p.Tyr28Ala) previously shown to negatively influence PALB2 binding capacity to BRCA1 and HR repair (*156*) and truncating mutation c.196C>T (p.Gln66Ter). The internal control for our model system was CRISPR-based *PALB2* knock-out (KO) (Table 50; Figure 22).

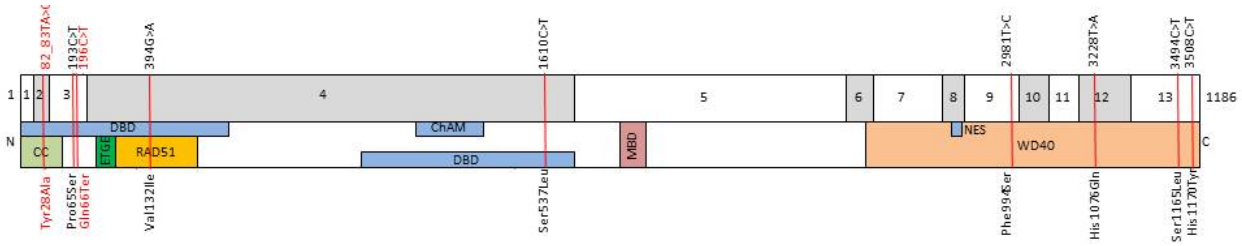

Figure 22. Modified diagram of PALB2 protein (Figure 4) with selected *PALB2* variants for functional analysis.
Upper part: 13 exons of PALB2.
Bottom part: Functional domains of PALB2. **CC** (Coiled Coil domain); **DBD** (DNA Binding Domain); **ChAM** (Chromatin-Association Motif); **MBD** (MRG15 Binding Domain); **NES** (Nuclear Export Signal).
RED - positive controls.

Four of the variants lie in the WD40 protein binding domain (c.2981T>C, c.3228T>A, c.3494C>T and c.3508C>T), variant c.1610C>T is in the DNA binding domain, variant c.394G>A in RAD51 binding domain and variant c.193C>T is not part of any known functional domain. The prediction tools showed high damaging probability for two variants (c.2981T>C and c.3494C>T).

Exon	Nucleotide change	Protein change	Variant frequency			Variant prediction							
			ExAC*	BC patients (N=409)	PDAC patients (N=152)	SIFT	PP-2	MA	Phylop	GERP	CADD scaled	Spidex	Clin Var class
2, PC	c.82_83delinsGC	p.Tyr28Ala	NA	0	0	NA	NA	NA	NA	NA	23.30	NA	--
3	c.193C>T	p.Pro65Ser	0	0.001	0	0.85	0.01	0.29	-0.57	-4.82	2.22	0.47	--
3, PC	c.196C>T	p.Gln66Ter	0	0	0	0.17	NA	NA	1.38	4.69	33	-76.95	4-5
4	c.394G>A	p.Val132Ile	0	0.001	0	0.63	0.04	1.45	0.14	0.69	4.89	0.11	--
4	c.1610C>T	p.Ser537Leu	0	0.001	0	0.42	0.01	0.72	-0.47	-3.63	0.03	-0.03	--
9	**c.2981T>C**	**p.Phe994Ser**	**0**	0.001	**0**	**0**	**0.99**	**2.02**	**2.23**	**5.84**	**25.30**	**0.78**	**--**
12	c.3228T>A	p.His1076Gln	0	0.001	0	0.20	0.24	1.30	-0.32	-0.24	22.30	1.80	--
13	**c.3494C>T**	**p.Ser1165Leu**	**0**	**0**	**0.003**	**0**	**1.00**	**2.24**	**2.80**	**5.90**	**31.00**	**NA**	**--**
13	c.3508C>T	p.His1170Tyr	0	0	0.003	0.79	0.98	2.08	2.80	4.86	24.00	NA	--

Table 50. Missense variants included in knock-in experiments.
* – European non-Finnish population; RED – prediction values above threshold (Table 15); **BOLD** – variants with at least six prediction programs values above threshold; PC – positive control.

3.5.3 Genome Modification

For the genome modification of *PALB2* we used an RNA-guided endonuclease CRISPR-Cas9 system following the protocol by Ran et al. (*154*). In order to minimize the off-target effect of CRISPR we used Cas9 mutant – Nickase. This CRISPR paralog is capable to introduce a single-strand break to target DNA molecule based on homology-mediated interaction of guiding RNA (gRNA) within CRISPR-Nickase and chromosomal DNA. DDSB is achieved by cooperative action of CRISPR dimer consisting of two Nickase subunits. This significantly increases the specificity and minimizes the off-target effect. The genome modification was achieved by endogenous homology-mediated DNA repair mechanism. Donor plasmid containing studied sequence alteration was co-transfected into the model cells together with CRISPR vectors. This donor contained sequence variant (point mutation) with adjacent left and right arms fully complementary to the target sequence in chromosome locus (Figure 23) (*154*).

To gain a *PALB2* KO cell line we have ordered the *PALB2* CRISPR-Cas9 Plasmids (Santa Cruz Biotechnology) consisting of 3 vectors each encoding different gRNA targeting *PALB2* sequence. Cells

were co-transfected with homology direct repeat (HDR) plasmid serving as a donor sequence of mCherry protein. Successfully recombined cells were therefore able to be visualised by fluorescent microscopy.

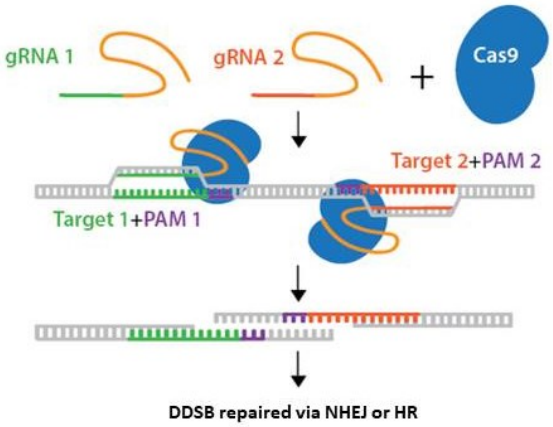

Figure 23. A CRISPR-Cas9 system overview.
A pair of CRISPR-Nickases nick DNA and yield to two single-stranded breaks resulting in DDSB which is repaired by NHEJ or HR. This increase the specificity of target recognition (https://www.addgene.org/crispr/nick/). PAM – protospacer adjacent motif.

3.5.3.1 Preparation of CRISPR Vectors

The CRISPR for targeted *PALB2* modification was prepared by insertion of synthetic gRNA into the px462 vector (Addgene) backbone (Figure 24). The px462 plasmid encodes for structural RNA (sgRNA scaffold) and protein part (spCas9) of ribonucleoprotein CRISPR complex. The expression is driven by U6 promoter. Within the structural RNA there is a unique BbsI restriction site that enables insertion of gRNA that target the whole complex to the DNA by homology between the gRNA and target DNA. The gRNA is double stranded molecule containing 19-25 bp long homologous region without protospacer adjacent motif (PAM, consensus sequence 5´-NGG-3´ recognized by the CRISPR as the site of cleavage) followed by 5´- and 3´- BbsI recognition site. The BbsI is type II restriction endonuclease, so once the gRNA is inserted into the px462 vector it can not be cleaved out by this enzyme again. This enables highly effecient restriction/ligation procedure.

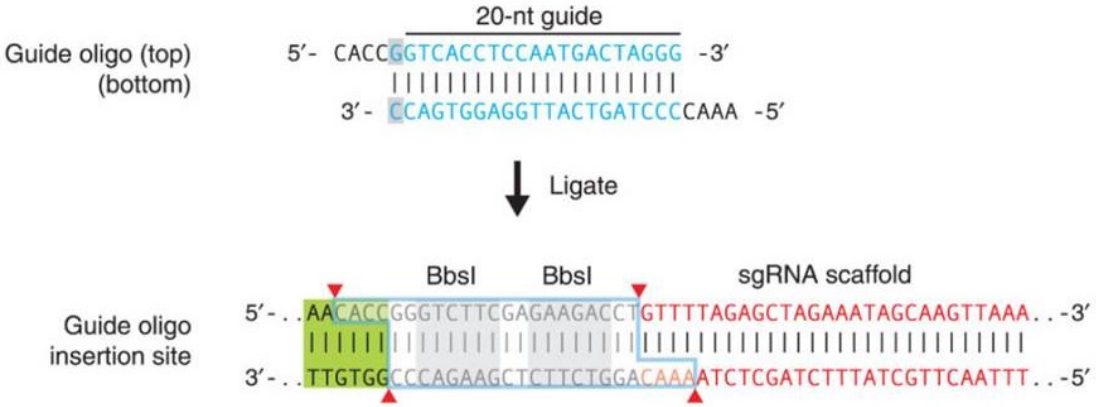

Figure 24. Target sequence is encoded in 19-25 nucleotide oligos with overhangs for ligation into BbsI digested px462 (pSpCas9(BB)-2A-Puro) vector backbone (Addgene).
sgRNA – structural RNA scaffold. (Adapted from *154*).

3.5.3.1.1 Designing CRISPR Vectors

The gRNA was designed as two complementary single stranded DNA oligonucleotides. For each couple of CRISPR-Nickase two double-stranded gRNA (i.e. four single-stranded oligonucleotides) were designed using publicly available CRISPR Design Tool – crispor.org (Table 51). Target sequence has to be directly adjacent to the PAM sequence. The major selection criteria were: 1) the vicinity of PAM to the studied VUS – maximally 50 bp upstream, or downstream from the VUS position; 2) minimal off-target effect; and 3) maximal predicted efficiency calculated by CRISPOR. The most optimal gRNA was designed for each analysed sequence alteration. The sequences are listed in Table 51.

Exon	Nucleotide change	Sense A Sequence 5´-3´ (Target-PAM sequence)	Off-targets for 0-1-2-3-4 mismatches*	Sense B Sequence 5´-3´ (Target-PAM sequence)	Off-targets for 0-1-2-3-4 mismatches*
2, PC	c.82_83delinsGC	GAAATTAGCATTCTTGAAA-AGG	0-0-9-60-404	GATTCACTTACCTGAAGGC-GGG	0-0-1-5-68
3	c.193C>T	CAAGATTGTTTGTCTCAGC-AGG	0-1-0-16-156	TAAAGCAGGCATAAGTGAA-TGG	0-0-3-51-492
3, PC	c.196C>T				
4	c.394G>A	CTGTGGGGAAAATGTTCTT-GGG	0-0-2-24-198	ACAGGGTCAGTGACCCTAG-TGG	0-0-1-9-129
4	c.1610C>T	GGCTAGAAGTTGGCAAAAG-TGG	0-0-3-30-251	TCGATTGTTAACAGGTCCA-AGG	0-0-0-1-40
9	c.2981T>C	TCTACTTGTTGATCAGAAA-GGG	0-0-4-35-202	TGACGTTTGCAGAAGATGG-AGG	0-0-1-23-129
12	c.3228T>A	TATTTTTCTCCGAAATTAG-GGG	0-0-2-25-259	CGCAACGACTCACTCTCTT-TGG	0-0-1-3-42
13	c.3494C>T	TTTCACAAAAGACCAATGT-TGG	0-1-1-42-248	GGTACAGACTCTCATTTGC-TGG	0-0-0-15-112
13	c.3508C>T				

Table 51. List of gRNA oligonucleotides and their predicted off-targets.
* - Numbers signify amount of predicted off-targets according to number of mismatches.

3.5.3.1.2 Ligation to px462 Vector

The particular single-stranded oligonucleotides of gRNA are first phosphorylated on their 5´ ends, than annealed to double-stranded molecule and finally ligated into the px462 vector backbone in single reaction consisting of two steps – BbsI restriction and T7 DNA-mediated ligation repeated several times.

Sense and antisense oligos were phosphorylated and annealed in the mixture described in Table 52 under following conditions: 37°C for 30 min, 95°C for 5 min, and cooling down to room temperature for 30 min. Oligos were then diluted 1:200 with ddH_2O.

Oligo sense (100 µM)	1 µl
Oligo antisense (100 µM)	1 µl
T4 DNA Ligase Buffer 10x (NEB)	1 µl
ddH_2O	6.5 µl
T4 Polynucleotide kinase (NEB)	0.5 µl

Table 52. Reaction mixture for phosphorylation and annealing of sense and antisense oligos.

Ligation reaction of annealed and diluted oligos into px462 plasmid was mixed according the Table 53. Reaction mixture of annealed oligonucleotides ligation with vectors.. Reaction was left to incubate for 1h and then six cycles of 37°C 5 min and 21°C 5 min were repeated.

Vector px462 (100 ng/µl)	1 µl
Diluted Annealed Oligos	2 µl
DTT (10 mM) (NEB)	1 µl
ATP (10 mM) (NEB)	1 µl
BbsI Enzyme (NEB)	1 µl
Buffer 2.1 10x (NEB)	2 µl
T7 DNA Ligase (NEB)	0.5 µ
ddH_2O	11 µl

Table 53. Reaction mixture of annealed oligonucleotides ligation with vectors.

Residual linearized DNA was digested with a Plasmid-Safe DNase (Epicentre) for 37°C 20 min (Table 54).

Ligation Reaction	11 µl
Plasmid Safe Reaction Buffer 10x (Epicentre)	1.5 µl
ATP (25 mM) (Epicentre)	1.5 µl
ATP Dependent Plasmid-Safe DNase (10 U/µl) (Epicentre)	1 µl

Table 54. Reaction mixture for DNase treatment of ligated vectors.

Two µl of DNase treated ligation reaction was added into 50 µl One Shot TOP10 Escherichia coli chemical competent bacteria (Invitrogen), incubated on ice for 30 min, heat-shocked at 42°C for 30 s and returned on ice for 2 min. Pre-heated 250 µl of SOC medium was added, bacteria were left to recover for 1 hour at 37°C and they were then plated on LB-agar plates (Invitrogen) containing ampicillin antibiotics (final concentration 100 µg/ml, Sigma Aldrich) and incubated overnight at 37°C. Subsequently, colonies were inoculated into 1 ml LB medium (Broth EZMIX Powder, Sigma Life Science) with ampicillin and incubated shaking overnight at 37°C. Plasmid DNA was isolated using Miniprep NucleoSpin Plasmid Kit (Macherey-Nagel) and sequence was checked using U6-Fwd primer (5´-CGCCAGGGTTTTCCCAGTCACGAC) in 5 µl sequence reaction (Table 55) on 96°C 5 min and 30 cycles of 96°C 1 min, 50°C 10 s, and 60°C 4 min.

Plasmid DNA (100 ng/µl)	2 µl
BigDye Terminator Sequencing Buffer 5x (MCLAB)	1 µl
Sequencing Primer (30 pmol/µl)	0.2 µl
BigDye Ready Reaction Premix	1 µl

Table 55. Reaction mixture of sequencing reaction.

3.5.3.2 Preparation of Donor Sequences

Donor sequences have to be transfected to the cells together with CRISPR vectors for the knock-in experiments. Donor sequences are about 400 – 500 bp long DNA fragments, they contain the sequence alteration in the middle and homology arm on each side. Donor sequences were prepared by PCR from U2 OS DNA and ligated into pCR2.1 vector backbone. The specific alterations were introduced by side directed mutagenesis (SDM).

3.5.3.2.1 Ligation to pCR2.1 Vector

Donor sequences were gained by PCR of U2 OS cell's DNA with primers (Table 56) designed to match the same reaction criteria 94°C 1 min, 35 cycles 94°C 20 s, 61°C 30 s, 68°C 7 min and final 72°C 10 min in 5 µl reaction (Table 57).

Exon	Nucleotide change	Forward Primer Sequence 5´-3´	Reverse Primer Sequence 5´-3´	Length of fragment (bp)
2, PC	c.82_83delinsGC	GGACATGTTCCAGATGATAGGAAC	GCTCTTTGGGCACGCTAGAG	395
3	c.193C>T	CGCCTTCAGGTAAGTGAATCG	GGTAACAAAGAGTGAGACTCTGTC	398
3, PC	c.196C>T			
4	c.394G>A	CACCTGTAAATTCATCTGCCTG	CTGTAACTGGTTCTGGAGAATCTG	583
4	c.1610C>T	TCCAATGAGGAAACTGACCAAAG	ACTTGGCCCTGTCACTTTTTAGA	433
9	c.2981T>C	ATTAAAAGGTTACTCCTCACATCACC	CTATGTCATAACCTAGTGTTGATGCG	362
12	c.3228T>A	GGGAAAAAAATCAAGCCAGTGG	GTGTTTGCACAGTGCCTTTC	362
13	c.3494C>T	TTTGGATATGTAATCTGAATTATATCTTCT TTG	GTCTGTCTGGACATAAACAAGC	380
13	c.3508C>T			

Table 56. Primers used for PCR of donor sequences.

ddH_2O	9.975 µl
LA PCR Buffer II 10x ($Mg2^+$ plus)	1.5 µl
dNTP Mixture (2.5 mM each)	2.4 µl
Primer Forward (30 pmol/µl)	0.025 µl
Primer Reverse (30 pmol/µl)	0.025 µl
DNA (100 ng/µl)	1 µl
TAKARA LA Taq Polymerase (5 U/µl)	0.075 µl

Table 57. Reaction mixture with TAKARA LA Taq Polymerase PCR reaction.

PCR products were purified on 1% gel electrophoresis (Chapter 3.1.3) by Gel DNA Recovery Kit (Zymoclean) and ligated into pCR2.1 plasmid backbone by TA cloning Kit (Invitrogen) in 10 µl ligation mixture left overnight at 22°C (Table 58).

ddH_2O	3.5 µl
T4 DNA Ligase Reaction Buffer 5x	1.5 µl
pCR2.1 Vector (25 ng/µl)	2 µl
DNA Fragment (25 ng/µl)	2 µl
ExpressLink T4 DNA Ligase (5 U/µl)	1 µl

Table 58. Reaction mixture of donor sequences ligation to pCR2.1 plasmid backbone.

Ligated plasmids were transformed into One Shot TOP10 Escherichia coli chemical competent bacteria (Invitrogen) following the protocol from Chapter 3.5.3.1.2. Primers M13F (5´-

GTAAAACGACGGCCAG) and M13R (5´-CAGGAAACAGCTATGAC) were used to check plasmid sequence.

3.5.3.2.2 Site Directed Mutagenesis

Side directed mutagenesis (SDM) requires synthetic primers complementary to the template DNA and containing the desired mutation. Primers hybridise to plasmids with donor sequences and they are polymerised by DNA polymerase according the rest of the plasmid. Specific primers with one or two base modification (Table 59) were designed at www.bioinformatics.org/primerx/, added into 12.5 µl reaction (Table 60) and incubated at 98°C 3 min, 17 cycles 98°C 10 s, 60°C 30 s, 72°C, 11 min and final 72°C 10 min. SDM reaction was treated by DpnI restrictase to digest input plasmid DNA (5 µl SDM reaction, 0.2 µl DpnI restrictase (20 U/µl) (BioLabs), 0.8 µl Cutsmart Buffer 10x (BioLabs), 2 µl ddH_2O) for 6 hours at 37°C. Restriction reaction was then transformed into bacteria and plasmids were sequenced as in Chapter 3.5.3.2.1.

Exon	Nucleotide change	Forward Primer Sequence 5´-3´	Reverse Primer Sequence 5´-3´
2, PC	c.82_83delinsGC	GCATTCTTGAAAAGGGAAGCCAGCAAGACACTAGCC	GGCTAGTGTCTTGCTGCTTCCCTTTTCAAGAATGC
3	c.193C>T	GTCTCAGCAGGATCTCTCATCGCAGCTAAAACACTCAGG	CCTGAGTGTTTTAGCTGCGATGAGAGATCCTGCTGAGAC
3, PC	c.196C>T	GATCTCTCACCGTAGCTAAAACACTCAGAAC	GGTTCTGAGTGTTTTAGCTACGGTGAGAGATCCTGCTGA
4	c.394G>A	GAACATTTTCCCCACAGGATCAGTGACCCTAGTGGTG	CACCACTAGGGTCACTGATCCTGTGGGGAAAATGTTC
4	c.1610C>T	GCCAACTTCTAGCCTGTTGATTGTTAACAGGTCC	GGACCTGTTAACAATCAACAGGCTAGAAGTTGGC
9	c.2981T>C	CAACAAGTAGAAGTCATGACGTCTGCAGAAGATGGAGGG	CCCTCCATCTTCTGCAGACGTCATGACTTCTACTTGTTG
12	c.3228T>A	CTTTATTGTCCTGAGTCAACCCTGTGCCAAAGAGAG	CTCTCTTTGGCACAGGGTTGACTCAGGACAATAAAG
13	c.3494C>T	GGTCTTTTGTGAAATGGTTGGGTACAGACTCTCATTTGC	GCAAATGAGAGTCTGTACCCAACCATTTCACAAAAGACC
13	c.3508C>T	CGGGTACAGACTCTTATTTGCTGGCTGGACAAAAAG	CTTTTTGTCCAGCCAGCAAATAAGAGTCTGTACCCG

Table 59. Primers used for donor sequences SDM modification.
The desired mutations are in red.

Pfu DNA Polymerase (2.5 U) (Thermo Scientific)	0.5 µl
ddH_2O	4 µl
Buffer 5x	2.5 µl
dNTPs (FastStart)	0.5 µl
Primer forward (2.5 pM)	2 µl
Primer reverse (2.5 pM)	2 µl
Plasmid DNA (30 ng/µl)	1 µl

Table 60. Reaction mixture of SDM.

3.5.3.3 CRISPR-Cas9 Transfection

3.5.3.3.1 U2 OS Cells Maintenance

The stable adherent human osteosarcoma-derived cell line U2 OS with stably integrated Direct repeat – green fluorescent protein (DR-GFP) cassette was used as a model system for in vitro functional analysis. This cell line enables direct scoring of HR activity by DR-GFP assay, and was kindly provided by Dr. Simon Powell (*155*).

Cells were cultivated in DMEM (Dulbecco´s modified eagle´s medium, Sigma Aldrich) medium supplemented with 10% fetal bovine serum (FBS, Sigma Life Science) and 10 ml/l of L-glutamine-penicillin-streptomycin solution (GPS, Sigma Life Science) at 37°C and 5% CO_2. When reaching 80-90%

of sub-confluency the cells were passaged. Briefly, the cultivation media was aspirated and cells were washed one time with PBS (Dulbecco´s phosphate buffered saline, Sigma Life Science). Then the cells were released from surface by incubation with Trypsin-EDTA Solution (Sigma Life Science) for 5 min at 37°C. Dissociated cells were resuspended in cultivation media and seeded into the new cultivation flask in the density 20,000 cells/1 cm^2. The cells were regularly checked by optical microscopy. The cell viability was checked during each passage by automated cell-counter Luna 3000 (LogosBio) using the crystal violet staining protocol. Briefly, 15 µl of cell suspension obtained during passaging was mixed directly with 15 µl of crystal violet staining solution, immediately applied onto the micro-counter slide and analysed.

3.5.3.3.2 CRISPR-Cas9 Transfection

Transfection was performed according to optimised transfection protocol of transfecting cells with pMAX-GFP (Amaxa) plasmid according to the manufacturer's recommendation. The transfection efficiency was scored by fluorescence-activated cell sorter (FACS) analysis.

U2 OS cells were seeded onto 24-wells plate at a density of $30x10^3$ cells per well 24 hours before transfection. Cultivation medium was supplemented with an NHEJ inhibitor SCR7 (1 µl/ml, Sigma Aldrich, (*157*)). Two hours prior the transfection it was exchanged with 250 µl of Opti-MEM I Reduced Serum Medium (Gibco by Life Technologies).

Opti-MEM I medium and Lipofectamine 3000 Reagent (Invitrogen by Thermo Fisher Scientific) were mixed together in tube A while donor sequence vector, two px462 plasmids, P 3000 Reagent and Opti-MEM I medium were mixed in tube B (Table 61). Contents of tube A and B were put together and left to incubate at room temperature for 5 minutes. Mixture was added to the cells in drop wise manner. After 24 hours of incubation cells were washed with PBS and incubate for 24 hours in standard cultivation media with SCR7 supplement.

Tube A	Opti-MEM I	25 µl
	Lipofectamine 3000 Reagent	1.5 µl
Tube B	Opti-MEM I	25 µl
	P 3000 Reagent	2.5 µl
	px462 A (100 ng/µl)	2 µl
	px462 B (100 ng/µl)	2 µl
	Donor vector (100 ng/µl)	25 µl

Table 61. Reagent mixture of CRISPR-Cas9 system transfection to cells.

After 24 hrs recovery the cells were released by Trypsin/EDTA and diluted to 300 cells/ml of media. One ml of diluted cell suspension was applied onto the 10 cm diameter Petri dish and cultivated for 10 days with replacing media every third day. Subsequently, isolated single cells colonies were picked and transferred separately to 96-wells plate and cultivated until reaching nearly confluent state. Cell

colonies were moved in a new 24-wells plate and left to grow. When the colonies sub-confluency reached about 80% the DNA was isolated by Wizard Genomic DNA Purification System (Promega). The isolated DNA was diluted into 50 µl DNA Rehydration Buffer and genome modification were checked by Sanger sequencing (Chapters 3.1.2-3.1.4) with primers listed in Table 62.

Name	Sequence 5´-3´	Tm (°C)
PB2_1F	AGCTGATCGCGCACTGAGG	59.3
PB2_1R	GACACAAAGCCAGGCCTAAA	54.8
PB2_2F	GACTCCACCTTTCCACTTGC	55.2
PB2_2R	GAGACAAAAACAGCCCCAGAAA	55.4
PB2_9F	ATTAAAAGGTTACTCCTCACATCACC	54.8
PB2_9R	TTACCCAACTTTCTCTGAAACCTG	54.8
PB2_13F	TTTGGATATGTAATCTGAATTATATCTTCTTTG	53.0
PB2_13R	AGGCCCAATATATCCAGAAAATTG	53.0

Table 62. Primers used for checking the CRISPR-Cas9 modification.

3.5.3.3.3 Santa Cruz Biotechnology CRISPR-Cas9 Transfection Protocol

For the KO experiment we ordered *PALB2* CRISPR-Cas9 Plasmids from Santa Cruz Biotechnology. The protocol for CRISPR-Cas9 genome modification was similar to Chapter 3.5.3.3.2. The mixture for tube B contained *PALB2* CRISPR-Cas9 KO and *PALB2* HDR Plasmids (Table 63). Successful transfection of these plasmids can be confirmed by detection of mCherry by fluorescent microscopy.

Tube A	Opti-MEM I	25 µl
	Lipofectamine 3000 Reagent	1.5 µl
Tube B	Opti-MEM I	25 µl
	P 3000 Reagent	2.5 µl
	PALB2 CRISPR-Cas9 KO Plasmid (1 µg/µl)	1 µl
	PALB2 HDR Plasmid (1 µg/µl)	1 µl

Table 63. Reagent mixture of CRISPR-Cas9 system transfection to cells with Santa Cruz Biotechnology plasmids.

3.5.3.4 HR Assay

Functional analysis of impact of variants on HR, the key PALB2 protein mediated cell process, was tested by DR-GFP assay. The assay is based on stable incorporation of construct into the model cell. This construct consists of two cassettes. The first cassette contains complete coding sequence of GFP with unique SceI recognition site. The coding sequence in first cassette however contains premature termination codon disabling the expression of fully functional GFP. Second cassette contains incomplete, however correct GFP coding sequence complementary to the mutated part of the first cassette. Upon the SceI – mediated introduction of DDSB into the first cassette the cell will use the second cassette for homologous-mediated DNA repair. If so it will unblock the expression of fully functional GFP that can be detected by flow cytometry (Figure 25) (*155*).

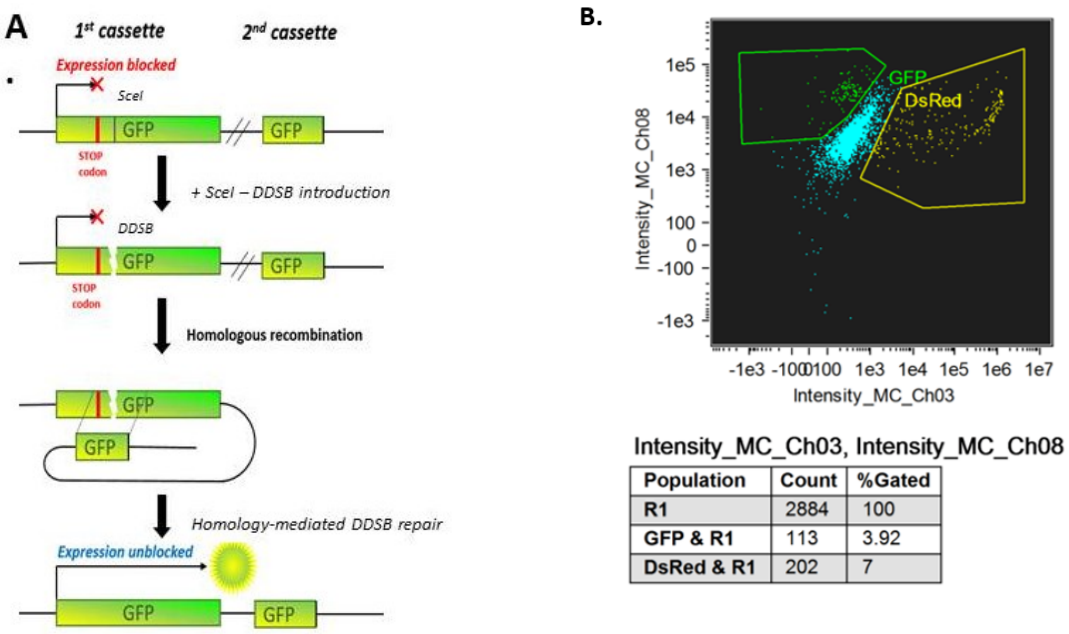

Intensity_MC_Ch03, Intensity_MC_Ch08

Population	Count	%Gated
R1	2884	100
GFP & R1	113	3.92
DsRed & R1	202	7

Figure 25. Determination of the activity of HR by a DR-GFP assay.
The assay is based on two cassette construct stably incorporated into the U2 OS genome A. The first cassette contains the complete GFP coding sequence with a premature STOP codon at the 5´ end disabling expression of fully functional GFP and unique SceI recognition site. The second cassette contains incomplete coding sequence of GFP complementary to the 5´-region of the first cassette without the premature stop codon. The site specific DDSB is introduced to the first cassette by SceI endonuclease. If the DDSB is repaired by HR using the second cassette as a template the premature stop codon is removed and expression of GFP is unblocked. B. The activity of HR is subsequently scored by flow cytometry as a number of GFP positive cells in relation to the internal control – number of dsRed positive cells.

The cells were seeded onto the 6-well plate and cultivated under the standard cultivation conditions till reaching approximately 75% of sub-confluency. A day before transfection the cultivation medium was replaced with fresh one. Two hours prior to the transfection the cultivation media was replaced by 0.5 ml of serum free OPTI-MEM medium. The cells were co-transfected by 0.5 µg of highly pure circular pSceI plasmid (expressing the SceI restriction endonuclease) together with 0.2 µg of dsRed plasmid (TAKARA) as an internal control using the chemical transfection with Lipofectamine 3000 as described in Chapter 3.5.3.3.2. After the transfection the cells were recovered for 24 hours under the standard cultivation conditions.

Subsequently, cells were washed by PBS and released by Trypsin/EDTA. The cell suspension was centrifuged at 700 g for 10 minutes at 4°C, media was aspirated and cells washed with ice cold PBS. Finally, the cells were resuspended in 200 µl of PBS and fixed immediately with 4 ml of ice cold 100% ethanol upon continuous mixing.

Prior to the flow cytometry analysis, the cells were spin down by centrifugation 1,000 g for 10 minutes at 4°C, washed twice with PBS and resuspended in 0.5 ml PBS. The cell clumps were removed by filtration and cells were analysed by AMNIS ImageStream X mkII on INSPIRE® software (Amnis – EMD Millipore). The dot plot representing intensity/area ratio parameter was used to gate and analysed the cell samples. The cells exclusively positive for dsRed and for GFP were gated and

counted. The experiment was done in biological replicates while each of them analysed in triplet. The results are expressed as mean ± standard deviation. The activity of HR is quantified directly as a ratio of GFP/dsRed positive cell within sample. The statistical significance was calculated by Mann-Whitney test.

4 Results

4.1 Mutation Analysis of the *PALB2* Gene in Unselected Pancreatic Cancer Patients in the Czech Republic

Sequencing of the *PALB2* gene in 152 unselected PDAC Czech patients revealed three pathogenic truncating mutations (1.97%) – c.509_510del, c.697del, and c.1838del (Table 64, Figure 26). No CNV was identified by MLPA analysis. The mean age at PDAC diagnosis of mutation carriers was significantly lower (50 years; range 48-56) than in non-carriers (63 years; range 40-82; p=0.016). Genotyping of *PALB2* variants in 1,226 control samples by HRM analysis revealed one carrier of c.509_510del (0.08%, p=0.005, genotyped previously by Janatova et al. (*61*)). One of the carriers had a family cancer history of father suffering from gastric cancer at 74 years and mother suffering from unknown cancer at 50 years. Another carrier´s mother had BC at 53 years. Neither of the patients had a family history of PDAC (Table 64).

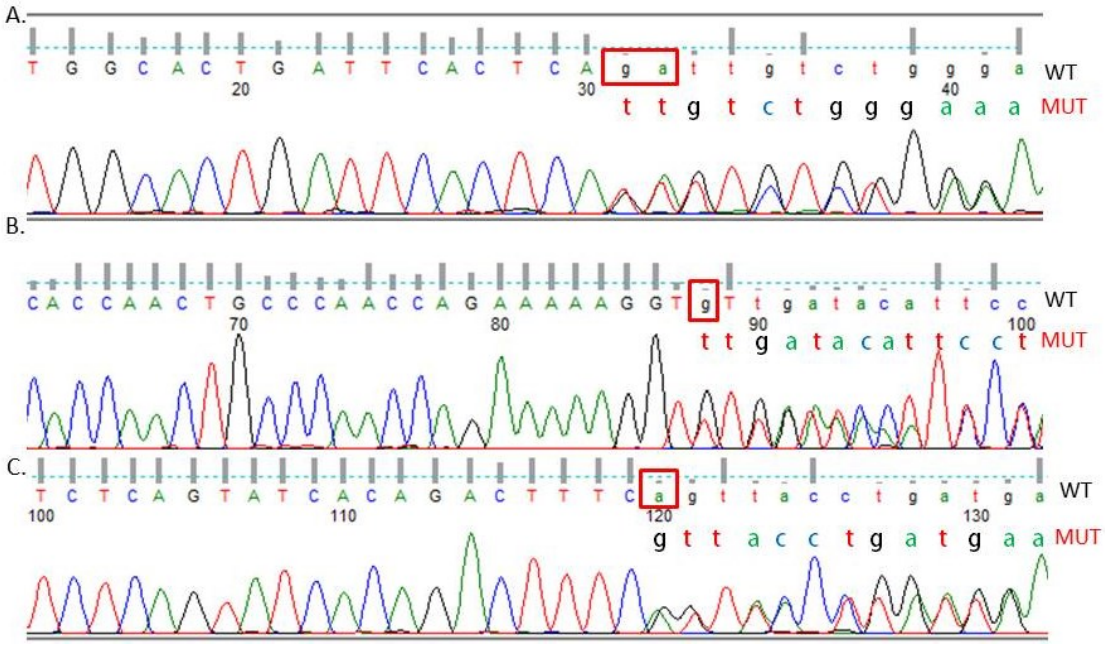

Figure 26. Found *PALB2* truncating mutations visualised by Sanger sequencing.

A. *PALB2* frameshift mutation c.509_510del.
B. *PALB2* frameshift mutation c.697del.
C. *PALB2* frameshift mutation c.1838del.

Patient no.	Nucleotide change	Protein change	Age at PDAC diagnosis; gender	Family cancer history (age at diagnosis)	Controls (N=1,226)	References
PC110391	c.509_510del	p.Arg170IlefsTer14	48; male	0	1	(*60, 61, 158-162*)
PC110074	c.697del	p.Val233LeufsTer5	50; male	M-unknown tumour (50); F-gastric (74)	0	(*163, 164*)
PC110511	c.1838del	p.Gln613LeufsTer23	56; male	M-breast (53)	0	Novel

Table 64. List of truncating *PALB2* variants found in 152 unselected Czech patients with PDAC.
M – mother; F – father. Since our article was published the mutation c.509_510del was found in other BC and OC patients *(92, 165-172)*.

Other 13 single nucleotide variants (SNVs) were detected. Three of them were considered pathogenic by all 6 prediction programs (Table 65). Patient carrying c.2816T>G (p.Leu939Trp) variant was a female diagnosed at 63. The functional studies described this variant as likely benign (*173-176*) and classification in ClinVar database ranges from benign to uncertain significance (class 1-3). The variant c.2993G>A (p.Gly998Glu) is classified as benign or likely benign (class 1-2) because of high population frequency. Two male patients with this variant were diagnosed at 51 and 68 years. Their family medical reports were not available. The novel variant c.3494C>T (p.Ser1165Leu) identified in a male patient diagnosed with PDAC at 50 years with no family cancer history was classified as of uncertain significance in a ClinVar database. The same ClinVar status also had a variant c.3508C>T (p.His1170Tyr) which was considered pathogenic by five prediction programs and found in a male patient of 60 years old with unknown family medical history.

Nucleotide change	Protein change	Variant frequency		Variant prediction							
		PDAC patients (N=152)	ExAC*	SIFT	PP-2	MA	Phylop	GERP	CADD scaled	Spidex	ClinVar class
c.1010T>C	p.Leu337Ser	0.023	0.019	0.04	0.18	1.95	0.43	2.61	11.35	-0.04	1-3
c.1572A>G	p.Ser524=	0.003	0.004	NA	NA	NA	NA	NA	1.33	0.05	1-2
c.1676A>G	p.Gln559Arg	0.066	0.100	1	0	-0.76	-0.61	-2.73	0.08	0.33	1-2
c.2014G>C	p.Glu672Gln	0.013	0.028	0.15	0.05	2.80	0.41	1.83	10.78	0.01	1-2
c.2379C>T	p.Gly793=	0.003	0	NA	NA	NA	NA	NA	0.53	-0.01	2-3
c.2590C>T	p.Pro864Ser	0.003	0.004	0.58	0.16	1.39	0.36	2.82	19.49	0.96	1-2
c.2794G>A	p.Val932Met	0.003	0.008	0.29	0.99	1.58	1.45	4.85	25.30	-0.12	1-2
c.2816T>G	**p.Leu939Trp**	**0.003**	**0.002**	**0**	**1.00**	**2.36**	**2.23**	**5.81**	**29.40**	**-0.08**	**2-3**
c.2993G>A	**p.Gly998Glu**	**0.007**	**0.021**	**0**	**1.00**	**2.36**	**2.77**	**5.84**	**27.70**	**0.61**	**1-2**
c.3300T>G	p.Thr1100=	0.013	0.028	NA	NA	NA	NA	NA	13.44	3.92	1-2
c.3494C>T	**p.Ser1165Leu**	**0.003**	**0**	**0**	**1.00**	**2.24**	**2.80**	**5.90**	**31.00**	**NA**	**3**
c.3495G>A	p.Ser1165=	0.010	0.001	NA	NA	NA	NA	NA	14.23	NA	2
c.3508C>T	p.His1170Tyr	0.003	0	0.79	0.98	2.08	2.80	4.86	24.00	NA	3

Table 65. List of identified *PALB2* SNVs found in 152 unselected Czech patients with PDAC.
* – Allele frequency in European non-Finnish population. RED – prediction values above threshold limits (Table 15). **BOLD** – variants with at least six prediction programs values above threshold.

4.2 The c.657_661del Variant in the *NBN* Gene Predisposes to Pancreatic Cancer

A heterozygous germline mutation c.657_661del of *NBN* gene was revealed in PDAC patient BRCA1291 (diagnosed at 64 years) from multiple cancer family (Figure 27) in our laboratory. The presence of the mutation was also detected in a sample of the proband´s sister FFPE gastric tumour confirming the segregation of the mutation with cancer phenotype in the family.

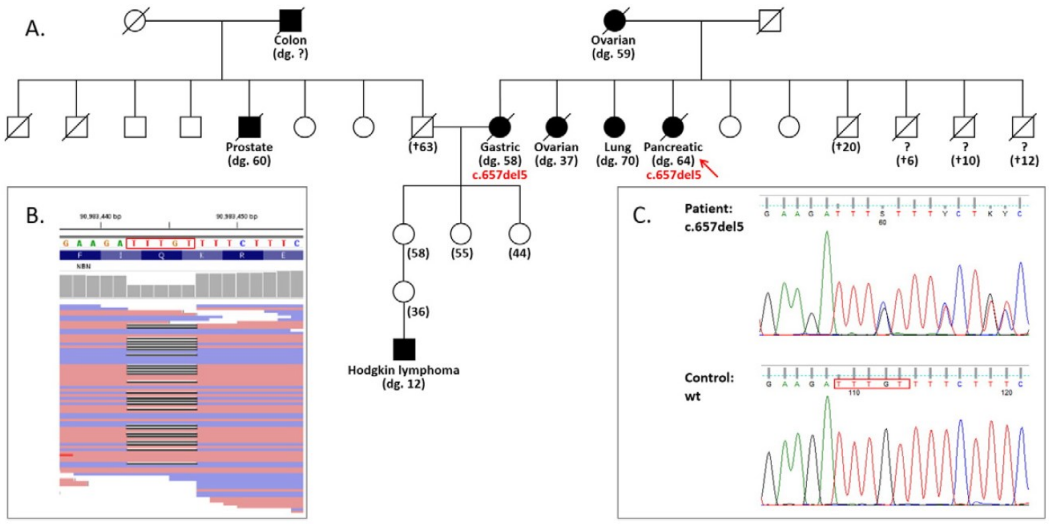

Figure 27. Sequencing and segregation of mutation *NBN* c.657_661del in BRCA1291 family.

A. A family tree of the multiple cancer family showing the proband with PDAC (marked by an arrow) and her sister, both carrying c.657_661del. The ages of cancer diagnosis (dg.) or death (†) are indicated.
B. The deletion showed in IGV software.
C. The deletion showed by Sanger sequencing.

In a following experiment we genotyped *NBN* c.657_661del mutation in 241 PDAC patients by HRM analysis and detected five carriers (2.08%). In contrast, frequency in 915 non-cancer controls was significantly lower (2/915; 0.2%; p=0.006; genotyped previously by Mateju et al. (*149*)). Our results showed that this *NBN* mutation increases the PDAC risk (OR=9.7; 95% CI 1.9-50.2; p=0.0006). The mean age at diagnosis of the mutation carriers was 65.8 years (ranged 59-73) and non-carriers 63.5 years (range 38-84). Characteristics of *NBN* mutation carriers PDAC patients are summarised in Table 66.

Patient No.	Gender	Age at PDAC diagnosis	Family cancer history (age at diagnosis)
PDAC patient from a multiple cancer family			
BRCA1291	Female	64	M-ovarian (59); S1-gastric (58); S2-ovarian (37); S3-lung (70)
Unselected PDAC patients			
PC110023	Male	65	S-gastric
PC110231	Female	73	None
PC110235	Female	59	None
46PA	Female	64; BC at 46	None
61PA	Male	68	None

Table 66. Characteristics of PDAC patients carrying *NBN* mutation.
M – mother; S – sister.

4.3 Germline Multi-gene Panel Testing in PDAC Patients

Sequencing of 113 unselected PDAC patients on CZECANCA panel revealed over 200,000 variants. The initial prioritisation according to Chapter 3.3.3 resulted in a set of 629 variants. This included 32 deletion/insertion, 8 nonsense, 1 CNV, 6 splicing, 345 missense, and 237 silent variants. Pathogenic mutations were checked in IGV software and those in PDAC/HBOC genes were confirmed by Sanger sequencing.

Study	PDAC patients (N)	Frequency of mutations	Panel (N genes)	Country	PDAC predisposition genes						Genes predisposing to both HBOC and PDAC									
					APC	*CDKN2A*	*FANCC*	*FANCG*	*MUTYH*	*PRSS1*	*ATM*	*BRCA1*	*BRCA2*	*EPCAM*	*MLH1*	*MSH2*	*MSH6*	*PALB2*	*PMS2*	*STK11*
fPDAC patients; 8.58% (82/956) in PDAC genes; 9.52% (91/956) in all main predisposing genes																				
Jones et al. (2009)(*28*)	1	100%	WES	USA	0	0	0	0	0	0	0	0	0	0	0	0	0	1	0	0
Roberts et al. (2012)(*11*)	2	100%	WGS/WES	USA	0	0	0	0	0	0	2	0	0	0	0	0	0	0	0	0
Grant et al. (2013)(*78*)	5	40%	WES	Canada	0	0	0	0	0	0	1	0	0	0	0	0	0	1	0	0
Grant et al. (2015)(*66*)	71	1.41%	13	Canada	0	0	-	-	-	0	1	0	0	-	0	0	0	0	0	0
Roberts et al. (2016)(*79*)	638	7.99%	WGS	USA	1	4	3	4	0	0	19	2	5	0	0	1	0	5	1	0
Takai et al. (2016)(*80*)	54	9.26%	21	Japan	-	-	-	-	0	-	2	0	3	-	1	0	0	2	0	0
Chaffee et al. (2018)(*81*)	185	14.05%	25	USA	0	4	-	-	0	-	6	2	8	0	0	1	0	1	1	0
Mutations (N)					**1**	**8**	**3**	**4**	**0**	**0**	**31**	**4**	**16**	**0**	**1**	**2**	**0**	**10**	**2**	**0**
Tested patients (N)					**902**	**902**	**646**	**646**	**885**	**717**	**956**	**956**	**956**	**831**	**956**	**956**	**956**	**956**	**956**	**956**
Carrier frequency					**0.11**	**0.89**	**0.46**	**0.62**	**0.00**	**0.00**	**3.24**	**0.42**	**1.67**	**0.00**	**0.10**	**0.21**	**0.00**	**1.5**	**0.21**	**0.00**
Sporadic or unselected PDAC patients; 7.15% (688/9,624) in PDAC genes; 8.58% (826/9,624) in all main predisposing genes																				
Grant et al. (2015)(*66*)	180	3.89%	13	Canada	0	0	-	-	-	0	1	1	1	-	0	0	0	0	0	0
Hu et al. (2015)(*67*)	96	13.54%	22	USA	-	0	-	-	-	-	4	1	2	-	0	0	2	0	0	0
Susswein et al. (2016)(*68*)	190	10.53%	6 - 29	USA	0	1	0	-	2	-	8	0	5	0	1	0	0	3	0	0
Humphris et al. (2017)(*69*)	385	2.60%	WGS/WES	Aus/USA/Italy	0	0	0	0	0	0	1	0	7	0	0	0	0	1	1	0
Mandelker et al. (2017)(*70*)	176	24.43%	76	USA	7	3	-	-	3	-	5	6	11	0	0	0	0	1	0	0
Shindo et al. (2017)(*71*)	854	3.63%	32	USA	-	1	0	0	-	0	10	3	12	-	2	0	0	2	0	0
Brand et al. (2018)(*72*)	298	9.73%	32	USA	0	1	-	-	0	-	10	4	4	0	0	0	1	1	1	0
Grant et al. (2018)(*73*)	437	8.01%	WES/WGS	USA/Canada/Aus	0	0	2	0	1	0	5	4	17	0	1	1	1	1	0	0
Hu et al. (2018a)(*74*)	3,030	8.28%	21	USA	-	10	8	-	-	-	69	18	59	0	5	1	7	12	2	-
Hu et al. (2018b)(*75*)	1,256	14.33%	7 - 49	USA	1/1,133	14/1,057	-	-	0/708	-	46/1,213	12/1,184	44/1,184	0/1,190	1/1,186	3/1,190	12/1,190	20/1,217	1/1,190	0/1,637
Young et al. (2018)(*76*)	274	5.84%	14- 59	USA	0/274	1/274	-	-	0/213	-	4/274	1/274	3/274	-	0/274	0/274	2/274	2/274	0/274	1/274
Yurgelun et al. (2019)(*77*)	289	9.34%	24	USA	1	2	-	-	-	0	4	3	4	-	0	1	2	1	0	0
LaDuca et al. (2020)(*65*)	2,046	7.48%	5 - 49	USA	0/1,313	16/1,249	-	-	0/489	-	36/1,344	11/1,324	45/1,324	0/1,343	1/1,343	2/1,343	5/1,343	18/1,352	4/1,343	0/1,345
Our study	113	13.27%	219	Czech	0	0	0	0	0	-	1	3	5	0	0	0	0	1	-	0
Mutations (N)					**9**	**49**	**10**	**0**	**6**	**0**	**204**	**67**	**219**	**0**	**11**	**8**	**32**	**63**	**9**	**1**
Tested patients (N)					**4,788**	**8,628**	**5,009**	**1,789**	**3,009**	**2,145**	**8,879**	**8,830**	**8,830**	**7,162**	**8,851**	**8,855**	**8,855**	**8,891**	**8,742**	**6,274**
Carrier frequency					**0.19**	**0.57**	**0.20**	**0.00**	**0.20**	**0.00**	**2.30**	**0.76**	**2.48**	**0.00**	**0.12**	**0.09**	**0.36**	**0.71**	**0.10**	**0.02**

Table 67A. Overview of NGS studies on germline mutations among PDAC patients.

Study	PDAC patients (N)	Frequency of mutations	Panel (N genes)	Country	HBOC predisposition genes									
					BARD1	*BRIP1*	*CDH1*	*CHEK2*	*NBN*	*NF1*	*PTEN*	*RAD51C*	*RAD51D*	*TP53*
fPDAC patients; 8.58% (82/956) in PDAC genes; 9.52% (91/956) in all main predisposing genes														
Jones et al. (2009)(*28*)	1	100%	WES	USA	0	0	0	0	0	0	0	0	0	0
Roberts et al. (2012)(*11*)	2	100%	WGS/WES	USA	0	0	0	0	0	0	0	0	0	0
Grant et al. (2013)(*78*)	5	40%	WES	Canada	0	0	0	0	0	0	0	0	0	0
Grant et al. (2015)(*66*)	71	1.41%	13	Canada	-	-	-	-	-	-	-	-	-	0
Roberts et al. (2016)(*79*)	638	7.99%	WGS	USA	0	2	0	1	0	1	0	0	0	2
Takai et al. (2016)(*80*)	54	9.26%	21	Japan	0	0	0	0	0	-	0	0	-	0
Chaffee et al. (2018)(*81*)	185	14.05%	25	USA	1	0	0	1	1	-	0	0	0	0
Mutations (N)					**1**	**2**	**0**	**2**	**1**	**1**	**0**	**0**	**0**	**2**
Tested patients (N)					**885**	**885**	**885**	**885**	**885**	**646**	**885**	**885**	**831**	**956**
Carrier frequency					**0.11**	**0.23**	**0.00**	**0.23**	**0.11**	**0.15**	**0.00**	**0.00**	**0.00**	**0.21**
Sporadic or unselected PDAC patients; 7.15% (688/9,624) in PDAC genes; 8.58% (826/9,624) in all main predisposing genes														
Grant et al. (2015)(*66*)	180	3.89%	13	Canada	-	-	-	-	-	-	-	-	-	1
Hu et al. (2015)(*67*)	96	13.54%	22	USA	1	0	0	2	1	-	0	0	0	0
Susswein et al. (2016)(*68*)	190	10.53%	6 - 29	USA	0	0	0	0	0	-	0	0	0	0
Humphris et al. (2017)(*69*)	385	2.60%	WGS/WES	Aus/USA/Italy	0	0	0	0	0	0	0	0	0	0
Mandelker et al. (2017)(*70*)	176	24.43%	76	USA	0	0	0	7	0	-	0	0	0	0
Shindo et al. (2017)(*71*)	854	3.63%	32	USA	-	0	-	-	-	-	-	0	0	1
Brand et al. (2018)(*72*)	298	9.73%	32	USA	1	0	0	5	0	0	0	0	0	1
Grant et al. (2018)(*73*)	437	8.01%	WES/WGS	USA/Canada/Aus	0	0	0	0	2	0	0	0	0	0
Hu et al. (2018a)(*74*)	3,030	8.28%	21	USA	4	5	1	33	4	4	0	3	0	6
Hu et al. (2018b)(*75*)	1,256	14.33%	7 - 49	USA	2/552	2/552	1/584	13/563	2/552	0/467	0/749	0/689	0/689	6/1,252
Young et al. (2018)(*76*)	274	5.84%	14- 59	USA	0/213	0/213	0/213	2/274	0/274	0/147	0/213	0/213	-	0/274
Yurgelun et al. (2019)(*77*)	289	9.34%	24	USA	-	3	0	3	1	-	0	1	0	1
LaDuca et al. (2020)(*65*)	2,046	7.48%	5 - 49	USA	1/479	1/480	1/502	8/491	1/479	1/415	0/509	0/480	0/416	1/1,370
Our study	113	13.27%	219	Czech	0	1	0	3	1	0	0	0	0	0
Mutations (N)					**9**	**12**	**3**	**76**	**12**	**5**	**0**	**4**	**0**	**17**
Tested patients (N)					**6,258**	**7,113**	**6,313**	**6,342**	**6,319**	**5,292**	**6,485**	**7,250**	**6,973**	**8,944**
Carrier frequency					**0.14**	**0.17**	**0.05**	**1.20**	**0.19**	**0.10**	**0.00**	**0.06**	**0.00**	**0.19**

Table 67B. Overview of NGS studies on germline mutations among PDAC patients, 2nd part. Aus – Australia.

4.3.1 Mutation in PDAC/HBOC Genes

All PDAC genes which harboured pathogenic mutations were simultaneously members of HBOC genes group. Therefore these two groups were joined into PDAC/HBOC genes group. Together we identified fifteen (15/113; 13.27%) pathogenic mutations in PDAC/HBOC genes in 15 patients. Ten of them (10/113; 8.85%) were among known PDAC associated predisposing genes. PDAC/HBOC genes pathogenic mutations included 12 truncating mutations, 1 CNV (recurrent *CHEK2* deletion of exons 9 and 10), and 2 missense variants described as pathogenic in ClinVar database (Table 68). There were no splice-site mutations in PDAC/HBOC genes.

Gene	Nucleotide change	Protein change	Patient no.	Variant frequency		PDAC genes	HBOC genes
				Controls (N=766)	ExAC*		
Truncating mutations							
ATM	c.7327C>T	p.Arg2443Ter	PKM1585	0	0	Y	Y
BRCA1	c.3770_3771del	p.Glu1257GlyfsTer9	BRCA2971	0	$0.15x10^{-4}$	Y	Y
	c.2263G>T	p.Glu755Ter	BRCA249	0	0		
	c.2411_2412del	p.Gln804LeufsTer5	PKM1156	0	0		
BRCA2	c.1813dup	p.Ile605AsnfsTer11	PKM1478	0	$0.47x10^{-4}$	Y	Y
	c.1989del	p.Phe663LeufsTer5	PKM309	0	0		
	c.3545_3546del	p.Phe1182Ter	PKM439	0	$0.60x10^{-4}$		
	c.7415dup	p.Cys2473ValfsTer2	BRCA3793	0	0		
BRIP1	c.1328_1334del	p.Cys443SerfsTer5	PKM2089	0	0	N	Y
CHEK2	c.1100del	p.Thr367MetfsTer15	PKM764	$6.53x10^{-4}$	$23.41x10^{-4}$	N	Y
NBN	c.657_661del	p.Lys219AsnfsTer16	BRCA1291	$10x10^{-4}$	$3.22x10^{-4}$	N	Y
PALB2	c.509_510del	p.Arg170IlefsTer14	PKM1552	$6.53x10^{-4}$	$1.05x10^{-4}$	Y	Y
CNV							
CHEK2	c.909-2028_1095+330del	Δ9-10	PKM1597	0	0	N	Y
Missense mutations							
BRCA2	c.475G>A	p.Val159Met	BRCA129	0	0	Y	Y
CHEK2	c.917G>C	p.Gly306Ala	PKM641	0	$1.05x10^{-4}$	N	Y

Table 68. Pathogenic mutations in PDAC/HBOC genes found during NGS sequencing of PDAC patients.
* – Allele frequency in European non-Finnish population; Δ – deletion of exons.

Two missense variants were considered pathogenic based on ClinVar database and functional analysis results. The *BRCA2* variant c.475G>A (p.Val159Met) is a variant altering splicing and resulting in in-frame skipping of exon 5. It has been previously found in a Czech HBOC family (*177*). Variant in *CHEK2* gene c.917G>C (p.Gly306Ala) is localised in a protein kinase domain and it was classified as pathogenic by a functional assay in our recent work (*178*).

The control group of 766 non-cancer individuals from Czech Republic was sequenced with CZECANCA panel and underwent the same variant prioritisation as our patient´s cohort. To find out the association of particular genes with PDAC incidence we calculated the OR comparing frequencies of mutations in the patients and control groups. The association between *BRCA1*, *BRCA2* and *CHEK2* genes pathogenic variants and PDAC was statistically significant (p-value <0.05). Together they represent 73.3% (11/15) of PDAC/HBOC pathogenic variants (Figure 28). Mutations in genes *ATM, BRIP1, NBN*, and *PALB2* were found only in one patient each.

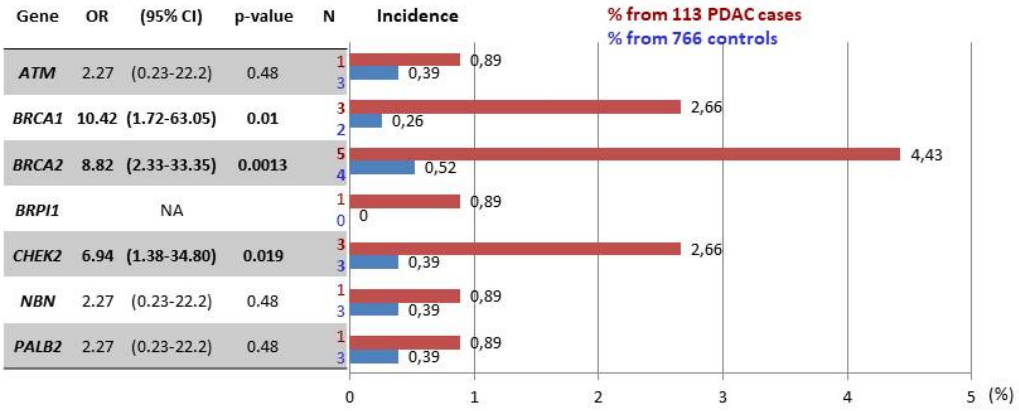

Figure 28. Frequency of mutations and associated PDAC risks of pathogenic germline mutations in known PDAC/HBOC predisposition genes.
N – number of found mutations; statistically significant OR are in **bold**.

Remaining 55 missense variants in PDAC/HBOC genes were further prioritised according to the ClinVar database and to the seven prediction programs. Seven variants were predicted as pathogenic by at least six programs (Table 69). Three of them were classified as VUS in ClinVar. Functional analysis will be necessary for further characterisation of these VUSs.

Gene	Nucleotide change	Protein change	Patient no.	Variant frequency		Variant prediction							
				Controls (N=766)	ExAC*	SIFT	PP-2	MA	Phylop	GERP	CADD scaled	Spidex	ClinVar class
BRCA1	c.5005G>T	p.Ala1669Ser	PKM1462	$6.53x10^{-4}$	$0.75x10^{-4}$	0.00	1.00	1.93	2.60	5.24	24.70	-0.42	1-3
	c.536A>G	p.Tyr179Cys	PKM1270	0	$3.30x10^{-4}$	0.00	1.00	2.00	2.30	5.16	24.70	-0.09	1
BRIP1	c.139C>G	p.Pro47Ala	PKM152 PKM654	0	$3.90x10^{-4}$	0.00	1.00	2.51	2.62	5.26	25.20	0.75	2-3
MLH1	c.794G>A	p.Arg265His	PKM497	0	$0.45x10^{-4}$	0.00	1.00	4.45	2.70	5.70	32.00	-0.96	2-3
NBN	c.602A>T	p.Asp201Val	BRCA815	0	0	0.00	0.99	2.09	2.23	5.84	28.40	-0.11	3
PALB2	c.3296C>G	p.Thr1099Arg	PKM1066	$6.53x10^{-4}$	$0.60x10^{-4}$	0.00	1.00	2.18	2.94	6.14	26.50	-12.07	3
	c.3278T>C	p.Ile1093Thr	PKM58	0	$0.15x10^{-4}$	0.00	0.97	2.10	2.37	6.14	26.70	0.69	3

Table 69. List of missense variants in PDAC/HBOC genes meeting the threshold criteria in at least six prediction tools.
RED – prediction values above threshold (Table 15). * – European non-Finnish population.

4.3.2 Mutations in Other Genes

We have found 20 carriers (20/113; 17.70%) of pathogenic mutations in genes not yet associated with PDAC or HBOC risk (Other genes). These included 15 truncating, 5 splicing, and 2 missense variants described as pathogenic in ClinVar database (Table 70). Two patients were carriers of two such mutations (*LIG4* c.1271_1275del and *SMARCA4* c.4323_4337delinsGC; and *ATRIP* c.1152_1155del and *SMARCE1* c.816+2T>A) and one patient was also a *CHEK2* mutation heterozygote (*CHEK2* c.917G>C and *LIG4* c.2359C>T).

The OR calculations were only available for 9 out of 20 genes, because of lack of mutations in a control cohort. No OR was statistically significant. *LIG4* seems the most promising candidate gene with three mutation carriers in patients and no carrier in controls (Figure 29). Out of the other genes, *FAN1* is the only one already associated with PDAC occurrence. Smith el al. also suggested FAN1 missense variant c.149T>G (p.Met50Arg) as pathogenic (*179*).

Gene	Nucleotide change	Protein change	Patient no.	Variant frequency	
				Controls (N=766)	ExAC*
Truncating mutations					
ATRIP	c.1152_1155del	p.Gly385Ter	PKM1177	$10x10^{-4}$	$0.75x10^{-4}$
DNAJC21	c.1501del	p.Lys501AsnfsTer10	PKM600	$6.53x10^{-4}$	$4.96x10^{-4}$
ERCC5	c.2680G>T	p.Glu894Ter	PKM1593	0	$0.49x10^{-4}$
FAN1	c.922_923del	p.Val308CysfsTer5	PKM2140	0	$2.10x10^{-4}$
LIG4	c.2440C>T	p.Arg814Ter	PKM654	0	$1.05x10^{-4}$
	c.2359C>T	p.Gln787Ter	PKM641	0	0
	c.1271_1275del	p.Lys424ArgfsTer20	PKM2166	0	$1.80x10^{-4}$
MSH5	c.1561C>T	p.Arg521Ter	PKM845	0	$0.15x10^{-4}$
PIK3CG	c.88del	p.Ala30ProfsTer41	PKM1446	0	0
PPM1D	c.1288del	p.Val430Ter	PKM1318	0	0
PRF1	c.185_195del	p.Asp62ValfsTer12	PKM771	0	0
RAD54B	c.7C>T	p.Arg3Ter	PKM994	0	$2.71x10^{-4}$
SETX	c.5308_5311del	p.Glu1770IlefsTer15	PKM1774	0	$0.16x10^{-4}$
SMARCA4	c.4323_4337delinsGC	p.Ser1442ArgfsTer49	PKM2166	0	0
ZNF365	c.1065G>A	p.Trp355Ter	PKM965	0	$0.60x10^{-4}$
Splicing mutations					
EXT2	c.1038+1G>A	–	PKM1164	0	0
HELQ	c.2677-1G>A	–	PKM400	0	$4.06x10^{-4}$
NAT1	c.102-1G>C	–	PKM1499	0	0
RET	c.2136+2T>G	–	BRCA2831	0	0
SMARCE1	c.816+2T>A	–	PKM1177	0	0
Missense mutations					
HOXB13	c.251G>A	p.Gly84Glu	PKM1925	$6.53x10^{-4}$	$31.20x10^{-4}$
TELO2	c.2296G>A	p.Val766Met	PKM1167	$6.53x10^{-4}$	$3.82x10^{-4}$

Table 70. Pathogenic mutations in Other genes found during NGS sequencing of PDAC patients.
* – Allele frequency in European non-Finnish population.

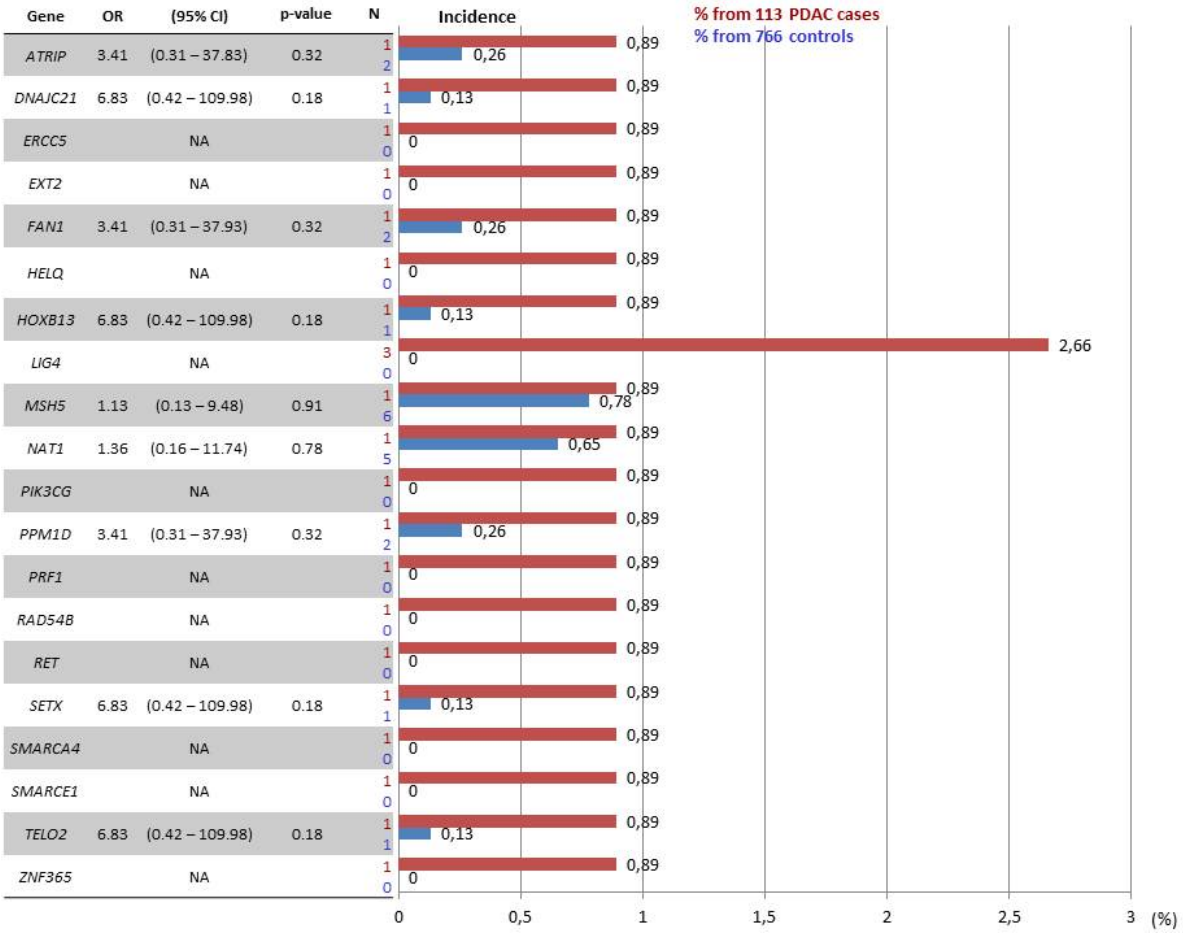

Figure 29. Frequency of mutations and associated PDAC risks of pathogenic germline mutations in „Other genes".
N – number of found mutations; statistically significant OR are in **bold**.

Out of 290 missense variants only 38 were suggested as pathogenic by at least six prediction programs (Table 71), among them eight were classified as VUS in ClinVar database.

Gene	Nucleotide change	Protein change	Patient no.	Variation frequency		Variant prediction							
				Controls (N=766)	ExAC*	SIFT	PP-2	MA	Phylop	GERP	CADD scaled	Spidex	ClinVar class
ALK	c.4738AG>	p.Gly1580Arg	PKM1837	0	$0.15x10^{-4}$	0.00	1.00	2.13	2.32	4.69	27.10	0.00	3
ATMIN	c.643G>A	p.Glu215Lys	PKM873	0	$13.61x10^{-4}$	0.17	0.99	2.32	2.70	5.71	29.50	-2.20	–
BABAM1	c.844G>A	p.Val282Met	BRCA2726	0	0	0.00	0.94	2.25	1.39	4.10	25.30	0.00	–
BLM	c.2474C>T	p.Pro825Leu	PKM764	0	0	0.00	1.00	3.27	2.40	5.16	27.60	-0.26	3
	c.3872C>T	p.Pro1291Leu	PKM1774	0	$0.15x10^{-4}$	0.03	0.28	2.40	1.47	4.96	23.00	-2.74	3
EGFR	c.1606G>A	p.Val536Met	PKM1639	0	0	0.00	0.88	2.99	1.58	5.19	24.20	-0.57	–
EPHX1	c.466G>A	p.Glu156Lys	PKM994	0	0	0.00	1.00	3.94	2.77	5.84	32.00	-0.06	–
EXO1	c.505A>C	p.Thr169Pro	BRCA3793	0	0	0.00	1.00	4.44	2.27	5.93	27.30	-0.79	–
EYA2	c.782C>T	p.Pro261Leu	PKM1145	0	$1.58x10^{-4}$	0.00	1.00	2.71	2.86	6.03	27.50	-2.17	–
FAN1	c.149T>G	p.Met50Arg	PKM1446	$6.53x10^{-4}$	$25.64x10^{-4}$	0.01	0.97	1.91	2.08	5.15	25.60	-0.54	–
FANCA	c.2968G>T	p.Asp990Tyr	BRCA2971	0	0	0.00	0.97	2.34	1.34	4.25	23.10	2.03	–
FANCG	c.626C>T	p.Thr209Ile	PKM62	0	0	0.00	1.00	2.18	2.78	5.88	25.90	-0.50	–
FANCI	c.1412C>G	p.Pro471Arg	PKM774	0	$1.20x10^{-4}$	0.00	1.00	2.28	2.81	5.95	29.10	0.12	3
FH	c.994G>A	p.Ala332Thr	PKM1721	0	0	0.00	0.97	4.21	2.71	5.73	29.00	1.45	3
GATA2	c.30G>T	p.Trp10Cys	PKM1585	0	$1.88x10^{-4}$	0.00	1.00	2.55	2.15	4.72	34.00	-0.07	3
GRB7	c.796C>T	p.Arg266Trp	PKM1156	0	$0.15x10^{-4}$	0.00	1.00	2.34	2.57	5.47	32.00	-1.19	–
KIT	c.2012A>G	p.Glu671Gly	PKM158	0	0	0.00	0.99	2.90	2.27	5.93	32.00	0.25	–
LIG3	c.790C>T	p.Arg264Trp	BRCA2726	0	$0.45x10^{-4}$	0.03	1.00	2.42	0.79	2.65	25.70	-0.05	–
LRIG1	c.2195C>T	p.Pro732Leu	PKM771	0	$5.10x10^{-4}$	0.00	0.99	1.98	2.70	5.74	24.90	0.01	–
	c.2618G>C	p.Gly873Ala	BRCA2726	0	0	0.04	0.77	2.22	2.81	5.96	25.10	-4.12	–
MCPH1	c.362C>T	p.Pro121Leu	BRCA2008	0	0	0.00	1.00	2.71	2.73	5.49	26.10	-1.35	–
MRE11A	c.818C>G	p.Ser273Cys	PKM1403	$10x10^{-4}$	$1.65x10^{-4}$	0.00	0.93	3.32	2.72	5.45	26.60	0.29	–
MSH5	c.436C>T	p.Arg146Cys	BRCA2781	$6.53x10^{-4}$	$1.42x10^{-4}$	0.00	1.00	2.02	2.78	5.87	32.00	-0.42	–
MSR1	c.905C>T	p.Pro302Leu	PKM1837	0	0	0.03	0.93	2.38	1.11	3.47	25.30	-5.79	–
	c.881G>A	p.Gly294Glu	BRCA3228 PKM2057	0	$10.09x10^{-4}$	0.00	1.00	3.68	2.63	4.87	24.60	2.86	–
NF2	c.1022G>A	p.Arg341Gln	PKM1462	0	0	0.00	0.97	2.38	1.40	4.65	24.90	-1.17	3
PLA2G2A	c.185G>A	p.Arg62His	PKM350 PKM1585	$6.53x10^{-4}$	0	0.02	0.89	3.01	1.41	4.29	24.30	-6.12	–
POLD1	c.1385T>G	p.Val462Gly	PKM1499	0	0	0.01	0.71	2.64	1.92	4.76	30.00	-2.22	–
PRF1	c.529C>T	p.Arg177Cys	PKM845	0	$1.05x10^{-4}$	0.05	0.88	2.39	0.62	3.50	24.90	-0.21	–
RAD9A	c.254G>C	p.Arg85Pro	PKM908	0	0	0.00	0.99	2.75	2.03	3.63	26.60	-0.35	–
RFC1	c.698A>G	p.Asp233Gly	PKM915	0	0	0.14	1.00	2.14	1.06	4.70	25.80	-12.09	–
RECQL5	c.1261G>A	p.Gly421Arg	PKM497	$10x10^{-4}$	$4.92x10^{-4}$	0.00	0.99	3.37	2.73	5.76	27.90	-0.48	–
SMAD4	c.479A>G	p.Asp160Gly	BRCA129	0	0	0.05	0.92	1.94	2.33	5.77	27.50	-1.10	3
TLR2	c.787G>T	p.Asp263Tyr	PKM492	0	0	0.03	1.00	2.41	2.80	5.61	23.10	0.00	–
TSHR	c.1351T>C	p.Phe451Leu	PKM1639	0	0	0.00	1.00	2.51	2.20	5.74	29.10	0.00	–
XRCC5	c.1357G>T	p.Ala453Ser	PKM641	0	0	0.04	1.00	3.02	1.37	4.72	25.20	-0.21	–

Table 71. List of missense variants in Other genes meeting the threshold criteria in at least six prediction tools.
RED – prediction values above threshold (Table 15). * – European non-Finnish population.

4.3.3 Clinical and Histopathological Characteristics of Mutation Carriers

Median age at diagnosis of PDAC/HBOC genes pathogenic mutations carriers and non-carriers was 61.1 (range 47-82 years) and 64.0 (range 39-92.6 years; p=0.6356) respectively. Patients carrying pathogenic mutation in Other genes had median age of diagnosis 62.5 years (range 47-76.8) and patients not carrying any pathogenic mutation among Other genes had median age of diagnosis 64.2 years (range 39-92.6; p=0.6063) (Figure 30).

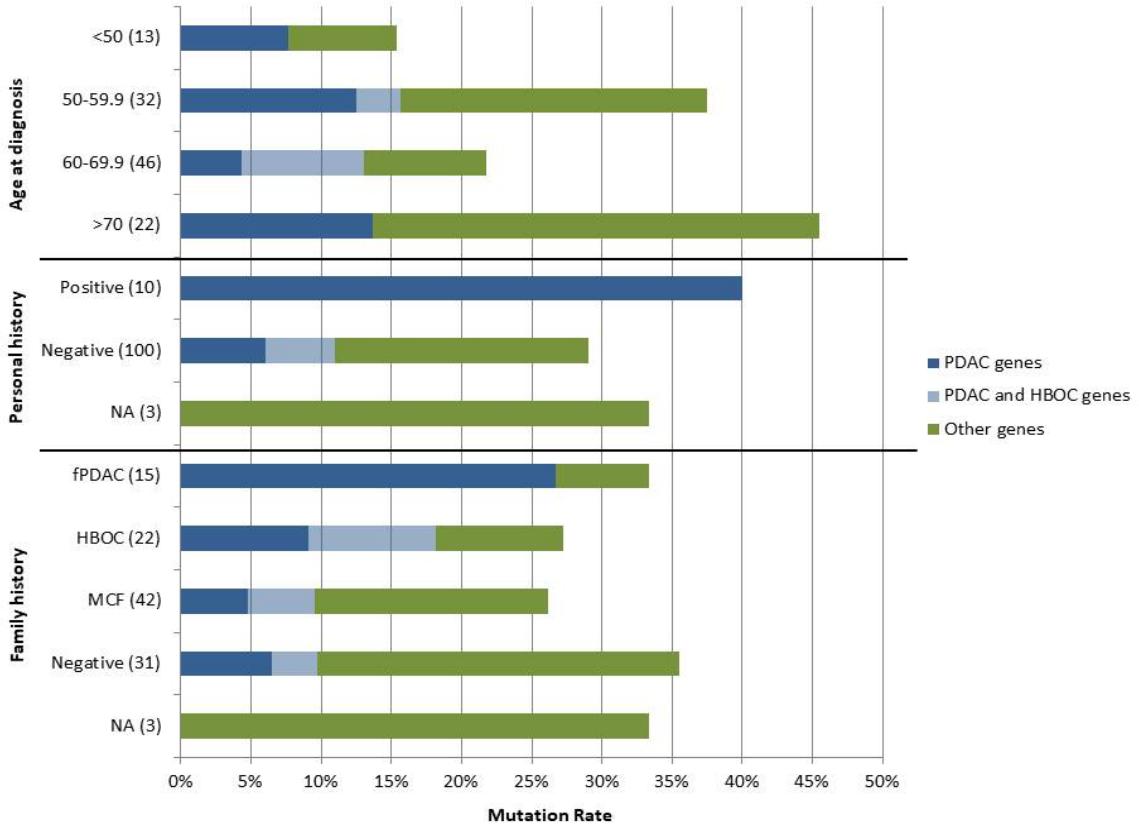

Figure 30. Percentage of pathogenic mutation carriers in subgroups based on personal/family history and age of diagnosis.
Patients with two mutations were counted once (patient with *CHEK2* as HBOC mutated and other two patients into Other genes group). In brackets is number of patients in specific subgroup.

The highest frequency of pathogenic mutations in PDAC/HBOC genes was in patients diagnosed with PDAC between 50-59.9 years (15.63%). Frequency of Other genes mutations was the highest among patients diagnosed after 70 years of age (31.82%). The lowest frequency of mutations was in patients diagnosed before 50 years (7.69%) for both PDAC/HBOC genes and for Other genes (Figure 30).

Among 10 patients who developed second primary cancer we found four mutations – all of them in *BRCA1/2* genes. Patient with *BRCA2* missense variant c.475G>A (p.Val159Met) had bilateral male BC at 70 and 74 years. PDAC cancer was diagnosed at 82 years. Patient with *BRCA2* c.7415dup was diagnosed with BC at 62 – ten years prior the diagnosis of PDAC. Carrier of *BRCA1* c.2263G>T (p.Glu755Ter) was diagnosed at 55 years while already having a personal history of BC (47 years) and OC (41 years). Patient with *BRCA1* c.3770_3771del was diagnosed at 47 years with both PDAC and OC.

Mutation frequency also correlated with family cancer history – 26.67% of patients with positive PDAC family history displayed PDAC genes mutations. Patients from families with history of BC and/or OC cancers diagnosis carried PDAC/HBOC genes mutations in 18.18% of cases (Figure 30).

In agreement with literature most of the patients (60.18%) had PDAC localised to head of pancreas (*180*) and 10.29% of them were carriers of PDAC/HBOC genes mutations (Figure 31). Among tumours localised to body of pancreas (14.16%) there were no germline mutation of PDAC/HBOC genes, only three variants in Other genes. In tumours localised to tail of pancreas (14.16%) we found three mutations in HBOC/PDAC genes and one mutation in Other genes. Diagnosis were determined from cytology therefore about half (50.44%) of tumours do not have specified grade status. PDACs are generally diagnosed in late stages thus there are 4.43% of tumours with grade one, 22.12% with grade two and 23.01% with grade three. The PDAC/HBOC genes mutations were found in 20% of grade one (1/5), 16% of grade two (4/25), and 7.69% of grade three (2/26) tumours.

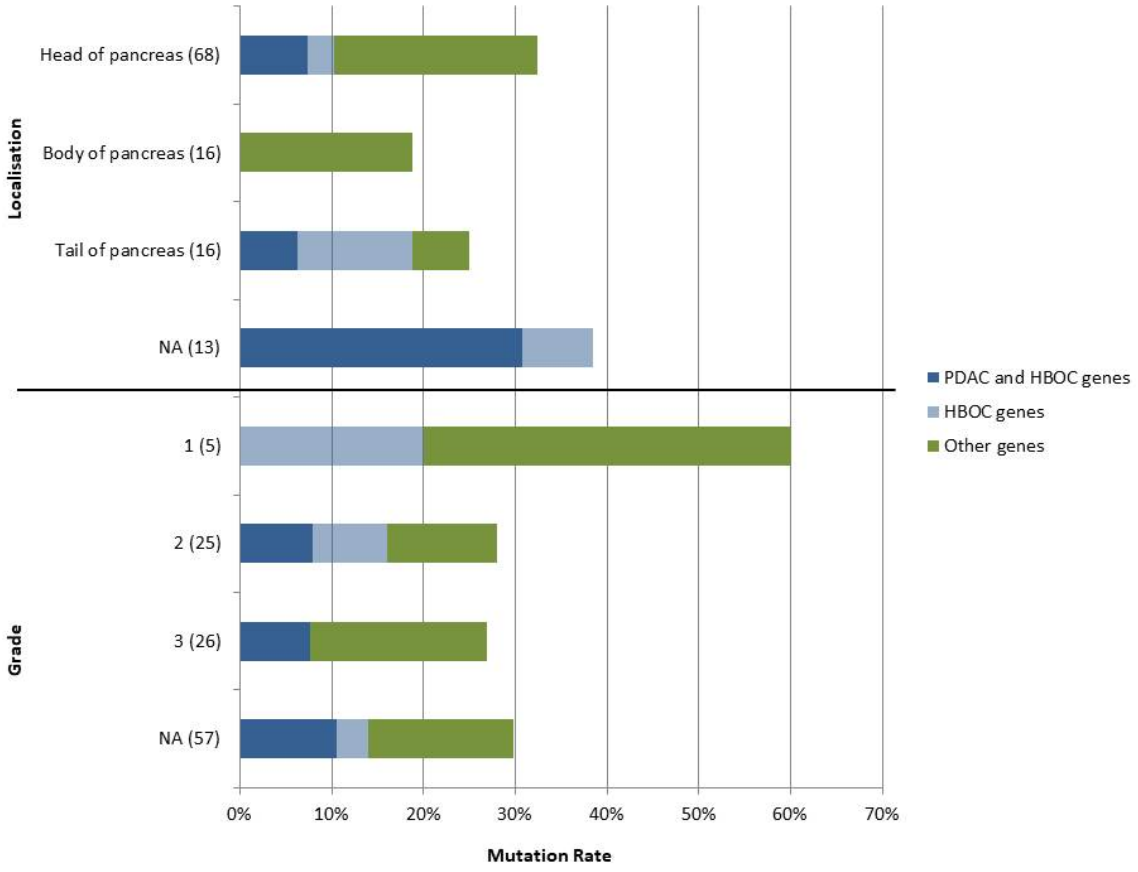

Figure 31. Percentage of pathogenic mutation carriers in clinicopathological subgroups.
Patients with two mutations were counted once (patient with *CHEK2* as HBOC mutated and other two patients into Other genes group). In brackets is number of patients in specific subgroup.

4.4 Genetic Analysis of Second Neoplasms in PDAC Long-term Survivors

Among 118 PDAC patients resected in University Hospital Olomouc between years 2006-2011 only 22 (18.64%) patients survived more than five years after surgery and 20 of them were analysed by NGS sequencing with CZECANCA panel. The mean age at PDAC diagnosis was 61.7 (range 44-75 years). A second malignant neoplasm (SMN) was developed by six of them (27.27%) within the median time to

SMN diagnosis 52.5 months after PDAC diagnosis. SMNs included prostate, urinary bladder, breast, malignant melanoma, and two rectal cancers. Two patients suffering from rectal cancers deceased before DNA samples could be collected.

Four patients out of 20 analysed long-term surviving PDAC patients harboured deleterious mutations in PDAC/HBOC genes (20.0%). One patient developed BC as a SMN and carried *CHEK2* deleterious missense variant c.349A>G (p.Arg117Gly) classified as likely/pathogenic in ClinVar database and confirmed by functional analysis (*178*). The remaining three patients did not develop any SMN. One patient harboured frameshift mutation in *ATM* c.3849del and nonsense variant c.390C>G (p.Tyr130Ter) in *MLH1* and had a positive family cancer history. Splicing variant in *RAD51D* c.345+2T>C had a patient whose mother had gastric cancer. Patient carrying c.1100del in *CHEK2* gene had no further family or personal cancer history (Table 72).

Patient	Gene	Nucleotide change	Protein change	Age at diagnosis; gender	SMN (age at diagnosis)	Family history
OL0138	*CHEK2*	c.349A>G	p.Arg117Gly	70; Female	Breast (71)	–
OL0132	*ATM*	c.3849del	p.Leu1283fs	52; Female	–	F – colon; FM – brain
	MLH1	c.390C>G	p.Tyr130Ter			
OL0130	*RAD51D*	c.345+2T>C	–	62; Male	–	M – gastric
PCI77	*CHEK2*	c.1100del	p.Thr367fs	55; Male	–	–

Table 72. List of found pathogenic mutations in long-term surviving PDAC patients.
F – father; M – mother; FM – father´s mother

Patient	Gene	Nucleotide change	Protein change	ExAC*	Variant prediction							
					SIFT	PP-2	MA	Phylop	GERP	CADD scaled	Spidex	ClinVar class
With SMN												
OL0134	*BLM*	c.11T>C	p.Val4Ala	$31.62x10^{-4}$	0	0.13	2.14	2.25	5.89	23.50	-1.87	1-3
OL0135	*PTCH1*	c.2597G>A	p.Gly866Glu	0	0.08	1.00	2.31	2.77	5.32	30.00	0.11	3
	ATM	c.3208G>A	p.Val1070Ile	0	0.35	0.03	2.14	1.51	4.72	21.60	0.06	3
OL0136	***PLA2G2A***	**c.185G>A**	**p.Arg62His**	**0**	**0.02**	**0.89**	**3.01**	**1.41**	**4.29**	**24.30**	**-6.12**	–
	LRIG1	**c.2195C>T**	**p.Pro732Leu**	**$5.10x10^{-4}$**	**0**	**0.99**	**1.98**	**2.70**	**5.74**	**24.90**	**0.01**	–
	RECQL5	c.1801G>A	p.Val601Met	0	0.30	0.04	1.91	2.53	5.39	23.20	-0.41	–
OL0138	*PREX2*	c.1672C>G	p.Pro558Ala	$2.10x10^{-4}$	0.15	0.15	0.46	2.63	5.59	22.10	0.06	–
	PARP1	c.659C>T	p.Ala220Val	$0.15x10^{-4}$	0.15	0.01	1.16	0.73	3.43	20.60	0.01	–
Without SMN												
OL0041	*BUB1B*	c.1042G>A	p.Ala348Thr	$0.15x10^{-4}$	0.33	0.85	2.18	2.77	5.85	26.50	0.24	–
	MRE11A	c.1475C>A	p.Ala492Asp	$50.52x10^{-4}$	0.43	0.75	1.74	1.48	4.97	23.00	0.73	1-3
OL0130	*XRCC1*	c.632A>G	p.Tyr211Cys	0	0.15	1.00	2.18	2.17	5.37	22.20	-1.64	–
OL0132	*GRB7*	c.1439T>C	p.Val480Ala	$6.74x10^{-4}$	0	0.85	3.70	1.85	3.75	25.80	-0.43	–
	RAD9A	c.215G>A	p.Arg72His	$0.30x10^{-4}$	0.58	0.02	1.20	1.00	3.30	22.90	-2.13	–
OL0133	***EXT2***	**c.1859C>T**	**p.Thr620Met**	**$7.661x10^{-4}$**	**0.02**	**1.00**	**2.24**	**2.40**	**5.15**	**25.30**	**-0.68**	**2-3**
	MLH3	c.3281-1G>C	–	0	NA	NA	NA	2.75	5.81	34.00	-25.64	–
OL0137	*PREX2*	c.2167A>G	p.Asn723Asp	$0.30x10^{-4}$	0.03	0.61	1.63	2.25	5.89	26.40	0.01	–
	HELQ	**c.1418G>A**	**p.Arg473His**	**$0.15 x10^{-4}$**	**0**	**1.00**	**4.55**	**2.64**	**5.31**	**32.00**	**-0.28**	–
	RFC4	c.908C>T	p.Ala303Val	$1.50x10^{-4}$	0.44	0.03	1.24	2.7	4.87	22.70	-1.41	–
OL0139	*RHBDF2*	c.940G>A	p.Ala314Thr	$9.57x10^{-4}$	0.33	0.95	1.78	2.60	5.54	24.70	0.16	–
	MDM4	c.1162C>G	p.Pro388Ala	$1.93x10^{-4}$	0.92	1.00	1.10	0.96	4.30	19.59	NA	–
OL0140	***FANCM***	**c.3407T>C**	**p.Leu1136Ser**	**$0.30x10^{-4}$**	**0.01**	**0.96**	**1.91**	**2.13**	**4.89**	**24.80**	**-0.06**	–
	POLE	**c.1601T>C**	**p.Leu534Pro**	**0**	**0**	**0.99**	**3.57**	**2.17**	**5.67**	**26.90**	**0.09**	–
OL0142	***RAD54L***	**c.1817G>A**	**p.Arg606Gln**	**$0.45x10^{-4}$**	**0**	**1.00**	**4.74**	**2.50**	**5.19**	**33.00**	**-0.61**	–
	POLD1	c.2116C>G	p.Pro706Ala	0	0.01	0.73	2.41	2.19	4.38	25.10	-0.02	3
OL0144	*CWF19L2*	c.2240A>C	p.Lys747Thr	0	0.08	0.70	1.92	2.29	4.53	26.30	0.82	–
	SETX	c.967A>G	p.Ser323Gly	$0.30x10^{-4}$	0	0.99	0.98	2.37	6.17	24.50	-0.07	–
OL0157	*TP53BP1*	c.2226A>T	p.Glu742Asp	$3.36x10^{-4}$	0.48	0.99	0.46	2.01	5.30	23.50	-0.01	–
PC115	*PTCH1*	c.3376G>A	p.Val1126Ile	$7.81x10^{-4}$	0.26	0.93	1.77	2.84	5.44	22.80	-0.02	3
	NCAM1	c.1481C>A	p.Thr494Asn	0	0.01	0.35	NA	1.49	3.58	22.40	0.16	–
PCO11	*BRCA1*	c.3929C>A	p.Thr1310Lys	0	0.01	0.79	1.90	2.61	5.10	22.20	-0.07	1-3
	AURKA	c.1028G>A	p.Arg343Gln	$3.00x10^{-4}$	0.04	0.03	0.71	2.48	3.82	22.70	0.04	–
	EXO1	c.820G>A	p.Gly274Arg	$27.27x10^{-4}$	0.16	1.00	1.30	2.65	5.64	31.00	-0.37	–

Table 73. List of identified VUSs in long-term surviving PDAC patients.
NA – not applicable. * – European non-Finnish population. RED – prediction values above threshold (Table 15). **BOLD** – potentially deleterious variants (meeting the threshold criteria in at least six prediction tools).

In other genes, we found one splicing mutation (c.3281-1G>C) in *MLH3* gene previously associated with hereditary nonpolyposis colorectal cancer type 7 (HNPCC7), but so far not associated with the occurrence of PDAC (*181*). Furthermore seven of 32 identified missense variants were suggested as pathogenic in at least six prediction programs (Table 73). *FANCM* was recently suggested as BC susceptibility gene (*182*). *PLA2G2A, LRIG1,* and *POLE* genes were associated with colorectal cancer diagnosis (*183-185*) and *EXT2* gene was found mutated in patients with multiple exostoses (*186*).

4.5 Functional Characterisations of *PALB2* Missense Variants

4.5.1 Preparation of CRISPRs

CRISPR-mediated targeted genome modification was used to introduce sequence alterations into the genome of model cell line. Guiding RNAs for each of the studied variant were designed and their off-targets were checked in CRISPOR software tool. Their sequences were ligated into expression vector backbone px462 according to the standard protocols and checked by sequencing (Figure 32). The px462-based Nickase construct was successfully prepared for each of the analysed *PALB2* sequence alteration. Together, 14 individual px462-based Nickases were prepared.

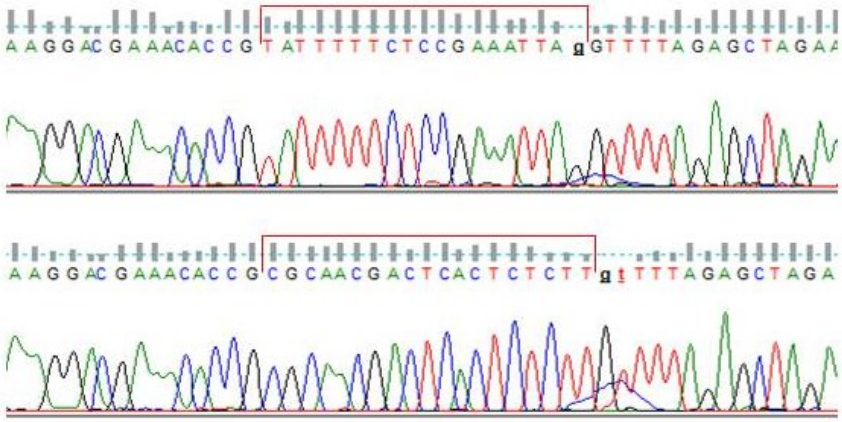

Figure 32. An example of gRNA designed for c.3228T>A mutation incorporated into CRISPR px462 vector backbone.
gRNA sequences: TATTTTTCTCCGAAATTAG and CGCAACGACTCACTCTCTT.

4.5.2 Preparation of Donor Sequences

The donor sequence for CRISPR-based genome modification was prepared in the form of circular plasmid. Donor sequence with homology arms was ligated into the pCR2.1 vector backbone and desired sequence alteration was subsequently introduced by a SDM (Figure 33). Donor sequence in the vector construct was prepared for each of the analysed sequence alteration.

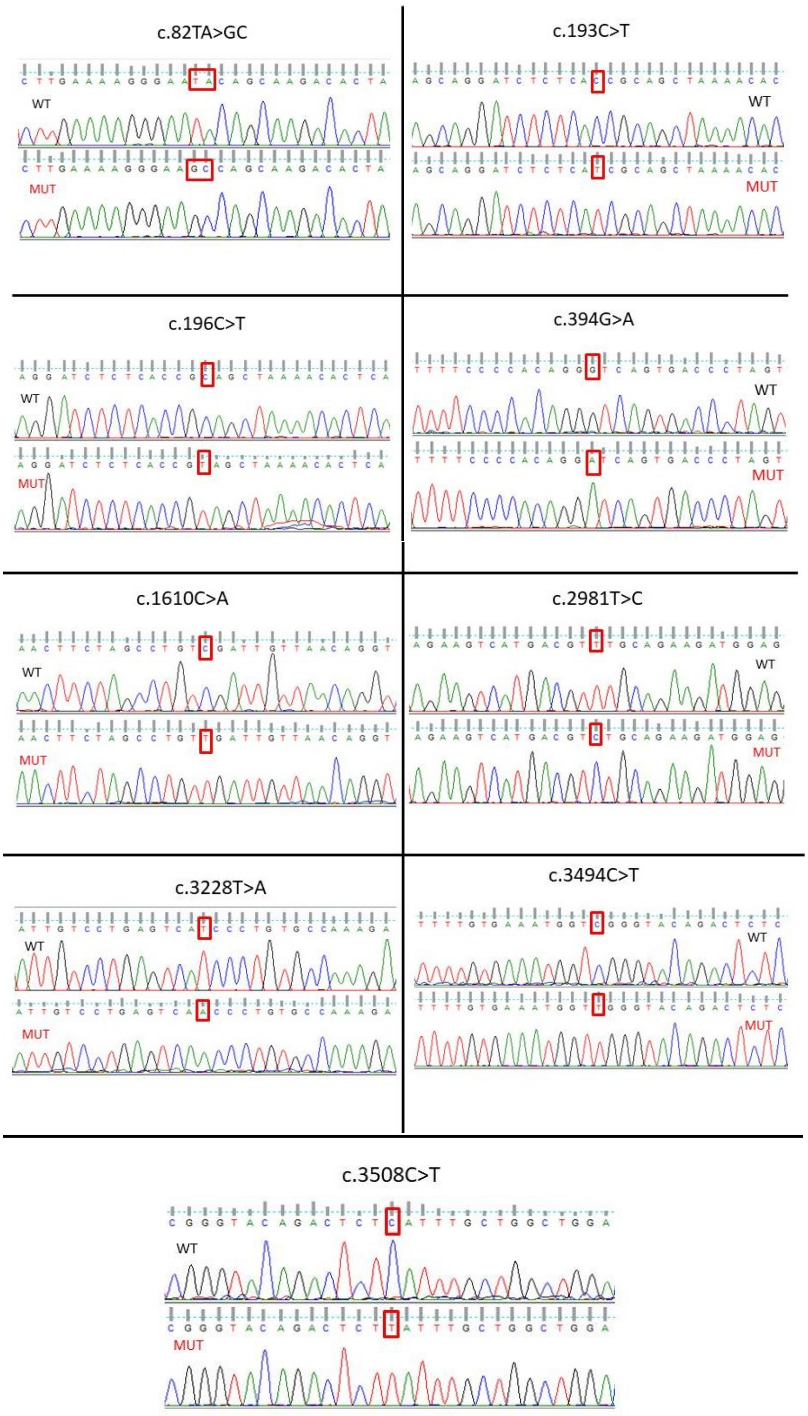

Figure 33. Donor construct for CRISPR-based genome modification.
The donor sequence for homology mediated DNA repair was prepared by ligation of portion of *PALB2* gene homologous to the region adjacent to the analysed sequence alteration. The donor consists of left and right homology arms with the sequence alteration in the middle. The analysed variant was introduced by a SDM. The donor construct was fully sequenced to prove the presence of particular sequence alteration.

4.5.3 Optimisation of Transfection

The functional analysis of sequence alteration was based on the selection of single-cell clones with targeted CRISPR-based knock-in. The clone selection is critical step highly dependent on the transfection efficiency and the viability and clonogenic potential of transfected cells. Thus, the

transfection of used model cells was optimised prior to the genome modification with respect to the above mention cell parameters. The optimal ratio of DNA and transfection reagent Lipofectamine 3000 together with total time of transfection was tested using the pMAX-GFP plasmid. The transfection efficiency was checked by fluorescent microscopy and scored by flow cytometry. The viability of cells was checked by crystal violet staining.

The optimal condition for chemical transfection by Lipofectamine 3000 reagent was selected with respect to the highest transfection efficiency and cell viability (Table 74; Figure 34). The highest transfection efficiency was reached with the Lipofectamine 3000 to circular DNA ratio 1:2 with a total transfection incubation time 24 hours. However, the cell viability and hence the cell clonogenic potential were significantly lower with the longer transfection. Regarding the critical importance of these cell parameters for further planed single-cell clone selection the shorter and slightly less efficient transfection conditions were preferred. Additionally, it was found that linear DNA is highly toxic for the cells decreasing the viability under the optimal transfection condition to less than 40%. Contrary to that the circular DNA was well tolerated by the model cell. With respect for the further planed genome modification the circular DNA donor were co-transfected with CRISPR px462 constructs.

Time	**24 hours**								
Sample	**1**	**2**	**3**	**4**	**5**	**6**	**7**	**8**	**9**
DNA (ng)	500			1,000			2,000		
Lipofectamine 3000 Reagent (µl)	0.8	1	1.5	0.8	1	1.5	0.8	1	1.5
Efficiency (%)	21±0.8	28±0.4	29±0.5	24±0.9	25±1	31±0.9	30±1	36±0.8	38±1.2
Viability (%)	82±3.5	84±3.9	85±4.4	85±3.6	82±4	82±5	78±3.8	82±3.3	80±4.2

Table 74A. Transfection optimisation.
Two separate parameters – total transfection time (24, or 48 hours) and Lipofectamine 3000 to DNA ratio were took into account within transfection optimisation. The optimal transfection condition after 24 or 48 hours incubation with Lipofectamine 3000 reagent was determined by scoring efficiency (counting GFP positive cells by flow cytometry) and viability (crystal violet staining) in three independent measurements.

Time	**48 hours**								
Sample	**10**	**11**	**12**	**13**	**14**	**15**	**16**	**17**	**18**
DNA (ng)	500			1,000			2,000		
Lipofectamine 3000 Reagent (µl)	0.8	1	1.5	0.8	1	1.5	0.8	1	1.5
Efficiency (%)	24±1.1	29±1.5	29±1.8	30±2	33±0.9	39±1.1	33±2	39±2	38±2.5
Viability (%)	77±4.9	76±4.1	74±4.2	72±4	70±5.1	70±5.7	68±4.6	70±3.9	68±4.4

Table 74B. Transfection optimisation, 2nd part.

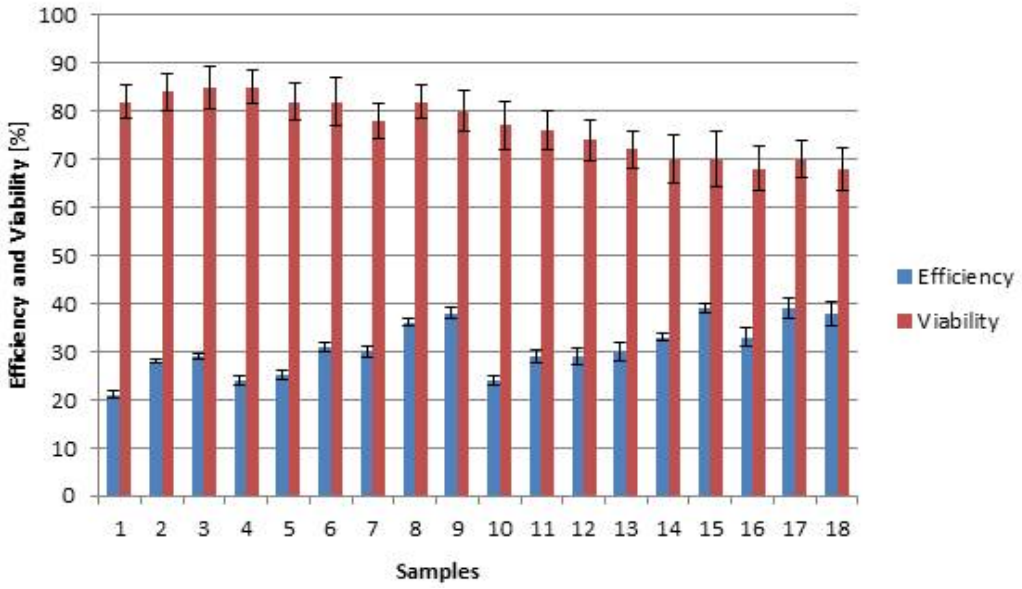

Figure 34. The results of transfection optimisation.
For the further experiments the conditions of sample 8 (24 hours, 1 µl of Lipofectamine 3000 Reagent and 2,000 ng of circular DNA) were chosen. Results are shown as mean value ± standard deviation.

4.5.4 Selection of Modified Clones

The CRISPR-Cas9 genome editing experiment plus knock-out was performed two times for each variant. From each separate experiment approximately one hundred single-clones were selected and individually analysed by the sequencing of the targeted region (in case of knock-in experiments) and by the fluorescent microscopy (in case of knock-out experiment). Despite the large number of analysed clones (almost 900) only two clones were found to harbour heterozygous mutations *PALB2* c.82_83delinsGC and c.3494C>T (Figure 35). Cells from transfection experiments with plasmids from Santa Cruz Biotechnology were checked by fluorescent microscopy, but we did not detect any mCherry signals.

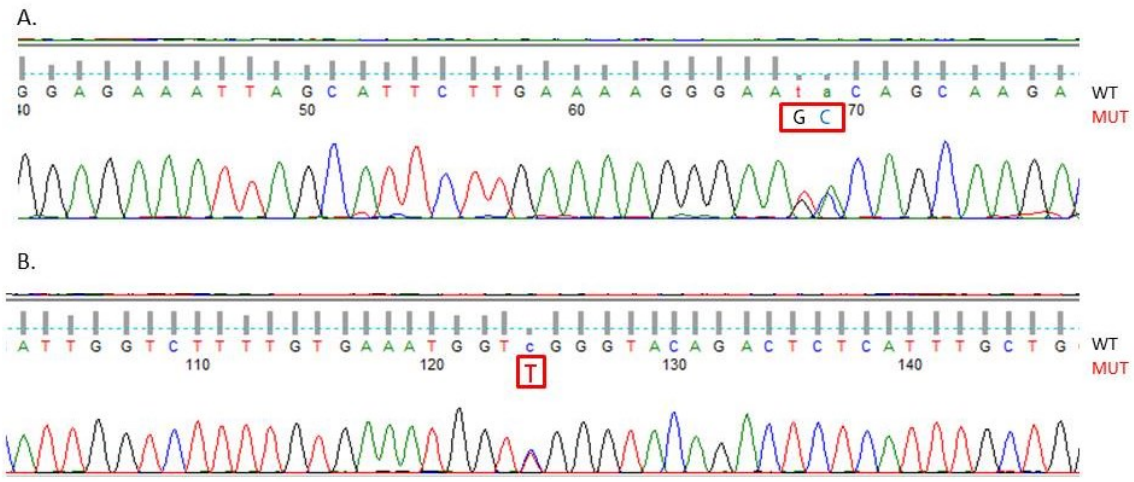

Figure 35. Selection of single-cell clones with modified *PALB2*.
The genome modification was checked by a direct sequencing of target region. Two of the selected clones were found to carry a heterozygous alteration – *PALB2* c.82_83delinsGC and c.3494C>T. The particular sequence alteration (MUT) is highlighted in the electrophereogram with respect to the WT sequence for each of the selected clone.

4.5.5 HR Assay Results

Genome instability is one of the cancer hallmarks. The generally accepted function of the PALB2 protein is its direct participation in the DDSB repair pathway by the HR mechanism. Further the impact of the analysed sequence alteration on the biological activity of the PALB2 protein was analysed by determining the activity of HR. The successfully established U2 OS-based clones harbouring heterozygous alteration were employed for the DR-GFP assay. This indirect assay is based on the scoring of the GFP positive cells, where the fully active GFP is formed only upon effective homology-mediated DDSB repair. Non-transfected U2 OS with the WT form of PALB2 were used as a control.

Cells were co-transfected with pSceI (for site specific induction of DDSB) and dsRed (as an internal control for quantification) plasmids and subsequently analysed by flow cytometry. The experiment was done in triplicate. As expected the highest HR activity was detected within the control cells with WT PALB2. For a relative quantification this was further taken as 100% HR activity. Modified cultures both had lower HR activity compare to WT culture, but neither statistically significant (c.82_83delinsGC – p=1; c.3494C>T – p=0.4).

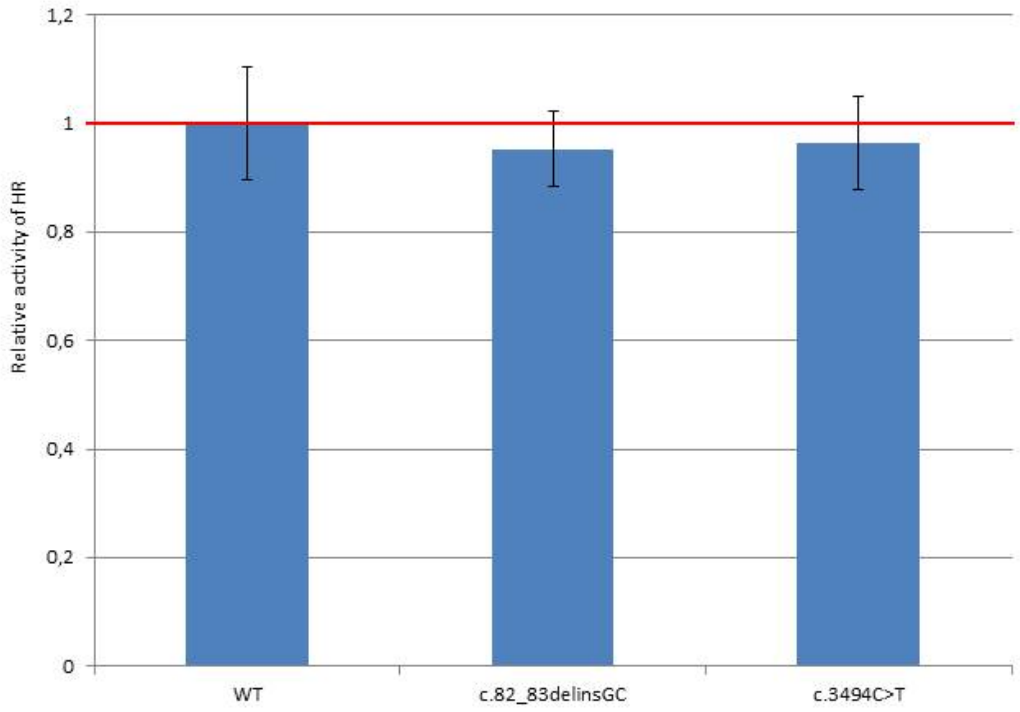

Figure 36. HR activity.
The HR activity was determined by a DR-GFP assay in the stable U2 OS-based clones harbouring the heterozygous alterations of *PALB2* gene c.82_83delinsGC or c.3494C>T. The HR activity in control non-transfected U2 OS cells with WT form of *PALB2* were taken as 100%. The results represent mean of three technical replicates ± standard deviation.

5 Discussion

Advanced genetic testing performed in PDAC patients has revealed a high number of mutation-bearing patients who do not meet the currently established genetic testing criteria for the mutated genes (*72, 187*).

Comparisons of sequencing results can be difficult due to variations in methodology, the selection of genes, and the patients' ethnicities. The mutation spectrum grows larger every year. Patients in sequencing studies are often selected according to changing criteria but are generally categorised as either fPDAC or unselected PDAC patients (Table 67). Recent papers have indicated that the main susceptibility genes among fPDAC patients remain *BRCA2*, *CDKN2A*, and *PALB2* (*11, 28, 66, 78-81*). Strong evidence has also supported the involvement of *ATM,* which, summarised from recent papers, had a 3.24% carrier frequency among fPDAC patients and a 2.30% frequency in unselected PDAC patients (Table 67).

The genetic predisposition to PDAC in the Czech Republic has not yet been extensively studied. After Jones et al. (*28*) suggested that *PALB2* may serve as a PDAC susceptibility gene and Janatova et al. (*61*) reported that 5.5% of hereditary BC patients in the Czech Republic are carriers of *PALB2* germline mutations, we decided to determine *PALB2* germline mutations frequency in Czech PDAC patients.

We identified three *PALB2* truncating mutations among 152 unselected Czech PDAC patients (1.97%), in contrast to a single truncation mutation among the group of 1,226 controls (0.08%; OR=24.66; 95% CI 2.55-238.64; p=0.005) (*61, 153*). This finding suggests that *PALB2* may serve as a high-risk PDAC susceptibility gene. Although this frequency was almost three times higher than the summarised frequencies obtained from the overall sequencing results reported for sporadic or unselected PDAC cases in recent papers (Table 67), this difference was not significant (0.71%; 95% CI 0.88-9.09; p=0.082). The carriers of *PALB2* mutations in our study had significantly lower mean age at diagnosis (51 years) than non-carriers (63 years; p=0.016). Similar results were to those from the study by Salo-Mullen et al. (*188*), who reported that the age at diagnosis of mutation carriers was 58.2 years, whereas the age at diagnosis for non-carriers was 64 years (p=0.02). However, other studies have indicated that the age of PDAC onset does not differ between carriers and non-carriers of pathogenic mutations in predisposition genes (*66, 189*).

All three patients with *PALB2* mutations in our cohort harboured truncating mutations that resulted in the loss of the WD40 domain function, resulting in the formation of a PALB2 protein that was unable to bind BRCA2 protein and perform HR. The patient carrying the c.509_510del *PALB2*

mutation was a 48-year-old male, with no family cancer history. This mutation is known to be a Central and Eastern European founder mutation and has been identified in breast, ovarian, and pancreatic cancer patients (*60, 162*). The *PALB2* c.697del mutation carrier was a 50-year-old male, with a father who suffered from gastric cancer (diagnosed at 74 years) and a mother who was diagnosed with unknown cancer at 50 years. This mutation has been described in patients of Italian and British origin with breast cancer (*163, 164*). The variant c.1838del was a novel mutation, and the patient with this mutation was a male, diagnosed with PDAC at 56 years, with a mother suffering from BC who was diagnosed at 56 years.

Although the frequency of *PALB2* mutation carriers in our study was low, our cohort represented a clinically meaningful population of patients with increased risks of PDAC development. The lack of indicative family cancer histories and the younger age at diagnosis may indicate that the *PALB2* analysis should be offered not only to patients with pancreatic and breast cancer family histories but also to younger patients (the mean age of diagnosis younger than 60 years), regardless of their family cancer history, which could be achieved by the implementation of NGS technologies in clinical settings.

We also identified 13 SNVs, described in the ClinVar database, with classifications ranging from benign to uncertain significance (classes 1-3). Only two of the SNVs identified in the present study were classified as class 3 (Table 65). Both variants, c.3494C>T (p.Ser1165Leu) and c.3508C>T (p.His1170Tyr), showed promising predictive results but were recently included in the functional analysis performed by Wiltshire et al. (*176*) and classified as likely benign. In conclusion, none of the identified SNVs are considered to be pathogenic. Until recently, only a few *PALB2* SNVs that influence *PALB2* splicing were classified as likely pathogenic in the ClinVar database (e.g. c.18G>T; c.48G>A; c.108G>A; c.2559C>T; and c.330G>A).

During previous NGS studies performed by our laboratory, we identified an *NBN* Slavic mutation, c.657_661del, in a PDAC patient. After confirming the segregation of this variant in the patient´s sister, who suffered from gastric cancer, we focused on genotyping this mutation in additional PDAC cases. In contrast with *PALB2*, the *NBN* gene was not previously suggested to be a PDAC susceptibility gene. We identified five mutation carriers among 241 (2.08%) unselected PDAC patients in the Czech Republic, compared with two mutations identified in the non-cancer control cohort (2/915; 0.22%; p=0.006). Our results suggested that *NBN* mutation carriers have an increased risk of developing PDAC (OR=9.65; 95% CI 1.9-50.2; p=0.006) (*140, 149*). The frequency of the c.657_661del mutation in the Czech Republic has been estimated at 0.33% (2/600) among high-risk BC patients (*BRCA1/2* WT) (*149*), at 0.31% (1/325) among other high-risk BC patients (*BRCA1/2/PALB2* WT) (*190*), at 0.84%

(1/119) among lymphoma patients (*135*), and at 0.39% (3/771) among colorectal cancer patients (*145*). The non-cancer control groups in these studies had a combined carrier frequency of 0.20% (4/2,001) (*135, 145, 149, 190*).

None of our patients with *NBN* mutations had any familial history of PDAC. One patient was diagnosed at 65 years, and his sister suffered from gastric cancer, with the confirmed presence of the mutation in tumour tissue. Another patient was diagnosed with PDAC at 64 years and BC at 46 years. These findings indicate that carriers of the c.657_661del mutation may develop a broader spectrum of tumours. The similar mean age at PDAC diagnosis between carriers and non-carriers in our analysis (65.8 and 63.5 years, respectively) suggested that the c.657_661del mutation is likely not associated with earlier disease onset.

A Polish study, from Lener et al. (*139*) suggested that *NBN* may serve as a PDAC susceptibility gene (8/383; 2.09%; OR=3.8; 95% CI 1.68-8.60). Together, in both of our studies combined, we identified 13 carriers of the c.657_661del mutation among 624 PDAC patients of Slavic origin, and 24 carriers were identified among 4,915 controls (OR=4.33; 95% CI 2.2-8.56; p=0.0001). This result suggests that c.657_661del may represent a novel PDAC-susceptibility allele that increases PDAC risk. In recent NGS studies, the frequency of *NBN* mutation carriers among unselected PDAC patients was estimated to be 0.19% ($p=7.13 \times 10^{-10}$; Table 67); however, the enrolled population cohorts were mostly non-Slavic.

To determine the frequency and importance of germline mutations in various known and candidate cancer-associated genes identified in PDAC patients from the Czech Republic, we analysed the mutation status of 219 genes among an additional 113 unselected PDAC patients, using panel-NGS. We identified 37 pathogenic mutations, in 34 PDAC patients (30.09%). Ten mutations (8.85%) were present in known PDAC susceptibility genes: *ATM* (1), *BRCA1* (3), *BRCA2* (5), and *PALB2* (1). An additional five (4.43%) mutations were identified in known HBOC susceptibility genes: *BRIP1* (1), *CHEK2* (3), and *NBN* (1). These findings suggested that a wider range of phenotypes may be associated with germ-line mutations in cancer-susceptibility genes than are currently acknowledged. The frequency of combined HBOC and PDAC gene mutation carriers in our cohort was 13.27% (15/113). In the literature, the germline mutation frequency in PDAC and HBOC susceptibility genes among unselected or sporadic PDAC patients have a combined frequency of 8.58% (range of 2.60%-24.43%, Table 67).

The age of diagnosis of our patients did not differ significantly between carriers of PDAC/HBOC gene mutations and non-carriers (61.1 years vs. 64.0 years, p=0.6356). The highest frequency of pathogenic mutations in PDAC/HBOC genes was identified in patients diagnosed with PDAC between

the ages of 50–59.9 years (15.63%). The lowest frequency was identified in patients diagnosed before the age of 50 years (7.69%). Four patients with mutations in *BRCA1* (2) and *BRCA2* (2) had personal histories of BC and/or OC, and two of them belonged to a subgroup of fPDAC patients.

The most prevalent PDAC/HBOC gene in our study, with five mutations, was *BRCA2* (4.42%), followed by *BRCA1* and *CHEK2,* with three mutations each (2.66%). The frequency of mutations in patients was compared to the frequency of mutations in a set of 766 non-cancer controls. Significant OR values were identified for *BRCA2* (OR=8.82; CI 95% 2.33-33.35; p=0.0013) and *CHEK2* (OR=6.94; CI 95% 1.38-34.80; p=0.019). Both *BRCA1* and *BRCA2* are known as PDAC susceptibility genes. The frequency of *BRCA2* mutations in our cohort (4.42%) was higher than the collective frequency reported among unselected PDAC patients in other NGS studies, which was 2.48% (Table 67). The mutation frequency of *BRCA1* in our cohort (2.66%) was also higher than the 0.76% frequency calculated for unselected PDAC patients in other published NGS studies (Table 67). These differences may be due to the small number of patients in our cohort. *CHEK2* has previously been identified as a susceptibility gene for BC. Recently, *CHEK2* has also been suggested to be a potential PDAC susceptibility gene (*67, 70, 72, 74-77*), with a carrier frequency in sporadic PDAC patients of 1.20% (Table 67). Our data also suggested that *CHEK2* may represent a PDAC susceptibility gene. The association between *CHEK2* mutations and PDAC risk was previously confirmed in a Czech population (*191*). Hu et al. (*74*) found a high frequency of *CHEK2* variants (1.09%; 95% CI 0.75%-1.53%) in 3,030 unselected PDAC patients. However, when compared with gnomAD (genome aggregation database) controls, the association was not significant.

We also identified 20 carriers, who each had one or two pathogenic mutations in genes that are not associated with either PDAC or HBOC cancer susceptibility (20/113; 17.70%). One of these patients was also a carrier for a *CHEK2* mutation. The median age of diagnosis for patients carrying pathogenic mutations was 62.2 years (range 47-82 years), compared with a median age of diagnosis among patients without pathogenic mutation of 64.6 years (range 39-92.6; p=0.953, Figure 30). The OR values for the Other genes group were not significantly associated with PDAC occurrence, which may be due to the small sample number and the low frequency of individual variants.

The most promising *LIG4* (DNA Ligase 4) gene mutations were found in three PDAC patients (frequency 2.66%; the same frequency as *BRCA1* and *CHEK2* mutations) and in no control subjects. LIG4 protein is essential for DDSBs repair by NHEJ. Homozygous mutations result in Lig4 syndrome, which is characterised by microcephaly, immunodeficiency, and growth and developmental delays (*192*). LIG4 protein contains two BRCT motifs (AAs 654-743 and 808-911) on the C-terminus, and their loss prevents interactions with XRCC4 and impairs ligation activity (*193*). A female patient with a

c.2359C>T (p.Gln787Ter) *LIG4* mutation was diagnosed at 60 years old and was also a carrier of the *CHEK2* pathogenic mutation c.917G>C (p.Gly306Ala). Her mother suffered from kidney cancer. Another male patient with the *LIG4* c.2440C>T (p.Arg814Ter) mutation had no family cancer history and was diagnosed with PDAC at 63 years old. The third patient was a female, diagnosed at 53 years old, who had mutations in *LIG4* (c.1271_1275del) and a novel mutation in the *SMARCA4* gene (SWI/SNF-related, matrix-associated, actin-dependent regulator of chromatin, subfamily a, member 4; c.4323_4337delinsGC). Both of her parents suffered from lung cancer (mother – 72 years; father – 82 years) and her paternal grandfather had gastric cancer. Mutations in *SMARCA4* cause rhabdoid tumour predisposition syndrome 2 and have been found in lung cancer patients (*194*).

Among the other mutated genes, *FAN1* (FANCD2/FANCI-associated nuclease 1) has been previously suggested as a colon cancer (*195*) and PDAC susceptibility gene (*179*). Smith et al. (*179*) found one frameshift mutation and two instances of a missense mutation, *FAN1* c.149T>G (p.Met50Arg), in a cohort of 93 high-risk PDAC cases (3.23%; 3/93). Both *FAN1* c.149T>G (p.Met50Arg) mutations segregated with PDAC in families (*179*). This variant affects a highly conserved amino acid residue in the RAD18-like ubiquitin-binding domain. In our cohort, a female patient with the *FAN1* c.149T>G (p.Met50Arg) was identified, who was also a carrier of a frameshift mutation in *PIK3CG* (c.88del), which has not yet been associated with any cancer risk. She was diagnosed at 70 years of age and had no family or personal cancer history. Another *FAN1* mutation, the truncating mutation c.922_923del, was found in a male patient, who was diagnosed at 58 years old, whose mother suffered from skin cancer and whose paternal grandfather suffered from gallbladder cancer. FAN1 is required for the HR repair of ICLs and has been suggested to be a candidate FA gene (*196*). Patients deficient in FAN1 suffer from karyomegalic interstitial nephritis (slow renal failure) (*197*) and display mild sensitivity to MMC (*198*).

Additional sequencing studies are necessary to confirm the roles played by these candidate predisposition genes in PDAC susceptibility.

Researchers are particularly interested in long-term surviving (5+ years) PDAC patients. Approximately 10%-20% of such patients develop SMN (*3, 199-201*), and 75% of their family members develop other malignancies. Compared with 51% from the non-SMNs long-term survival group, these results suggest genetic involvement in tumour development in these patients (*199*). Therefore, we sequenced a unique cohort of 20 five-year PDAC survivors. A subgroup of four (20%) patients also developed SMN (prostate, urinary bladder, BC, and melanoma). Only one of four patients with SMNs had a mutation in a known cancer-predisposing gene. This female patient

developed BC one year after PDAC diagnosis and had a pathogenic missense mutation in *CHEK2* (c.349A>G; p.Arg117Gly).

Four pathogenic mutations in the main cancer-predisposing genes (*ATM*, *CHEK2*, *MLH1*, and *RAD51D*) were found in three patients without SMNs (3/17; 18.75%). A female patient with an *MLH1* mutation, resulting in a Lynch syndrome diagnosis, was also a carrier of an *ATM* mutation. Her father suffered from colon cancer and her father´s mother suffered from brain cancer. Another male patient with a splicing *RAD51D* mutation had a mother with gastric cancer. The *CHEK2* frameshift mutation was present in a male patient with no family cancer history.

Our work represents the first study of genetic alterations in long-term surviving PDAC patients. The higher age at diagnosis (61.7 vs 66.7 years) and long-term survival (14% among unselected PDAC (*202*) vs 20% in our study) were the only risk factors for SMNs. The frequency of mutations between patients with SMNs and those without SMNs appeared comparable (20% vs 18.75%); however, we only had a small number of patients.

The genetic testing of PDAC patients facilitates the identification of high-risk individuals who may benefit from PDAC cancer prevention programs, such as the adoption of a no smoking/alcohol policy and screening for early PDAC stages (endoscopic ultrasonography and/or MRI/magnetic resonance cholangiopancreatography) while therapeutic interventions with curative potential are still available (*203*). Most previously reported PDAC susceptibility genes also increased the risks of other malignancies, and these extra-pancreatic neoplasms can be screened for, even in unaffected relatives, who can be offered appropriate clinical management strategies for extra-pancreatic tumours associated with particular mutations. Understanding the genetic basis of PDAC susceptibility offers opportunities for personalised therapies, as demonstrated by patients whose pancreatic cancers harbour defects in HR, associated with the inactivation of *BRCA1*, *BRCA2*, or *PALB2*. In these patients, targeting DNA repair with PARP inhibitors, platinum compounds, or MMC can result in major therapeutic benefits (*21*). Thus, global genomic analysis can result in the development of customised therapies, tailored to the genetic environments of a patient's tumour and the identification of new biomarkers for drug responses (*204*). Identifying new causative PDAC genes, using NGS techniques, will improve our knowledge regarding PDAC tumorigenesis and contribute to the epidemiological, functional, and clinical applications of these reported mutations, such as improving the estimation of mutation penetrance and revealing potential modifiers of cancer penetrance.

The second part of this work addressed the functional analysis and risk assessment of selected *PALB2* missense VUSs, which were ascertained during the genetic screening of Czech BC and PDAC patients

(*61, 153*). The primary aim of the functional analysis was to determine the influence of missense mutations on PALB2 activity during HR. The basis for this *in vitro* study was the establishment of U2 OS-derived clones with stably modified genomes. The CRISPR-Cas9 system was used to perform targeted genome editing. Subsequently, HR activity was determined using a DR-GFP assay.

Despite repeated attempts at various modifications (for instance, the use of NHEJ-inhibitors) we were unable to select *PALB2* knock-out clones, which were intended to serve as a control for further DR-GFP assays. Homozygous mutations in human *PALB2* are known to result in FA-N, and all patients are believed to carry two null alleles. However, evidence suggests that one of the mutations may be required to be hypomorphic, resulting in the expression of proteins with partial activity. Erkko et al. (*87*) showed that the frequency of heterozygotes expressing the Finnish *PALB2* founder mutation (c.1592del) in the control population was 1/416. The incidence of FA-N patients who are homozygotic for this mutation is therefore 1:692,000, and in a recent Finnish population, eight c.1592del homozygotes should have been identified (*87*). However, no FA-N patients have been diagnosed carrying this mutation, thus far. Xia et al. (*23*) have successfully derived a human *PALB2*-deficient cell culture, EUFA1341, from an FA-N patient's lymphoblasts and fibroblasts, which carry the pathogenic mutation p.Tyr551Ter in exon 4 and a second allele that was inactivated by the large deletion of exons 1-10. The 550-AA-long PALB2 protein expressed in these EUFA1341 cells may possess sufficient residual activity to maintain cell viability (*23*).

Additionally, the generation of *Palb2*-deficient mice has been attempted and has failed due to the massive apoptosis of modified embryonic cells between E9.5 and E12.5 (*205, 206*). The only viable *Palb2*-deficient murine ES (embryonic stem) cells were selected from cells that expressed the first three exons of *Palb2,* in concord with the previously described findings (207). Surprisingly, *p53* or *p21* depletion prior to *Palb2* knock-out significantly decreased embryonic lethality, enabling the development of a conditional *Palb2* knock-out (*206-208*). These findings indicated that Palb2 protein is essential for cell proliferation during embryogenesis and that its depletion leads to embryonic lethality. Although mouse and human PALB2 proteins have only share 58% of AA identity, it could be assumed that functions of these protein isoforms are identical within their respective species. This may explain our failure to knock-out *PALB2* in U2 OS cells, which are p53; p21 +/+ and are, thus, non-viable without PALB2 protein expression. Notwithstanding that, the designed system for genome modification is functional; however, any *PALB2* null clone generated by a targeted CRISPR-based modification is likely to die.

Next, we focused on the establishment of *PALB2* modified cell lines, using the CRISPR system, together with a homology donor sequence. We successfully selected two viable and stable clones

that were heterozygotic for *PALB2* c.82_83delinsGC and c.3494C>T. The efficiencies of genome modification and clone selection were very low, although our selection of clones with two different sequence alterations from the same genome modification system demonstrates that the designed CRISPR-donor system is functional. However, several factors may negatively influence the selection of homozygous clones. First, the preferable pathway for DDSBs repair is NHEJ, which is a competing mechanism with HR. Thus, the CRISPR-mediated induction of site-specific DDSB could be solved rapidly and easily by NHEJ, rather than HR. We attempted to prevent this problem by adding the SCR7 inhibitor of Ligase 4, which is mandatory for the NHEJ-mediated reparation of DNA breaks, during CRISPR transfection (*157*). However, NHEJ inhibition significantly impairs cell viability, which is critically important for single-cell clone selection. Although Maruyama et al. described a 19-fold increase in the efficiency of CRISPR-based genome editing, we were unable to confirm this observation (*157*). Further, the PALB2 protein plays a crucial role during the HR repair mechanism. Thus, the impairment of PALB2 functions while attempting to simultaneously modify its sequence through the CRISPR mechanism may be paradoxical. Finally, cells that are homozygous for PALB2 variants enter apoptosis due to the activation of the p53 pathway, as described and discussed above. Therefore, homozygous clones are less viable and more prone to apoptosis than heterozygous clones, which could result in the preferential growth of heterozygous clones.

We determined the HR activity of the c.82_83delinsGC and c.3494C>T heterozygous clones using the DR-GFP assay. Both modified cultures displayed reduced HR activity compared with *PALB2* WT cultures, although these differences were not significant. Variant c.3494C>T was recently included in a functional study by Wiltshire et al. (*176*) and, although it had a small negative effect on HR repair, they did not classify this variant as pathogenic. This variant occurs within the WD40 protein binding domain and, thus, could have severe effects on the ability of PALB2 to bind BRCA2, RAD51, and other proteins. A homozygous variant in the CC domain of *PALB2,* c.82_83delinsGC (p.Tyr28Ala), was designed to disrupt BRCA1-PALB2 interactions and impair the HR repair of DDSBs (*156*). A slightly different variant, p.Tyr28Cys, was studied by Wiltshire et al. (*176*), which demonstrated an effect on HR repair that did not exceed the threshold for pathogenic variants. The criteria for pathogenic variants are very narrow. Variants outside the pathogenic window might not have immediate effects on HR, but they can result in the accumulation of DNA lesions and DNA instability over time.

The results of this study showed that the designed model system is functional; however, the efficiency of genome modification was very low. Therefore, the designed model system may not be suitable for the functional analysis of large numbers of sequence variants.

6 Conclusion

PDAC is one of the most devastating malignancies, worldwide. In the Czech Republic, the incidence (21/100,000 individuals) and mortality (19/100,000 individuals) of PDAC are almost identical, and 5-year survival ranges from 5% to 9%. Approximately 5%-10% of PDAC cases are hereditary, but the genetic background is not fully understood. This study, therefore, focused on the genetic background of PDAC in the Czech Republic.

In this study, we confirmed the role of *PALB2* as a PDAC-predisposition gene. We found that the frequency of pathogenic mutations was 1.97% in PDAC patients, compared with a frequency of 0.08% in control subjects, which suggested that *PALB2* mutations may be associated with a high risk of PDAC development among carriers (OR=24.66).

We also examined the role of *NBN* in PDAC predisposition. *NBN* was previously established as a BC susceptibility gene. We found that *NBN* germline mutations in PDAC patients occurred with a 2.08% frequency, compared with a 0.2% frequency in controls. We, therefore, suggested that *NBN* may also represent a high-risk PDAC susceptibility gene (OR=9.65).

By performing an NGS analysis, using a panel of 219 genes, we aimed to examine the broader genetic background of PDAC. We detected mutations in known PDAC predisposition genes, namely *BRCA1*, *BRCA2*, and *ATM.* We also identified an association between other HBOC predisposition genes, *CHEK2* and *BRIP1,* and PDAC risk. We observed that the combined frequency of pathogenic mutations in known cancer predisposition genes in unselected PDAC patients was 13.27%. We proposed *LIG4* and *FAN1* to be promising PDAC susceptibility gene candidates. However, their functions must be confirmed in further studies.

We chose several candidate *PALB2* missense variants to perform a functional analysis of their impacts on the protein product function and prepared CRISPR-Cas9 knock-in systems and donor sequences for each of them. We performed several transfection experiments and selected two stable, heterozygous cell lines expressing the mutations c.82_83delinsGC and c.3494C>T. Both clones underwent the HR assay, showing insignificantly decreased HR activity compared with the WT control.

Our findings corresponded with the NCCN guidelines, published in 2020, which recommend germline genetic testing for any patient with confirmed exocrine pancreatic cancer, using comprehensive gene panels for hereditary cancer syndromes. More studies remain necessary to properly determine the risks for established and candidate PDAC predisposition genes. These findings are important for

patients and their family members and can have immense impacts on the tailored therapies and preventive strategies for high-risk patients.

7 List of Publications

Mutation Analysis of the *PALB2* Gene in Unselected Pancreatic Cancer Patients in the Czech Republic.
Borecka M, Zemankova P, Vocka M, Soucek P, Soukupova J, Kleiblova P, Sevcik J, Kleibl Z, Janatova M.
Cancer Genet. 2016 May;209(5): 199–204.
IF=2.183

The c.657del5 Variant in the *NBN* Gene Predisposes to Pancreatic Cancer.
Borecka M, Zemankova P, Lhota F, Soukupova J, Kleiblova P, Vocka M, Soucek P, Ticha I, Kleibl Z, Janatova M.
Gene. 2016 Aug 10;587(2): 169–172.
IF=2.638

Genetic Analysis of Subsequent Second Primary Malignant Neoplasms in Long-term Pancreatic Cancer Survivors Suggests New Potential Hereditary Genetic Alterations.
Lovecek M, Janatova M, Skalicky P, Zemanek T, Havlik R, Ehrmann J, Strouhal O, Zemankova P, Lhotova K, Borecka M, Soukupova J, Svebisova H, Soucek P, Hlavac V, Kleibl Z, Neoral C, Melichar B., Mohelnikova-Duchonova B.
Cancer Manag Res. 2019 Jan 10;11:599-609.
IF=2.243

8 References

1. D. C. Whitcomb, C. A. Shelton, R. E. Brand, Genetics and Genetic Testing in Pancreatic Cancer. *Gastroenterology* **149**, 1252-1264 e1254 (2015).
2. L. Dusek *et al.*, Cancer incidence and mortality in the Czech Republic. *Klin Onkol* **23**, 311-324 (2010).
3. N. L. Jacobs *et al.*, Cumulative morbidity and late mortality in long-term survivors of exocrine pancreas cancer. *J Gastrointest Cancer* **40**, 46-50 (2009).
4. R. L. Siegel, K. D. Miller, A. Jemal, Cancer statistics, 2019. *CA Cancer J Clin* **69**, 7-34 (2019).
5. Z. Krska, J. Svab, D. Hoskovec, J. Ulrych, Pancreatic Cancer Diagnostics and Treatment--Current State. *Prague Med Rep* **116**, 253-267 (2015).
6. A. P. Klein *et al.*, Evidence for a major gene influencing risk of pancreatic cancer. *Genet Epidemiol* **23**, 133-149 (2002).
7. Z. S. Kanji, S. Gallinger, Diagnosis and management of pancreatic cancer. *CMAJ* **185**, 1219-1226 (2013).
8. A. P. Klein *et al.*, Prospective risk of pancreatic cancer in familial pancreatic cancer kindreds. *Cancer Res* **64**, 2634-2638 (2004).
9. J. LaRusch, D. C. Whitcomb, Genetics of pancreatitis. *Curr Opin Gastroenterol* **27**, 467-474 (2011).
10. C. J. van Asperen *et al.*, Cancer risks in BRCA2 families: estimates for sites other than breast and ovary. *Journal of medical genetics* **42**, 711-719 (2005).
11. N. J. Roberts *et al.*, ATM mutations in patients with hereditary pancreatic cancer. *Cancer Discov* **2**, 41-46 (2012).
12. M. S. van der Heijden, C. J. Yeo, R. H. Hruban, S. E. Kern, Fanconi anemia gene mutations in young-onset pancreatic cancer. *Cancer Res* **63**, 2585-2588 (2003).
13. A. Sud, D. Wham, M. Catalano, N. M. Guda, Promising outcomes of screening for pancreatic cancer by genetic testing and endoscopic ultrasound. *Pancreas* **43**, 458-461 (2014).
14. M. I. Canto *et al.*, Risk of Neoplastic Progression in Individuals at High Risk for Pancreatic Cancer Undergoing Long-term Surveillance. *Gastroenterology* **155**, 740-751 e742 (2018).
15. B. Tran *et al.*, Platinum-based chemotherapy (Pt-chemo) in pancreatic adenocarcinoma (PC) associated with BRCA mutations: A translational case series. *Journal of Clinical Oncology* **30**, 217-217 (2012).
16. M. S. van der Heijden *et al.*, Functional defects in the fanconi anemia pathway in pancreatic cancer cells. *Am J Pathol* **165**, 651-657 (2004).
17. T. Golan *et al.*, Overall survival and clinical characteristics of pancreatic cancer in BRCA mutation carriers. *British journal of cancer* **111**, 1132-1138 (2014).
18. D. R. Fogelman *et al.*, Evidence for the efficacy of Iniparib, a PARP-1 inhibitor, in BRCA2-associated pancreatic cancer. *Anticancer research* **31**, 1417-1420 (2011).
19. B. Kaufman *et al.*, Olaparib monotherapy in patients with advanced cancer and a germline BRCA1/2 mutation. *Journal of clinical oncology : official journal of the American Society of Clinical Oncology* **33**, 244-250 (2015).
20. M. J. Pishvaian *et al.*, A phase I/II study of ABT-888 in combination with 5-fluorouracil (5-FU) and oxaliplatin (Ox) in patients with metastatic pancreatic cancer (MPC). *Journal of Clinical Oncology* **31**, 147-147 (2013).
21. R. Pihlak, J. W. Valle, M. G. McNamara, Germline mutations in pancreatic cancer and potential new therapeutic options. *Oncotarget* **8**, 73240-73257 (2017).
22. B. Xia *et al.*, Control of BRCA2 cellular and clinical functions by a nuclear partner, PALB2. *Molecular cell* **22**, 719-729 (2006).
23. B. Xia *et al.*, Fanconi anemia is associated with a defect in the BRCA2 partner PALB2. *Nature genetics* **39**, 159-161 (2007).
24. N. Rahman *et al.*, PALB2, which encodes a BRCA2-interacting protein, is a breast cancer susceptibility gene. *Nature genetics* **39**, 165-167 (2007).

25. S. M. H. Sy, M. S. Y. Huen, Y. Y. Zhu, J. J. Chen, PALB2 Regulates Recombinational Repair through Chromatin Association and Oligomerization. *J Biol Chem* **284**, 18302-18310 (2009).
26. F. Zhang *et al.*, PALB2 links BRCA1 and BRCA2 in the DNA-damage response. *Current biology : CB* **19**, 524-529 (2009).
27. F. Zhang, Q. Fan, K. Ren, P. R. Andreassen, PALB2 functionally connects the breast cancer susceptibility proteins BRCA1 and BRCA2. *Mol Cancer Res* **7**, 1110-1118 (2009).
28. S. Jones *et al.*, Exomic sequencing identifies PALB2 as a pancreatic cancer susceptibility gene. *Science* **324**, 217 (2009).
29. A. W. Oliver, S. Swift, C. J. Lord, A. Ashworth, L. H. Pearl, Structural basis for recruitment of BRCA2 by PALB2. *EMBO reports* **10**, 990-996 (2009).
30. R. Buisson *et al.*, Breast Cancer Proteins PALB2 and BRCA2 Stimulate Polymerase eta in Recombination-Associated DNA Synthesis at Blocked Replication Forks. *Cell reports* **6**, 553-564 (2014).
31. J. Y. Park, F. Zhang, P. R. Andreassen, PALB2: the hub of a network of tumor suppressors involved in DNA damage responses. *Biochim Biophys Acta* **1846**, 263-275 (2014).
32. J. Y. Park *et al.*, Breast cancer-associated missense mutants of the PALB2 WD40 domain, which directly binds RAD51C, RAD51 and BRCA2, disrupt DNA repair. *Oncogene* **33**, 4803-4812 (2014).
33. J. Pauty *et al.*, Cancer-causing mutations in the tumor suppressor PALB2 reveal a novel cancer mechanism using a hidden nuclear export signal in the WD40 repeat motif. *Nucleic Acids Res* **45**, 2644-2657 (2017).
34. M. Ducy *et al.*, The Tumor Suppressor PALB2: Inside Out. *Trends Biochem Sci*, (2019).
35. R. Buisson, J. Y. Masson, PALB2 self-interaction controls homologous recombination. *Nucleic Acids Res* **40**, 10312-10323 (2012).
36. F. Zhang, G. Bick, J. Y. Park, P. R. Andreassen, MDC1 and RNF8 function in a pathway that directs BRCA1-dependent localization of PALB2 required for homologous recombination. *J Cell Sci* **125**, 6049-6057 (2012).
37. R. Buisson *et al.*, Cooperation of breast cancer proteins PALB2 and piccolo BRCA2 in stimulating homologous recombination. *Nature structural & molecular biology* **17**, 1247-+ (2010).
38. J. Y. Bleuyard, R. Buisson, J. Y. Masson, F. Esashi, ChAM, a novel motif that mediates PALB2 intrinsic chromatin binding and facilitates DNA repair. *EMBO reports* **13**, 135-141 (2012).
39. S. M. H. Sy, M. S. Y. Huen, J. J. Chen, MRG15 Is a Novel PALB2-interacting Factor Involved in Homologous Recombination. *J Biol Chem* **284**, 21127-21131 (2009).
40. J. Y. Bleuyard *et al.*, MRG15-mediated tethering of PALB2 to unperturbed chromatin protects active genes from genotoxic stress. *Proceedings of the National Academy of Sciences of the United States of America* **114**, 7671-7676 (2017).
41. A. Gardini, D. Baillat, M. Cesaroni, R. Shiekhattar, Genome-wide analysis reveals a role for BRCA1 and PALB2 in transcriptional co-activation. *EMBO J* **33**, 890-905 (2014).
42. R. Buisson *et al.*, Coupling of Homologous Recombination and the Checkpoint by ATR. *Molecular cell* **65**, 336-346 (2017).
43. S. Matsuoka *et al.*, ATM and ATR substrate analysis reveals extensive protein networks responsive to DNA damage. *Science* **316**, 1160-1166 (2007).
44. J. K. Ahlskog, B. D. Larsen, K. Achanta, C. S. Sorensen, ATM/ATR-mediated phosphorylation of PALB2 promotes RAD51 function. *EMBO reports* **17**, 671-681 (2016).
45. J. Ma *et al.*, PALB2 interacts with KEAP1 to promote NRF2 nuclear accumulation and function. *Mol Cell Biol* **32**, 1506-1517 (2012).
46. A. Orthwein *et al.*, A mechanism for the suppression of homologous recombination in G1 cells. *Nature* **528**, 422-426 (2015).
47. T. Hayakawa *et al.*, MRG15 binds directly to PALB2 and stimulates homology-directed repair of chromosomal breaks. *J Cell Sci* **123**, 1124-1130 (2010).

48. T. Uziel *et al.*, Requirement of the MRN complex for ATM activation by DNA damage. *EMBO J* **22**, 5612-5621 (2003).
49. L. Pellegrini *et al.*, Insights into DNA recombination from the structure of a RAD51-BRCA2 complex. *Nature* **420**, 287-293 (2002).
50. E. Dray *et al.*, Enhancement of RAD51 recombinase activity by the tumor suppressor PALB2. *Nature structural & molecular biology* **17**, 1255-1259 (2010).
51. A. K. Murphy *et al.*, Phosphorylated RPA recruits PALB2 to stalled DNA replication forks to facilitate fork recovery. *J Cell Biol* **206**, 493-507 (2014).
52. S. A. Hartford *et al.*, Interaction with PALB2 Is Essential for Maintenance of Genomic Integrity by BRCA2. *PLoS genetics* **12**, e1006236 (2016).
53. J. Nikkila *et al.*, Heterozygous mutations in PALB2 cause DNA replication and damage response defects. *Nat Commun* **4**, 2578 (2013).
54. A. Gueiderikh, F. Rosselli, J. B. C. Neto, A never-ending story: the steadily growing family of the FA and FA-like genes. *Genet Mol Biol* **40**, 398-407 (2017).
55. K. Knies *et al.*, Biallelic mutations in the ubiquitin ligase RFWD3 cause Fanconi anemia. *J Clin Invest* **127**, 3013-3027 (2017).
56. S. Reid *et al.*, Biallelic mutations in PALB2 cause Fanconi anemia subtype FA-N and predispose to childhood cancer. *Nature genetics* **39**, 162-164 (2007).
57. K. Myers *et al.*, The clinical phenotype of children with Fanconi anemia caused by biallelic FANCD1/BRCA2 mutations. *Pediatr Blood Cancer* **58**, 462-465 (2012).
58. P. J. Byrd *et al.*, A Hypomorphic PALB2 Allele Gives Rise to an Unusual Form of FA-N Associated with Lymphoid Tumour Development. *PLoS genetics* **12**, e1005945 (2016).
59. A. Serra *et al.*, Shared Copy Number Variation in Simultaneous Nephroblastoma and Neuroblastoma due to Fanconi Anemia. *Mol Syndromol* **3**, 120-130 (2012).
60. A. Dansonka-Mieszkowska *et al.*, A novel germline PALB2 deletion in Polish breast and ovarian cancer patients. *BMC medical genetics* **11**, 20 (2010).
61. M. Janatova *et al.*, The PALB2 Gene Is a Strong Candidate for Clinical Testing in BRCA1- and BRCA2-Negative Hereditary Breast Cancer. *Cancer Epidem Biomar* **22**, 2323-2332 (2013).
62. X. Yang *et al.*, Cancer Risks Associated With Germline PALB2 Pathogenic Variants: An International Study of 524 Families. *Journal of clinical oncology : official journal of the American Society of Clinical Oncology*, JCO1901907 (2019).
63. F. Aloraifi *et al.*, Protein-truncating variants in moderate-risk breast cancer susceptibility genes: a meta-analysis of high-risk case-control screening studies. *Cancer Genet* **208**, 455-463 (2015).
64. B. P. Alter, A. F. Best, Frequency of heterozygous germline pathogenic variants in genes for Fanconi anemia in patients with non-BRCA1/BRCA2 breast cancer: a meta-analysis. *Breast cancer research and treatment* **182**, 465-476 (2020).
65. H. LaDuca *et al.*, A clinical guide to hereditary cancer panel testing: evaluation of gene-specific cancer associations and sensitivity of genetic testing criteria in a cohort of 165,000 high-risk patients. *Genetics in medicine : official journal of the American College of Medical Genetics* **22**, 407-415 (2020).
66. R. C. Grant *et al.*, Prevalence of germline mutations in cancer predisposition genes in patients with pancreatic cancer. *Gastroenterology* **148**, 556-564 (2015).
67. C. Hu *et al.*, Prevalence of pathogenic mutations in cancer predisposition genes among pancreatic cancer patients. *Cancer epidemiology, biomarkers & prevention : a publication of the American Association for Cancer Research, cosponsored by the American Society of Preventive Oncology*, (2015).
68. L. R. Susswein *et al.*, Pathogenic and likely pathogenic variant prevalence among the first 10,000 patients referred for next-generation cancer panel testing. *Genetics in medicine : official journal of the American College of Medical Genetics* **18**, 823-832 (2016).
69. J. L. Humphris *et al.*, Hypermutation In Pancreatic Cancer. *Gastroenterology* **152**, 68-74 e62 (2017).

70. D. Mandelker *et al.*, Mutation Detection in Patients With Advanced Cancer by Universal Sequencing of Cancer-Related Genes in Tumor and Normal DNA vs Guideline-Based Germline Testing. *JAMA* **318**, 825-835 (2017).
71. K. Shindo *et al.*, Deleterious Germline Mutations in Patients With Apparently Sporadic Pancreatic Adenocarcinoma. *Journal of clinical oncology : official journal of the American Society of Clinical Oncology* **35**, 3382-3390 (2017).
72. R. Brand *et al.*, Prospective study of germline genetic testing in incident cases of pancreatic adenocarcinoma. *Cancer* **124**, 3520-3527 (2018).
73. R. C. Grant *et al.*, Exome-Wide Association Study of Pancreatic Cancer Risk. *Gastroenterology* **154**, 719-722 e713 (2018).
74. C. Hu *et al.*, Association Between Inherited Germline Mutations in Cancer Predisposition Genes and Risk of Pancreatic Cancer. *JAMA* **319**, 2401-2409 (2018).
75. C. Hu *et al.*, Multigene Hereditary Cancer Panels Reveal High-Risk Pancreatic Cancer Susceptibility Genes. *JCO Precision Oncology*, 1-28 (2018).
76. E. L. Young *et al.*, Pancreatic cancer as a sentinel for hereditary cancer predisposition. *BMC cancer* **18**, 697 (2018).
77. M. B. Yurgelun *et al.*, Germline cancer susceptibility gene variants, somatic second hits, and survival outcomes in patients with resected pancreatic cancer. *Genetics in medicine : official journal of the American College of Medical Genetics* **21**, 213-223 (2019).
78. R. C. Grant *et al.*, Exome sequencing identifies nonsegregating nonsense ATM and PALB2 variants in familial pancreatic cancer. *Human genomics* **7**, 11 (2013).
79. N. J. Roberts *et al.*, Whole Genome Sequencing Defines the Genetic Heterogeneity of Familial Pancreatic Cancer. *Cancer Discov* **6**, 166-175 (2016).
80. E. Takai *et al.*, Germline mutations in Japanese familial pancreatic cancer patients. *Oncotarget* **7**, 74227-74235 (2016).
81. K. G. Chaffee *et al.*, Prevalence of germ-line mutations in cancer genes among pancreatic cancer patients with a positive family history. *Genetics in medicine : official journal of the American College of Medical Genetics* **20**, 119-127 (2018).
82. S. J. Ramus *et al.*, Germline Mutations in the BRIP1, BARD1, PALB2, and NBN Genes in Women With Ovarian Cancer. *Journal of the National Cancer Institute* **107**, (2015).
83. J. Kotsopoulos *et al.*, Frequency of germline PALB2 mutations among women with epithelial ovarian cancer. *Familial cancer* **16**, 29-34 (2017).
84. B. M. Norquist *et al.*, Inherited Mutations in Women With Ovarian Carcinoma. *JAMA oncology* **2**, 482-490 (2016).
85. K. Lhotova *et al.*, Multigene Panel Germline Testing of 1333 Czech Patients with Ovarian Cancer. *Cancers (Basel)* **12**, (2020).
86. S. Pakkanen *et al.*, PALB2 variants in hereditary and unselected Finnish prostate cancer cases. *Journal of negative results in biomedicine* **8**, 12 (2009).
87. H. Erkko *et al.*, A recurrent mutation in PALB2 in Finnish cancer families. *Nature* **446**, 316-319 (2007).
88. M. Tischkowitz *et al.*, Analysis of the gene coding for the BRCA2-interacting protein PALB2 in hereditary prostate cancer. *The Prostate* **68**, 675-678 (2008).
89. L. G. Aoude *et al.*, Assessment of PALB2 as a candidate melanoma susceptibility gene. *PloS one* **9**, e100683 (2014).
90. N. Sabbaghian, R. Kyle, A. Hao, D. Hogg, M. Tischkowitz, Mutation analysis of the PALB2 cancer predisposition gene in familial melanoma. *Familial cancer* **10**, 315-317 (2011).
91. T. Heikkinen *et al.*, The breast cancer susceptibility mutation PALB2 1592delT is associated with an aggressive tumor phenotype. *Clinical cancer research : an official journal of the American Association for Cancer Research* **15**, 3214-3222 (2009).
92. C. Cybulski *et al.*, Clinical outcomes in women with breast cancer and a PALB2 mutation: a prospective cohort analysis. *Lancet Oncol* **16**, 638-644 (2015).

93. M. Tischkowitz *et al.*, Analysis of PALB2/FANCN-associated breast cancer families. *Proceedings of the National Academy of Sciences of the United States of America* **104**, 6788-6793 (2007).
94. A. C. Antoniou, W. D. Foulkes, M. Tischkowitz, Breast-cancer risk in families with mutations in PALB2. *The New England journal of medicine* **371**, 1651-1652 (2014).
95. J. E. A. Lee *et al.*, Molecular analysis of PALB2-associated breast cancers. *The Journal of pathology* **245**, 53-60 (2018).
96. A. Li *et al.*, Homologous recombination DNA repair defects in PALB2-associated breast cancers. *NPJ Breast Cancer* **5**, 23 (2019).
97. A. Potapova, A. M. Hoffman, A. K. Godwin, T. Al-Saleem, P. Cairns, Promoter hypermethylation of the PALB2 susceptibility gene in inherited and sporadic breast and ovarian cancer. *Cancer Res* **68**, 998-1002 (2008).
98. C. M. Scott *et al.*, Methylation of Breast Cancer Predisposition Genes in Early-Onset Breast Cancer: Australian Breast Cancer Family Registry. *PloS one* **11**, e0165436 (2016).
99. T. Mikeska *et al.*, No evidence for PALB2 methylation in high-grade serous ovarian cancer. *J Ovarian Res* **6**, 26 (2013).
100. N. Poumpouridou *et al.*, Development and validation of molecular methodologies to assess PALB2 expression in sporadic breast cancer. *Clin Biochem* **49**, 253-259 (2016).
101. L. Spugnesi *et al.*, Germline mutations in DNA repair genes may predict neoadjuvant therapy response in triple negative breast patients. *Genes, chromosomes & cancer* **55**, 915-924 (2016).
102. K. P. Pennington *et al.*, Germline and somatic mutations in homologous recombination genes predict platinum response and survival in ovarian, fallopian tube, and peritoneal carcinomas. *Clinical cancer research : an official journal of the American Association for Cancer Research* **20**, 764-775 (2014).
103. M. C. Villarroel *et al.*, Personalizing cancer treatment in the age of global genomic analyses: PALB2 gene mutations and the response to DNA damaging agents in pancreatic cancer. *Molecular cancer therapeutics* **10**, 3-8 (2011).
104. S. Boeck *et al.*, Mismatch-repair-deficient metastatic pancreatic ductal adenocarcinoma with a germline PALB2 mutation: unusual genetics, unusual clinical course. *Ann Oncol* **28**, 438-439 (2017).
105. M. A. Smith *et al.*, Initial testing (stage 1) of the PARP inhibitor BMN 673 by the pediatric preclinical testing program: PALB2 mutation predicts exceptional in vivo response to BMN 673. *Pediatr Blood Cancer* **62**, 91-98 (2015).
106. K. P. Hopfner, C. D. Putnam, J. A. Tainer, DNA double-strand break repair from head to tail. *Curr Opin Struct Biol* **12**, 115-122 (2002).
107. B. J. Lamarche, N. I. Orazio, M. D. Weitzman, The MRN complex in double-strand break repair and telomere maintenance. *FEBS Lett* **584**, 3682-3695 (2010).
108. R. Varon *et al.*, Nibrin, a novel DNA double-strand break repair protein, is mutated in Nijmegen breakage syndrome. *Cell* **93**, 467-476 (1998).
109. H. Tauchi, S. Matsuura, J. Kobayashi, S. Sakamoto, K. Komatsu, Nijmegen breakage syndrome gene, NBS1, and molecular links to factors for genome stability. *Oncogene* **21**, 8967-8980 (2002).
110. J. Falck, J. Coates, S. P. Jackson, Conserved modes of recruitment of ATM, ATR and DNA-PKcs to sites of DNA damage. *Nature* **434**, 605-611 (2005).
111. H. Tauchi *et al.*, The forkhead-associated domain of NBS1 is essential for nuclear foci formation after irradiation but not essential for hRAD50[middle dot]hMRE11[middle dot]NBS1 complex DNA repair activity. *J Biol Chem* **276**, 12-15 (2001).
112. R. Rai *et al.*, NBS1 Phosphorylation Status Dictates Repair Choice of Dysfunctional Telomeres. *Molecular cell* **65**, 801-817 e804 (2017).
113. X. Wu *et al.*, ATM phosphorylation of Nijmegen breakage syndrome protein is required in a DNA damage response. *Nature* **405**, 477-482 (2000).

114. J. Wen, K. Cerosaletti, K. J. Schultz, J. A. Wright, P. Concannon, NBN phosphorylation regulates the accumulation of MRN and ATM at sites of DNA double-strand breaks. *Oncogene* **32**, 4448-4456 (2013).
115. J. Wu *et al.*, Skp2 E3 ligase integrates ATM activation and homologous recombination repair by ubiquitinating NBS1. *Molecular cell* **46**, 351-361 (2012).
116. G. J. Williams, S. P. Lees-Miller, J. A. Tainer, Mre11-Rad50-Nbs1 conformations and the control of sensing, signaling, and effector responses at DNA double-strand breaks. *DNA Repair (Amst)* **9**, 1299-1306 (2010).
117. K. P. Hopfner *et al.*, Structural biochemistry and interaction architecture of the DNA double-strand break repair Mre11 nuclease and Rad50-ATPase. *Cell* **105**, 473-485 (2001).
118. K. P. Hopfner *et al.*, The Rad50 zinc-hook is a structure joining Mre11 complexes in DNA recombination and repair. *Nature* **418**, 562-566 (2002).
119. M. Hohl *et al.*, Interdependence of the rad50 hook and globular domain functions. *Molecular cell* **57**, 479-491 (2015).
120. R. A. Deshpande *et al.*, ATP-driven Rad50 conformations regulate DNA tethering, end resection, and ATM checkpoint signaling. *EMBO J* **33**, 482-500 (2014).
121. T. T. Paull, R. A. Deshpande, The Mre11/Rad50/Nbs1 complex: recent insights into catalytic activities and ATP-driven conformational changes. *Exp Cell Res* **329**, 139-147 (2014).
122. S. F. Tseng, C. Y. Chang, K. J. Wu, S. C. Teng, Importin KPNA2 is required for proper nuclear localization and multiple functions of NBS1. *J Biol Chem* **280**, 39594-39600 (2005).
123. J. Kobayashi *et al.*, NBS1 localizes to gamma-H2AX foci through interaction with the FHA/BRCT domain. *Current biology : CB* **12**, 1846-1851 (2002).
124. M. Gatei *et al.*, ATM protein-dependent phosphorylation of Rad50 protein regulates DNA repair and cell cycle control. *J Biol Chem* **286**, 31542-31556 (2011).
125. Y. Shiloh, Y. Ziv, The ATM protein kinase: regulating the cellular response to genotoxic stress, and more. *Nat Rev Mol Cell Biol* **14**, 197-210 (2013).
126. S. Burma, B. P. Chen, M. Murphy, A. Kurimasa, D. J. Chen, ATM phosphorylates histone H2AX in response to DNA double-strand breaks. *J Biol Chem* **276**, 42462-42467 (2001).
127. V. Borde, The multiple roles of the Mre11 complex for meiotic recombination. *Chromosome Res* **15**, 551-563 (2007).
128. K. C. Manthey *et al.*, NBS1 mediates ATR-dependent RPA hyperphosphorylation following replication-fork stall and collapse. *J Cell Sci* **120**, 4221-4229 (2007).
129. K. H. Chrzanowska, H. Gregorek, B. Dembowska-Baginska, M. A. Kalina, M. Digweed, Nijmegen breakage syndrome (NBS). *Orphanet J Rare Dis* **7**, 13 (2012).
130. M. Digweed, K. Sperling, Nijmegen breakage syndrome: clinical manifestation of defective response to DNA double-strand breaks. *DNA Repair (Amst)* **3**, 1207-1217 (2004).
131. R. S. Maser, R. Zinkel, J. H. Petrini, An alternative mode of translation permits production of a variant NBS1 protein from the common Nijmegen breakage syndrome allele. *Nature genetics* **27**, 417-421 (2001).
132. E. Seemanova *et al.*, Nijmegen breakage syndrome (NBS) with neurological abnormalities and without chromosomal instability. *Journal of medical genetics* **43**, 218-224 (2006).
133. R. Varon *et al.*, Clinical ascertainment of Nijmegen breakage syndrome (NBS) and prevalence of the major mutation, 657del5, in three Slav populations. *European journal of human genetics : EJHG* **8**, 900-902 (2000).
134. J. Drabek, M. Hajduch, L. Gojova, E. Weigl, V. Mihal, Frequency of 657del(5) mutation of the NBS1 gene in the Czech population by polymerase chain reaction with sequence specific primers. *Cancer Genet Cytogenet* **138**, 157-159 (2002).
135. P. Soucek *et al.*, Multiplex single-tube screening for mutations in the Nijmegen Breakage Syndrome (NBS1) gene in Hodgkin's and non-Hodgkin's lymphoma patients of Slavic origin. *European journal of human genetics : EJHG* **11**, 416-419 (2003).

136. I. B. Resnick *et al.*, 657del5 mutation in the gene for Nijmegen breakage syndrome (NBS1) in a cohort of Russian children with lymphoid tissue malignancies and controls. *Am J Med Genet A* **120A**, 174-179 (2003).
137. K. H. Chrzanowska *et al.*, Carrier frequency of mutation 657del5 in the NBS1 gene in a population of Polish pediatric patients with sporadic lymphoid malignancies. *International journal of cancer. Journal international du cancer* **118**, 1269-1274 (2006).
138. J. Steffen *et al.*, Increased risk of gastrointestinal lymphoma in carriers of the 657del5 NBS1 gene mutation. *International journal of cancer. Journal international du cancer* **119**, 2970-2973 (2006).
139. M. R. Lener *et al.*, Do founder mutations characteristic of some cancer sites also predispose to pancreatic cancer? *International journal of cancer. Journal international du cancer* **139**, 601-606 (2016).
140. M. Borecka *et al.*, The c.657del5 variant in the NBN gene predisposes to pancreatic cancer. *Gene* **587**, 169-172 (2016).
141. F. Damiola *et al.*, Rare key functional domain missense substitutions in MRE11A, RAD50, and NBN contribute to breast cancer susceptibility: results from a Breast Cancer Family Registry case-control mutation-screening study. *Breast Cancer Res* **16**, R58 (2014).
142. G. Zhang, Y. Zeng, Z. Liu, W. Wei, Significant association between Nijmegen breakage syndrome 1 657del5 polymorphism and breast cancer risk. *Tumour Biol* **34**, 2753-2757 (2013).
143. P. Gao, N. Ma, M. Li, Q. B. Tian, D. W. Liu, Functional variants in NBS1 and cancer risk: evidence from a meta-analysis of 60 publications with 111 individual studies. *Mutagenesis* **28**, 683-697 (2013).
144. R. Pearlman *et al.*, Prevalence and Spectrum of Germline Cancer Susceptibility Gene Mutations Among Patients With Early-Onset Colorectal Cancer. *JAMA oncology* **3**, 464-471 (2017).
145. B. Pardini *et al.*, NBN 657del5 heterozygous mutations and colorectal cancer risk in the Czech Republic. *Mutat Res* **666**, 64-67 (2009).
146. P. Meyer *et al.*, Molecular genetic analysis of NBS1 in German melanoma patients. *Melanoma Res* **17**, 109-116 (2007).
147. C. Cybulski *et al.*, NBS1 is a prostate cancer susceptibility gene. *Cancer Res* **64**, 1215-1219 (2004).
148. K. G. Buslov *et al.*, NBS1 657del5 mutation may contribute only to a limited fraction of breast cancer cases in Russia. *International journal of cancer. Journal international du cancer* **114**, 585-589 (2005).
149. M. Mateju *et al.*, Germline mutations 657del5 and 643C>T (R215W) in NBN are not likely to be associated with increased risk of breast cancer in Czech women. *Breast cancer research and treatment* **133**, 809-811 (2012).
150. E. M. Stoffel *et al.*, Evaluating Susceptibility to Pancreatic Cancer: ASCO Provisional Clinical Opinion. *Journal of clinical oncology : official journal of the American Society of Clinical Oncology* **37**, 153-164 (2019).
151. J. Soukupova *et al.*, Validation of CZECANCA (CZEch CAncer paNel for Clinical Application) for targeted NGS-based analysis of hereditary cancer syndromes. *PloS one* **13**, e0195761 (2018).
152. K. V. Voelkerding, S. A. Dames, J. D. Durtschi, Next-generation sequencing: from basic research to diagnostics. *Clin Chem* **55**, 641-658 (2009).
153. M. Borecka *et al.*, Mutation analysis of the PALB2 gene in unselected pancreatic cancer patients in the Czech Republic. *Cancer Genet* **209**, 199-204 (2016).
154. F. A. Ran *et al.*, Genome engineering using the CRISPR-Cas9 system. *Nat Protoc* **8**, 2281-2308 (2013).
155. R. S. Bindra, A. G. Goglia, M. Jasin, S. N. Powell, Development of an assay to measure mutagenic non-homologous end-joining repair activity in mammalian cells. *Nucleic Acids Res* **41**, e115 (2013).

156. S. M. Sy, M. S. Huen, J. Chen, PALB2 is an integral component of the BRCA complex required for homologous recombination repair. *Proceedings of the National Academy of Sciences of the United States of America* **106**, 7155-7160 (2009).
157. T. Maruyama *et al.*, Increasing the efficiency of precise genome editing with CRISPR-Cas9 by inhibition of nonhomologous end joining. *Nat Biotechnol* **33**, 538-542 (2015).
158. S. Casadei *et al.*, Contribution of Inherited Mutations in the BRCA2-Interacting Protein PALB2 to Familial Breast Cancer. *Cancer Res* **71**, 2222-2229 (2011).
159. M. A. Adank, S. E. van Mil, J. J. Gille, Q. Waisfisz, H. Meijers-Heijboer, PALB2 analysis in BRCA2-like families. *Breast cancer research and treatment* **127**, 357-362 (2011).
160. N. Bogdanova *et al.*, PALB2 mutations in German and Russian patients with bilateral breast cancer. *Breast cancer research and treatment* **126**, 545-550 (2011).
161. T. Walsh *et al.*, Detection of inherited mutations for breast and ovarian cancer using genomic capture and massively parallel sequencing. *Proceedings of the National Academy of Sciences of the United States of America* **107**, 12629-12633 (2010).
162. E. P. Slater *et al.*, PALB2 mutations in European familial pancreatic cancer families. *Clinical genetics* **78**, 490-494 (2010).
163. M. Sluiter, S. Mew, E. J. van Rensburg, PALB2 sequence variants in young South African breast cancer patients. *Familial cancer* **8**, 347-353 (2009).
164. L. Papi *et al.*, A PALB2 germline mutation associated with hereditary breast cancer in Italy. *Familial cancer* **9**, 181-185 (2010).
165. A. Kluska *et al.*, PALB2 mutations in BRCA1/2-mutation negative breast and ovarian cancer patients from Poland. *BMC Med Genomics* **10**, 14 (2017).
166. A. Myszka *et al.*, Targeted massively parallel sequencing characterises the mutation spectrum of PALB2 in breast and ovarian cancer cases from Poland and Ukraine. *Familial cancer* **17**, 345-349 (2018).
167. P. Wojcik *et al.*, Recurrent mutations of BRCA1, BRCA2 and PALB2 in the population of breast and ovarian cancer patients in Southern Poland. *Hereditary cancer in clinical practice* **14**, 5 (2016).
168. M. Noskowicz *et al.*, Prevalence of PALB2 mutation c.509_510delGA in unselected breast cancer patients from Central and Eastern Europe. *Familial cancer* **13**, 137-142 (2014).
169. C. Cybulski *et al.*, Mutations predisposing to breast cancer in 12 candidate genes in breast cancer patients from Poland. *Clinical genetics* **88**, 366-370 (2015).
170. P. Domagala *et al.*, Prevalence of Germline Mutations in Genes Engaged in DNA Damage Repair by Homologous Recombination in Patients with Triple-Negative and Hereditary Non-Triple-Negative Breast Cancers. *PloS one* **10**, e0130393 (2015).
171. B. H. Shirts *et al.*, Improving performance of multigene panels for genomic analysis of cancer predisposition. *Genetics in medicine : official journal of the American College of Medical Genetics* **18**, 974-981 (2016).
172. A. Desmond *et al.*, Clinical Actionability of Multigene Panel Testing for Hereditary Breast and Ovarian Cancer Risk Assessment. *JAMA oncology* **1**, 943-951 (2015).
173. I. Catucci *et al.*, The PALB2 p.Leu939Trp mutation is not associated with breast cancer risk. *Breast Cancer Res* **18**, 111 (2016).
174. R. Boonen *et al.*, Functional analysis of genetic variants in the high-risk breast cancer susceptibility gene PALB2. *Nat Commun* **10**, 5296 (2019).
175. A. Rodrigue *et al.*, A global functional analysis of missense mutations reveals two major hotspots in the PALB2 tumor suppressor. *Nucleic Acids Res*, (2019).
176. T. Wiltshire *et al.*, Functional characterization of 84 PALB2 variants of uncertain significance. *Genetics in medicine : official journal of the American College of Medical Genetics*, (2019).
177. E. Machackova *et al.*, Spectrum and characterisation of BRCA1 and BRCA2 deleterious mutations in high-risk Czech patients with breast and/or ovarian cancer. *BMC cancer* **8**, 140 (2008).

178. P. Kleiblova *et al.*, Identification of deleterious germline CHEK2 mutations and their association with breast and ovarian cancer. *International journal of cancer. Journal international du cancer*, (2019).
179. A. L. Smith *et al.*, Candidate DNA repair susceptibility genes identified by exome sequencing in high-risk pancreatic cancer. *Cancer Lett* **370**, 302-312 (2016).
180. A. Artinyan *et al.*, The anatomic location of pancreatic cancer is a prognostic factor for survival. *HPB (Oxford)* **10**, 371-376 (2008).
181. H. X. Liu *et al.*, The role of hMLH3 in familial colorectal cancer. *Cancer Res* **63**, 1894-1899 (2003).
182. G. Figlioli *et al.*, The Spectrum of FANCM Protein Truncating Variants in European Breast Cancer Cases. *Cancers (Basel)* **12**, (2020).
183. I. Nimmrich *et al.*, Loss of the PLA2G2A gene in a sporadic colorectal tumor of a patient with a PLA2G2A germline mutation and absence of PLA2G2A germline alterations in patients with FAP. *Hum Genet* **100**, 345-349 (1997).
184. L. Raskin *et al.*, Targeted sequencing of established and candidate colorectal cancer genes in the Colon Cancer Family Registry Cohort. *Oncotarget* **8**, 93450-93463 (2017).
185. F. Bellido *et al.*, POLE and POLD1 mutations in 529 kindred with familial colorectal cancer and/or polyposis: review of reported cases and recommendations for genetic testing and surveillance. *Genetics in medicine : official journal of the American College of Medical Genetics* **18**, 325-332 (2016).
186. A. Jamsheer *et al.*, Mutational screening of EXT1 and EXT2 genes in Polish patients with hereditary multiple exostoses. *J Appl Genet* **55**, 183-188 (2014).
187. S. Holter *et al.*, Germline BRCA Mutations in a Large Clinic-Based Cohort of Patients With Pancreatic Adenocarcinoma. *Journal of clinical oncology : official journal of the American Society of Clinical Oncology* **33**, 3124-3129 (2015).
188. E. E. Salo-Mullen *et al.*, Identification of germline genetic mutations in patients with pancreatic cancer. *Cancer* **121**, 4382-4388 (2015).
189. C. R. Ferrone *et al.*, BRCA germline mutations in Jewish patients with pancreatic adenocarcinoma. *Journal of clinical oncology : official journal of the American Society of Clinical Oncology* **27**, 433-438 (2009).
190. F. Lhota *et al.*, Hereditary truncating mutations of DNA repair and other genes in BRCA1/BRCA2/PALB2-negatively tested breast cancer patients. *Clinical genetics* **90**, 324-333 (2016).
191. B. Mohelnikova-Duchonova *et al.*, CHEK2 gene alterations in the forkhead-associated domain, 1100delC and del5395 do not modify the risk of sporadic pancreatic cancer. *Cancer epidemiology* **34**, 656-658 (2010).
192. R. R. Joshi, S. I. Ali, A. K. Ashley, DNA Ligase IV Prevents Replication Fork Stalling and Promotes Cellular Proliferation in Triple Negative Breast Cancer. *J Nucleic Acids* **2019**, 9170341 (2019).
193. T. I. Ben-Omran, K. Cerosaletti, P. Concannon, S. Weitzman, M. M. Nezarati, A patient with mutations in DNA Ligase IV: clinical features and overlap with Nijmegen breakage syndrome. *Am J Med Genet A* **137A**, 283-287 (2005).
194. L. Witkowski *et al.*, The hereditary nature of small cell carcinoma of the ovary, hypercalcemic type: two new familial cases. *Familial cancer* **16**, 395-399 (2017).
195. N. Segui *et al.*, Germline Mutations in FAN1 Cause Hereditary Colorectal Cancer by Impairing DNA Repair. *Gastroenterology* **149**, 563-566 (2015).
196. C. MacKay *et al.*, Identification of KIAA1018/FAN1, a DNA repair nuclease recruited to DNA damage by monoubiquitinated FANCD2. *Cell* **142**, 65-76 (2010).
197. W. Zhou *et al.*, FAN1 mutations cause karyomegalic interstitial nephritis, linking chronic kidney failure to defective DNA damage repair. *Nature genetics* **44**, 910-915 (2012).
198. J. P. Trujillo *et al.*, On the role of FAN1 in Fanconi anemia. *Blood* **120**, 86-89 (2012).

199. B. Gerdes *et al.*, Multiple primaries in pancreatic cancer patients: indicator of a genetic predisposition? *Int J Epidemiol* **29**, 999-1003 (2000).
200. T. S. Riall *et al.*, Incidence of additional primary cancers in patients with invasive intraductal papillary mucinous neoplasms and sporadic pancreatic adenocarcinomas. *J Am Coll Surg* **204**, 803-813; discussion 813-804 (2007).
201. K. T. Chen, K. Devarajan, J. P. Hoffman, Morbidity among long-term survivors after pancreatoduodenectomy for pancreatic adenocarcinoma. *Ann Surg Oncol* **22**, 1185-1189 (2015).
202. T. Hackert *et al.*, Extrapancreatic malignancies in patients with pancreatic cancer: epidemiology and clinical consequences. *Pancreas* **41**, 212-217 (2012).
203. M. I. Canto *et al.*, International Cancer of the Pancreas Screening (CAPS) Consortium summit on the management of patients with increased risk for familial pancreatic cancer. *Gut* **62**, 339-347 (2013).
204. M. Y. Teo, E. M. O'Reilly, Is it time to split strategies to treat homologous recombinant deficiency in pancreas cancer? *J Gastrointest Oncol* **7**, 738-749 (2016).
205. P. Rantakari *et al.*, Inactivation of Palb2 gene leads to mesoderm differentiation defect and early embryonic lethality in mice. *Hum Mol Genet* **19**, 3021-3029 (2010).
206. P. Bouwman *et al.*, Loss of p53 partially rescues embryonic development of Palb2 knockout mice but does not foster haploinsufficiency of Palb2 in tumour suppression. *The Journal of pathology* **224**, 10-21 (2011).
207. C. Bowman-Colin *et al.*, Palb2 synergizes with Trp53 to suppress mammary tumor formation in a model of inherited breast cancer. *Proceedings of the National Academy of Sciences of the United States of America* **110**, 8632-8637 (2013).
208. Y. Huo *et al.*, Autophagy opposes p53-mediated tumor barrier to facilitate tumorigenesis in a model of PALB2-associated hereditary breast cancer. *Cancer Discov* **3**, 894-907 (2013).

9 Supplements